BLIND DETECTION DESIGNS WITH UNIQUE IDENTIFICATION IN TWO-WAY RELAY CHANNELS

A Dissertation by

Lun Li

Master of Science, Wichita State University, Wichita, Kansas, 2011

Submitted to the Department of Electrical Engineering and Computer Science
and the faculty of the Graduate School of
Wichita State University
in partial fulfillment of
the requirements for the degree of
Doctor of Philosophy

July 2016

BLIND DETECTION DESIGNS WITH UNIQUE IDENTIFICATION IN TWO-WAY RELAY CHANNELS

The following faculty members have examined the final copy of this dissertation for form and content, and recommend that it be accepted in partial fulfillment of the requirement for the degree of Doctor of Philosophy with a major in Electrical Engineering.

Yanwu Ding, Committee Chair

John Watkins, Committee Member

Venod Namboodiri, Committee Member

Yi Song, Committee Member

Tianshi Lu, Committee Member

Accepted for the College of Engineering

Royce Bowden, Dean

Accepted for the Graduate School

Dennis Livesay, Dean

ACKNOWLEDGEMENTS

I would like to thank my advisor, Dr. Yanwu Ding, who made it possible for me to complete this dissertation. Her support, knowledge, and patience have guided me from the very beginning to the end. I would also like to thank Dr. John Watkins, Dr. Venod Namboodiri, Dr. Yi Song, and Dr. Tianshi Lu for their kind help and for serving on my dissertation committee.

I am thankful to Dr. Hyuck Kwon, Dr. M. Edwin Sawan, and other professors at WSU, who put their faith in me and urge me to do better.

I am grateful to Allen Tang, Yu Bi, Xin Ding, Jiang Liu, Dr. Zhouxing Hu, Guo Chen, Dr. Guangxing Bai, Dr. Wenhao Xiong, Dr. Li Liang, Dr. Kanghee Lee, Shuang Xia, and all my friends and colleagues at WSU. Thank you all for continuous support and encouragement.

I would like to thank Zhe Shi for going through ups and downs with me in the past a few years.

I would like to express my gratitude to my family for always standing next to me, and showing me unconditional love. I know that my mother has been watching down on me. You are my motivation to achieve this. All I have been doing is to make you proud. Thank you mom.

ABSTRACT

In amplify-and-forward (AF) two-way relay networks, information is exchanged between two source nodes via a relay node by AF relaying. This dissertation develops the blind detection designs for various two-way relay systems such as one antenna AF two-way relay network with direct link, one antenna AF two-way relay network without direct link, and multiple antenna AF two-way relay network without direct link.

In the first system, an effective signalling and transmitting scheme using four M-ary phase-shift keying (M-PSK) constellation sets is proposed to achieve a unique identification of the transmitted symbols and the channel coefficients in a noise-free transmission. Blind receivers with full diversity are derived for Rayleigh fading channels with Gaussian noise by the generalized likelihood ratio test (GLRT) and least square error (LSE) criterions. Constellation selections are investigated for the source nodes to transmit at a uniform bit rate in each time slot. Power allocation schemes are discussed to further improve the average error probability of the source nodes in the blind detections.

In the second system, frequency selective fading channels are assumed between each node. The knowledge of channel state information (CSI) is assumed not available for all nodes. An efficient transmission and signaling scheme is proposed. To deal with the high complexity in implementing the LSE receiver, a parallel iterative sphere decoding scheme is investigated. The low complexity of this scheme allows that the joint estimation and detection of the channel coefficients and transmitted symbols can be efficiently implemented.

In the third system, multiple antennas are equipped on both source nodes. This part of work proposes an efficient transmission and signaling scheme with time-reversal space-time-block-coded (TR-STBC) blind detection design for frequency-selective two-way relay channels. The similar sphere decoder is derived and simulated for this system to reduce the computational complexity.

TABLE OF CONTENTS

Chapter **Page**

1 INTRODUCTION 1

1.1 Problem Statement 1

1.2 Research Contributions and Dissertation Organization 3

1.2.1 Dissertation Organization 3

1.2.2 Research Contributions 3

1.3 Notation 4

2 Blind Detection Design over Flat-Fading Channels: AF Two-Way Relay Network with Direct Link 6

2.1 Introduction 6

2.2 System Model and Transmission Scheme 8

2.3 Blind Unique Identification in Noise-Free Transmission 12

2.4 Blind Receivers 14

2.4.1 Receivers A1 and A2: GLRT and LSE receivers with SIC 15

2.4.2 Receivers B1 and B2: GLRT and LSE receivers without SIC 16

2.5 Performance of Derived Receivers 18

2.6 Constellation Selection 19

2.7 Simulation Results 20

2.8 Conclusion 26

3 Blind Detection Design over Frequency-Selective Fading Channels: AF Two-Way Relay Network without Direct Link 28

3.1 Introduction 28

3.2 System Model 29

TABLE OF CONTENTS (continued)

Chapter **Page**

3.3 Blind Receiver 35
3.3.1 LSE Receiver 35
3.3.2 Parallel Iterative Sphere Decoder 35
3.4 Simulation Results 42
3.5 Conclusion 45

4 Time-Reversal Space Time Block Coded Blind Detection Design over Frequency-Selective Fading Channels: Two Antenna AF Relay Network without Direct Link 47

4.1 Introduction 47
4.2 System Model 49
4.3 Blind Receiver 56
4.3.1 Sphere Decoding 56
4.3.2 Initialization of Channel Estimation 57
4.4 Simulation Results 61
4.5 Conclusion 63

5 Conclusion 64

REFERENCES 65

APPENDICES 73

A Proof for Theorem 1 74
B Proof of Receiver A1 77
C Proof for Receiver B1 78

LIST OF TABLES

Table **Page**

2.1 Signalling and Transmission Scheme for Flat-Fading Two-Way Relay System with Direct Link 11

2.2 Two-Point Constellation Selections 20

2.3 Power Allocations for Cost Functions 3, 4, and 5 24

3.1 Signalling and Transmission Scheme for Frequency-Selective Fading Two-Way Relay System without Direct Link 32

3.2 Number of Flops Algorithms for Various Operations 45

4.1 Signalling and Transmission Scheme for TR-STBC Frequency-Selective Fading Two-Way Relay System without Direct Link 52

LIST OF FIGURES

Figure **Page**

2.1 A Two-Way Relay Transmission System with Direct Links 10

2.2 SER at S_1 and Constellation Selections for Blind Receivers, $\delta_q^2 = \delta_g^2 = \delta_h^2 = 1$. . 22

2.3 Average SER, $\delta_q^2 = 1, \delta_g^2 = 5$, and $\delta_h^2 = 1$. 24

2.4 Worst SER, $\delta_q^2 = 1, \delta_g^2 = 5$, and $\delta_h^2 = 1$. 25

2.5 Average SER, $\delta_q^2 = 0.1, \delta_g^2 = 10$, and $\delta_h^2 = 1$. 25

2.6 Worst SER, $\delta_q^2 = 0.1, \delta_g^2 = 10$, and $\delta_h^2 = 1$. 26

2.7 SER at S_1 in Time Varying Channels. 27

3.1 A Frequency-Selective Two-Way Relay System without Direct Link 30

3.2 SER for LSE blind detector 43

3.3 SER for parallel iterative sphere decoder 44

3.4 Complexity comparison between two blind detectors 46

4.1 TR-STBC Two-Way Relay Transmission in Odd Time Slots 49

4.2 TR-STBC Two-Way Relay Transmission in Even Time Slots 50

4.3 Symbol error rate 62

4.4 Symbol error rate 62

CHAPTER 1

INTRODUCTION

A fundamental information-theoretic structure of general memoryless two-way relay channels was introduced in [1–3]. Two-way relaying has been adopted in more recent work as an extension of one-way relaying in order to improve spectral efficiency [4]. In two-way relay systems, source nodes exchange information with each other with the help of one or more relays. Source nodes transmit to the relays simultaneously, and the relays forward the signals received from the source nodes, unlike the traditional one-way relaying whereby only one source node transmits to the relay at one time, or the relays forward signals for only one source node. In this sense, two-way relaying, including bidirectional relaying [5–7] and analog network coding [8–11], have been reported on in the literature by other authors.

Two main operation strategies proposed for one-way relay communications, namely, amplify-and-forward (AF) and decode-and-forward (DF) [12, 13], have been applied to two-way relay systems. In an AF protocol, the relay nodes retransmit a scaled version of the signal received from the source nodes. In a DF protocol, relay nodes first decode the message, then re-encode it, and finally transmit it. Since an AF protocol does not need to decode the message, it is less complex than a DF protocol and also avoids error propagation due to decoding errors.

1.1 Problem Statement

However, AF relaying requires the receivers to have full channel state information (CSI) of all links in the system. Various channel estimation algorithms based on pilots or training have been discussed in flat-fading two-way relaying systems [14–16].

In [14], a two-stage weighted least squares channel estimation method is proposed for a two-way multiple-input multiple-output system. In [16], a maximum likelihood (ML) channel estimation is applied to the relay node, along with power loading techniques, by

maximizing the average effective signal-to-noise ratio and minimizing the mean square error of the channel estimation. These training-based estimation techniques must sacrifice some spectral efficiency to transmit the training symbols. Furthermore, if the fading coefficients of the channels vary rapidly, the coherence time of the channels may be too short for the training-based estimator to accurately estimate the channel coefficients. Some research has focused on blind and semi-blind channel estimations for two-way relay systems [17–19]. In [17], a relaxed blind ML channel estimator is developed for M-ary phase-shift keying (PSK) signals. In [18], a non-redundant linear precoding is applied at the source node for estimation on frequency selective channels with inter-symbol interference.In [19], a semi-blind channel estimation is proposed for constant-modulus constellations.

Except for the drawbacks mentioned above, these research works only focus on flat-fading environment. In radio propagation, the fading channels are not always flat. When the coherence bandwidth of channel is less than the signal bandwidth, different frequency components of signals experience different magnitude of fading, which is frequency-selective fading. Recently, blind estimations have been discussed for frequency selective fading two-way relay systems in which the frequency-selective CSI is assumed unavailable at the receivers [20–22].

Unfortunately, these estimators are typically associated with *phase or scalar* ambiguity, even in noise-free transmissions. As a result, a short training sequence needs to be applied to resolve the inherent phase or scalar ambiguity to ensure reliable recovery of the channel coefficients and transmitted signals.

Consequently, it is crucial to ensure unique identification of the channel coefficients and transmitted signals even in a noise-free environment, albeit all realistic systems are noisy. If the unique identifiability is not guaranteed in a noise-free environment, it is impossible for the blind detectors to reliably recover the transmitted symbols at the receivers in a noisy transmission, even at a high SNR.

1.2 Research Contributions and Dissertation Organization

Inspired by the results of signalling designs for unique identifications for flat and frequency selective channels in [23–25], my master thesis designed a blind detection scheme over flat-fading channels for a partial-connected two-way relay network, which is reported in [26]. Then, this dissertation develops and proposes the effective signalling and transmitting schemes to resolve the issue of ambiguity in the blind estimation and achieve the unique identifiability in a noise-free transmission for a single antenna fully-connected two-way relay system with flat-fading channels, a single antenna partial-connected two-way relay network with frequency-selective fading channels, respectively, and a multiple antenna partial-connected two-way relay network with frequency-selective fading channels.

1.2.1 Dissertation Organization

This dissertation consists of three main chapters as follows:

- Blind detection design over flat fading channels: one antenna AF two-way relay network with direct link
- Blind detection design over frequency-selective fading channels: one antenna AF two-way relay network without direct link
- Time-reversal space time block coded blind detection design over frequency-selective fading channels: mutiple antenna AF two-way relay network without direct link

The first item is included in Chapter 2, which is also reported in [27]. The Chapter 3 and 4 present the second and third item of work.

1.2.2 Research Contributions

The contributions of the first chapter of this research work are summarized as follows:

- An efficient signaling and transmission scheme using four PSK constellation sets is designed to uniquely identify the flat fading channel coefficients and transmitted symbols for a fully-connected two-way relay system in a noise-free environment.

- Blind receivers using the generalized likelihood ratio test (GLRT) are derived for the Gaussian noise and Rayleigh fading environment by maximizing the likelihood of the received signals conditioned on the fading channel coefficients and the transmitted signals. The diversity gain is justified for the derived GLRT receiver. Since the GLRT receiver needs knowledge of the noise variance for detection, the least square error (LSE) receivers are then studied to avoid the knowledge of the noise variance.

- A constellation selection scheme is applied to select a certain number of constellation points in each PSK set so that a uniform transmission bit rate is achieved at each time slot for the source nodes.

The contributions of the second chapter are as follows:

- An efficient signaling and transmission scheme using four PSK constellation sets is designed to uniquely identify the frequency-selective channel coefficients and transmitted symbols for a partial-connected two-way relay system in a noise-free environment.

- In the Gaussian noise and Rayleigh fading environment, the complexity of detection implementation is highly decreased by applying the joint sphere decoder derived.

The contributions of the third chapter are summarized as follows:

- A time-reversal space time block coded (TR-STBC) blind detection scheme is developed for two antenna equipped two-way relay system over frequency-selective fading channels.

- Simulation results evaluate the diversity gain benefitted from the TR-STBC scheme.

1.3 Notation

The transpose and Hermitian of vector $\mathbf{a}$ and matrix $\mathbf{A}$ are denoted by $\mathbf{a}^{\mathrm{T}}, \mathbf{A}^{\mathrm{T}}$ and $\mathbf{a}^{\mathrm{H}}, \mathbf{A}^{\mathrm{H}}$, respectively. LU($\mathbf{A}$) denotes the LU decomposition of matrix $\mathbf{A}$. The notation $\mathbb{E}[\cdot]$ is the expectation operator and log is the natural logarithm. The notation $\mathbf{n} \sim \mathcal{CN}(\mathbf{0}, \mathbf{\Sigma})$

indicates that vector $\mathbf{n}$ is a circular Gaussian vector with zero mean and covariance matrix $\mathbf{\Sigma}$. Two positive integers m and n are coprime, if the greatest common divisor is 1. Notation $a \equiv b(\mathrm{mod}\ c)$ denotes that $a - b$ is multiple of c. $\varphi(p)$ is the Euler function of integer p, i.e., the number of all positive integers that do not exceed p and are coprime to p. The variable $\angle(x)$is the angle of x. $\mathbb{Z}$ denotes the ring of rational integers. $\mathbb{Q}$ denotes the field of rational numbers; $\mathbb{C}$ denotes the field of complex numbers. $\zeta_\rho = \exp\left(\frac{j2\pi}{\rho}\right)$, $\mathbb{Z}[\zeta_\rho]$ denotes the cyclotomic ring generated by $\mathbb{Z}$ and the cyclotomic number ζ_ρ, and $\mathbb{Q}[\zeta_\rho]$ denotes the field generated by $\mathbb{Q}$ and ζ_ρ.

CHAPTER 2

Blind Detection Design over Flat-Fading Channels: AF Two-Way Relay Network with Direct Link

2.1 Introduction

Two-way or bidirectional relaying has been considered to improve spectral efficiency for relay systems, in which relay nodes forward signals received from all source nodes simultaneously, instead of from only one source node as in conventional one-way relay systems [4–8]. Popular relaying strategies applied to two-way relay systems include amplify-and-forward (AF) and decode-and-forward (DF) relaying [12, 13, 28–31]. In an AF protocol, the relay node simply transmits a scaled sum of the signals received from the source nodes. Since the AF protocol does not need to decode the message, it avoids error propagation caused by decoding errors and has a lower complexity than the DF counterpart. However, for detection purposes, AF relaying requires full channel state information of all links. While various channel estimations based on pilots or training have been discussed for two-way relay systems [14–16], these estimators require extra system bandwidth and overhead to transmit the training symbols and share the channel information among nodes in the systems [32, 33]. Recently, blind and semi-blind estimations have been studied for time-varying two-way relay systems in which the channel information is assumed unavailable at the receivers [17–19]. Unfortunately, these estimators are typically associated with a *phase or scaler* ambiguity, even in noise-free transmissions. As a result, a short training sequence is required to resolve the inherent phase or scaler ambiguity. Unique identification of the channel coefficients and transmitted signals in noise-free transmissions is essential for blind detectors to reliably recover the channel coefficients and transmitted signals in noisy transmissions.

While we proposed an effective signalling and transmission scheme to resolve the issue of ambiguity in the blind estimation for a two-way channel in [26], the direct link between the source nodes is assumed to be unavailable. The maximum diversity gain is one. In this sequel,

a two-way relay system is considered in which the direct link is assumed available. An effective signalling and transmission scheme is proposed for unique identification of the channel coefficients and transmitted symbols in noise-free transmissions. Then blind receivers with full diversity are derived for Rayleigh fading channels and Gaussian noise. A more realistic channel fading situation is assumed, whereby the channel coefficient between two nodes and that in the reverse link to the same node may undergo different fading. Such channels are referred as non-reciprocal; these channels are also referred to as *asymmetric* [34–37]. The fundamental limits for both reciprocal and non-reciprocal channels between the relay and source nodes are analyzed for DF relaying using the diversity multiplexing tradeoff framework, assuming there is perfect knowledge of channel state information at the receivers [34]. The error performance is studied for an asymmetric Nakagami-m two-way relay channel with an AF protocol [35]. A relay assignment is considered for asymmetric two-way relay systems [36]. The system outage behavior was studied for one-way asymmetric channels, whereby the source-relay, source-destination, and relay-destination channels are characterized with combinations of Rayleigh and Rician fading [37]. Studies on blind detection for non-reciprocal or asymmetric two-way relay channels seems sparse in the literature.

The contribution of this chapter is as follows: an effective signalling and transmission scheme is proposed to blindly and uniquely identify the transmitted symbols and channel coefficients in noise-free transmissions using four pairwise coprime phase-shift keying (PSK) constellations; full diversity blind receivers are derived for Rayleigh fading channels with Gaussian noise, using generalized likelihood ratio test (GLRT) and least square error (LSE) criterions; constellation schemes are provided to achieve a uniform bit rate for the system; and power allocation schemes are discussed to improve the average of the error probabilities of the source nodes.

The proposed transmission scheme is carried out block by block. A one-block transmission is sufficient for the source nodes to achieve the unique identifiability of the transmitted signals and channel coefficients in noise-free transmissions. If the coherent time of the

channels is long enough to allow the channels to remain static in more than one block, then the blind detection can be performed using multiple blocks (at a higher computational cost). The performance (of the detection) using multiple blocks is often improved over that using one block. In deriving the blind receivers, the GLRT receiver is obtained by maximizing the likelihood of the received signals conditioned on the fading channel coefficients and the transmitted signals. Since the GLRT receivers require the knowledge of noise variance for detection, to avoid this requirement, the LSE receivers are then studied. Because the symbols at a source node are known to itself, the self-interference terms related to those symbols can be removed before applying the GLRT or LSE detection. An interesting observation from our simulation results is that, regardless of the self-interference cancelations, the performance of GLRT and LSE receivers is almost identical for the system considered. Therefore, the LSE receivers can be considered replacements for the GLRT receivers, with little sacrifice in performance, easier implementation, and avoidance of the noise power knowledge requirement.

The remainder of this chapter is organized as follows: Section 2.2 presents the system model and describes the signaling and transmission strategy with the designed PSK symbols. Section 2.3 proves that the proposed scheme achieves unique identification of the transmitted symbols and channel coefficients in a noise-free transmission. Section 2.4 derives the GLRT and LSE receivers for the Rayleigh fading channels with Gaussian noise. Section 2.5 justifies that the derived receivers achieve full diversity. Section 2.6 describes the constellation selection schemes for the source nodes to achieve a uniform transmission bit rate. The power loading schemes and simulation results are provided in Section 2.7. Finally, Section 2.8 concludes the chapter.

2.2 System Model and Transmission Scheme

Fig. 2.1 illustrates a two-way system in which two source nodes S_1 and S_2 exchange information with each other with the help of a relay node R. We assume that the channels in the system are nonreciprocal, i.e., the channel coefficient from one node to another is not

identical to that in the reverse channel back to the same node. For instance, the channel coefficient from source node S_1 to the relay and that from the relay to S_1 is not identical. The channel coefficients from S_1 to S_2 and from S_2 to S_1 are denoted, respectively, by q_1 and q_2. The channel coefficients from S_1 to R and from R to S_1 are denoted, respectively, by h_1 and h_2. The channel coefficients from S_2 to R and from R to S_2 are denoted, respectively, by g_1 and g_2. These channel coefficients are independent zero-mean CSCG random variables, in particular, $q_i \sim \mathcal{CN}(0, \delta_q^2), h_i \sim \mathcal{CN}(0, \delta_h^2), g_i \sim \mathcal{CN}(0, \delta_g^2), i = 1, 2$. The channel coefficients are not known at either the source nodes or the relay node. Each source node recovers symbols from the other source node based on prior knowledge of its own transmitted symbols and signals from the direct and relaying links. The system operates in a half duplex mode in which the transmissions and receptions are not carried out simultaneously. Therefore, two time slots are required for S_1 to transmit one symbol to S_2, and vice versa. The transmissions are carried out in blocks. The assumptions on the block (quasi-static) Rayleigh fading channels [38, 39] are adopted for the theoretic necessity of the diversity analysis for our transmission scheme. The channel coefficients do not change within one block of observation; after that, they change to new independent values according to Rayleigh fading and are fixed in the next block, and so on.[1]

To develop the blind receivers, a signaling and transmission scheme using PSK constellations is first developed to ensure the unique identification of channel coefficients and transmitted symbols in a noise-free transmission. If this unique identifiability is not guaranteed, it is impossible for the blind receivers to reliably recover the transmitted signals in noisy transmissions. We are interested with a transmission scheme with a shortest possible block length and a highest possible symbol rate. A shorter block length helps reduce complexity in implementation of the blind receivers.

For the half-duplex two-way system in Fig. 2.1, we propose a transmission scheme in

[1]However, since the behaviors of time-varying channels are often caused by the movement of the transmitter and the receiver or environmental scatters, it would be more practical to assume that the channel coefficients change gradually within one block as well, instead of remaining unchanged within one block and making sudden changes in the next block.

blocks in nine time-slots length using four PSK constellations. Three symbols are exchanged between the source nodes in each block. The symbol rate is therefore one-third symbols per time slot for each source node (a maximum symbol rate for the half-duplex system in Fig. 2.1 is half symbol per time slot for each source node). As shown in Theorem 1, one block transmission is sufficient for the source nodes to achieve unique identification of the channel coefficients and transmitted signals in a noise-free transmission.

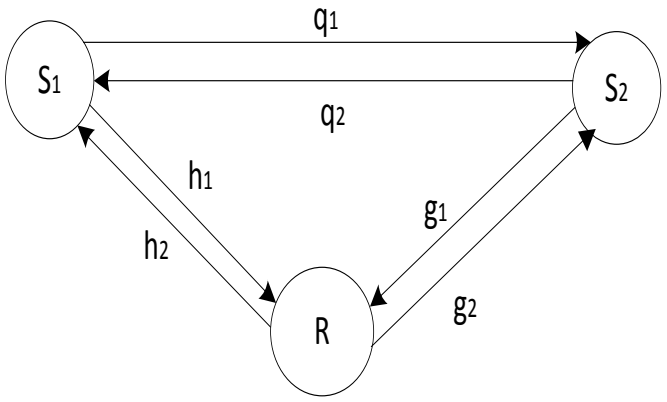

Figure 2.1: A Two-Way Relay Transmission System with Direct Links

If the channel coherence time is long enough such that the channels remain unchanged in more than one blocks, the proposed transmission and detection schemes can also be applied. Simulation results indicate that the performance of the blind receivers is further improved in multiple block detections. In the chapter, we illustrate the transmission scheme and blind receivers using one-block transmissions.

Let $p_i, i = 1, 2, 3, 4$ denote pairwise co-prime positive integers, and constellation set $\mathcal{S}_1$ collect all p_1-PSK symbols except symbol "0", $\mathcal{S}_1 = \{\exp(j2\pi m_1/p_1), m_1 = 1, \cdots, p_1\}$. Let the set $\mathcal{S}_i, i = 2, 3, 4$, collect p_i-PSK symbols, $\mathcal{S}_i = \{\exp(j2\pi m_i/p_i), m_i = 0, 1, \cdots, p_i\}$. Denote the transmitted symbols from S_1 and S_2, respectively, by x_k and $y_k, k = 1, 2, \cdots$. The

proposed signalling and transmission schemes are shown in Table 4.1. While the transmission is carried out in a block of nine time-slot lengths, transmissions in time slots $4-6$ and $7-9$ are carried out in a similar fashion to those in time slots $1-3$.

Table 2.1: Signalling and Transmission Scheme for Flat-Fading Two-Way Relay System with Direct Link

Time Slot	Transmiting/Receiving	Symbols and Constellations
1	$\mathrm{S}_1 \xrightarrow{x_1} \mathrm{R}, \mathrm{S}_2$	$x_1 \in \mathcal{S}_1$
2	$\mathrm{S}_2 \xrightarrow{y_1} \mathrm{R}, \mathrm{S}_1$	$y_1 \in \mathcal{S}_2$
3	$\mathrm{R} \xrightarrow{x_1, y_1} \mathrm{S}_1, \mathrm{S}_2$	
4	$\mathrm{S}_1 \xrightarrow{x_2} \mathrm{R}, \mathrm{S}_2$	$x_2 \in \mathcal{S}_2$
5	$\mathrm{S}_2 \xrightarrow{-y_2} \mathrm{R}, \mathrm{S}_1$	$y_2 \in \mathcal{S}_1$
6	$\mathrm{R} \xrightarrow{x_2, y_2} \mathrm{S}_1, \mathrm{S}_2$	
7	$\mathrm{S}_1 \xrightarrow{x_3} \mathrm{R}, \mathrm{S}_2$	$x_3 \in \mathcal{S}_3$
8	$\mathrm{S}_2 \xrightarrow{y_3} \mathrm{R}, \mathrm{S}_1$	$y_3 \in \mathcal{S}_4$
9	$\mathrm{R} \xrightarrow{x_3, y_3} \mathrm{S}_1, \mathrm{S}_2$	

In the first time slot, S_1 transmits x_1, a p_1-PSK symbols in set $\mathcal{S}_1$, to S_2 and R. The received signal at S_2 is $\zeta(1) = \sqrt{P_1} q_1 x_1 + u(1)$, and the received signal at the relay is $r_{\mathrm{R}}(1) = \sqrt{P_1} h_1 x_1 + \nu(1)$, where P_1 is the transmitting power at S_1, $u(i) \sim \mathcal{CN}(0, \sigma^2)$, and $\nu(i) \sim \mathcal{CN}(0, \sigma^2), i = 1, 2, \cdots$, are the independent zero-mean CSCG noise terms at S_2 and the relay node in the i-th time slot. In the second time slot, S_2 transmits y_1, a p_2-PSK symbols in set $\mathcal{S}_2$, to S_1 and R. The received signal at S_1 is $r(2) = \sqrt{P_2} q_2 y_1 + v(2)$, where P_2 is the transmitting power at S_2, and $v(i) \sim \mathcal{CN}(0, \sigma^2), i = 1, 2, \cdots$, is the independent zero mean CSCG noise terms at S_1 in the i-th time slot. The received signal at the relay is $r_{\mathrm{R}}(2) = \sqrt{P_2} g_1 y_1 + \nu(2)$. In the third time slot, the relay node R transmits $A\big(r_{\mathrm{R}}(1) + r_{\mathrm{R}}(2)\big)$ to both source nodes S_1 and S_2, where $A = \sqrt{P_r / (P_1 \delta_h^2 + P_2 \delta_g^2 + 2\sigma^2)}$ is the amplification coefficient at the relay node to ensure that the average power in forwarding

the received signals does not exceed the available power, and P_r is the available power at the relay. The received signals at S_1 and S_2 in the third time slot are, respectively, $r(3) = Ah_2\big(r_{\rm R}(1) + r_{\rm R}(2)\big) + v(3) = Ah_2\big(\sqrt{P_1}h_1x_1 + \nu(1) + \sqrt{P_2}g_1y_1 + \nu(2)\big) + v(3)$, and $\zeta(3) = Ag_2\big(r_{\rm R}(1) + r_{\rm R}(2)\big) + u(3) = Ag_2\big(\sqrt{P_1}h_1x_1 + \nu(1) + \sqrt{P_2}g_1y_1 + \nu(2)\big) + u(3)$. In time slots $4-6$ and $7-9$, another two pair of symbols, $x_2 \in \mathcal{S}_2$, $y_2 \in \mathcal{S}_1$, and $x_3 \in \mathcal{S}_3$, $y_3 \in \mathcal{S}_4$, are transmitted, following the same fashion as in time slots $1-3$. The transmitted symbols are specified as below:

$$x_1{=}\exp\Big(\frac{j2\pi\ell_1}{p_1}\Big), y_2{=}\exp\Big(\frac{j2\pi k_2}{p_1}\Big), \ell_1,k_2{\in}\{1,\cdots,p_1-1\} \tag{2.1}$$

$$x_2{=}\exp\Big(\frac{j2\pi\ell_2}{p_2}\Big), y_1{=}\exp\Big(\frac{j2\pi k_1}{p_2}\Big), \ell_2,k_1{\in}\{0,1,\cdots,p_2{-}1\} \tag{2.2}$$

$$x_3 = \exp\Big(\frac{j2\pi\ell_3}{p_3}\Big), \ell_3 \in \{0,1,2,\cdots,p_3-1\} \tag{2.3}$$

$$y_3 = \exp\Big(\frac{j2\pi k_3}{p_4}\Big), k_3 \in \{0,1,2,\cdots,p_4-1\}. \tag{2.4}$$

Let $\mathbf{h} = \begin{pmatrix} \sqrt{P_2}q_2 & A\sqrt{P_2}g_1h_2 \end{pmatrix}^T$ and $\mathbf{w} = \begin{pmatrix} 0 & A\sqrt{P_1}h_1h_2 \end{pmatrix}^T$. The received signals at S_1 are written as follows (the signals at S_2 admit a similar form):

$$\mathbf{r}_1 = \begin{pmatrix} r(2) & r(3) \end{pmatrix}^T = y_1\mathbf{h} + x_1\mathbf{w} + \mathbf{n}_1 \tag{2.5}$$

$$\mathbf{r}_2 = \begin{pmatrix} r(5) & r(6) \end{pmatrix}^T = -y_2\mathbf{h} + x_2\mathbf{w} + \mathbf{n}_2 \tag{2.6}$$

$$\mathbf{r}_3 = \begin{pmatrix} r(8) & r(9) \end{pmatrix}^T = y_3\mathbf{h} + x_3\mathbf{w} + \mathbf{n}_3 \tag{2.7}$$

where $\mathbf{r}_1, \mathbf{r}_2$, and $\mathbf{r}_3$ are, respectively, the received vectors at S_1 in time slots $1{-}3$, $4{-}6$, and $7{-}9$; and $\mathbf{n}_1, \mathbf{n}_2$, and $\mathbf{n}_3$ are, respectively, the noise vectors, $\mathbf{n}_1 = \begin{pmatrix} v(2) & Ah_2\big(\nu(1)+\nu(2)\big) + v(3) \end{pmatrix}^T$, $\mathbf{n}_2 = \begin{pmatrix} v(5) & Ah_2\big(\nu(4)+\nu(5)\big) + v(6) \end{pmatrix}^T$, and $\mathbf{n}_3 = \begin{pmatrix} v(8) & Ah_2\big(\nu(7)+\nu(8)\big) + v(9) \end{pmatrix}^T$.

2.3 Blind Unique Identification in Noise-Free Transmission

Since the unique identifiability of the transmitted symbols and channel coefficients in noise-free transmissions is critical for blind detection at the receivers, we justify that the transmission scheme described in Section 2.2 possesses this very desirable property. We use the received signals at S_1 for illustration, while similar results hold for S_2. Setting the noise

terms in (2.5) to (2.7) to zero, the received signal at S_1 in noise-free transmissions is

$$\tilde{\mathbf{r}}_1 = \big(\tilde{r}(2)\ \tilde{r}(3)\big)^T = y_1\mathbf{h} + x_1\mathbf{w} \tag{2.8}$$

$$\tilde{\mathbf{r}}_2 = \big(\tilde{r}(5)\ \tilde{r}(6)\big)^T = -y_2\mathbf{h} + x_2\mathbf{w} \tag{2.9}$$

$$\tilde{\mathbf{r}}_3 = \big(\tilde{r}(8)\ \tilde{r}(9)\big)^T = y_3\mathbf{h} + x_3\mathbf{w} \tag{2.10}$$

where $\tilde{r}(\cdot)$ designates the value of $r(\cdot)$ in the noise-free environment. Note that symbols $x_i, i = 1, 2, 3$, are known to S_1. The self-interference terms related to these symbols can be eliminated by linear combinations: $x_2\tilde{\mathbf{r}}_1 - x_1\tilde{\mathbf{r}}_2$, $x_2\tilde{\mathbf{r}}_3 - x_3\tilde{\mathbf{r}}_2$, and $x_3\tilde{\mathbf{r}}_1 - x_1\tilde{\mathbf{r}}_3$. For notation brevity, let vector $\tilde{\mathbf{z}} = (\tilde{z}_1\ \tilde{z}_2\ \tilde{z}_3\ \tilde{z}_4\ \tilde{z}_5\ \tilde{z}_6)^T$ collect the resulting linear combinations. We then have

$$\begin{pmatrix} \tilde{z}_1 & \tilde{z}_2 \end{pmatrix}^T = x_2\tilde{\mathbf{r}}_1 - x_1\tilde{\mathbf{r}}_2 = (x_2y_1 + x_1y_2)\mathbf{h} \tag{2.11}$$

$$\begin{pmatrix} \tilde{z}_3 & \tilde{z}_4 \end{pmatrix}^T = x_2\tilde{\mathbf{r}}_3 - x_3\tilde{\mathbf{r}}_2 = (x_2y_3 + x_3y_2)\mathbf{h} \tag{2.12}$$

$$\begin{pmatrix} \tilde{z}_5 & \tilde{z}_6 \end{pmatrix}^T = x_3\tilde{\mathbf{r}}_1 - x_1\tilde{\mathbf{r}}_3 = (x_3y_1 - x_1y_3)\mathbf{h}. \tag{2.13}$$

The transmitted symbols from S_2 and the corresponding channel gains can be uniquely identified at S_1 in noise-free transmissions. The solutions are given in Theorem 1.

Theorem 1 *For a noise-free two-way relay system described in* (2.8), (2.9), *and* (2.10), *the transmitted symbols from* S_2, y_1, y_2, *and* y_3, *and the entries in channel vectors* $\mathbf{h}$ *and* $\mathbf{w}$ *can be uniquely identified at* S_1 *for a given non-zero received vector* $\tilde{\mathbf{z}} \neq \mathbf{0}$. *The solutions are given by*

$$y_1 = \exp\Big(\frac{j2\pi k_1}{p_2}\Big), y_2 = \exp\Big(\frac{j2\pi k_2}{p_1}\Big), y_3 = \exp\Big(\frac{j2\pi k_3}{p_4}\Big), \tag{2.14}$$

$$\mathbf{h} = \begin{pmatrix} \tilde{z}_1 & \tilde{z}_2 \end{pmatrix}^T / (x_2y_1 + x_1y_2), \mathbf{w} = (\tilde{\mathbf{r}}_1 - y_1\mathbf{h})/x_1, \tag{2.15}$$

where

$$k_1 \equiv (\vartheta P/\pi)(P/p_2)^{\varphi(p_2)-1} mod\ p_2, P = p_1p_2p_3p_4,$$
$$2\pi > \vartheta \geq 0, \vartheta = \begin{cases} \angle(\tilde{z}_1/\tilde{z}_3), & for\ \tilde{z}_1 \neq 0, \\ \angle(\tilde{z}_2/\tilde{z}_4), & for\ \tilde{z}_1 = 0, \end{cases}$$
$$k_2 \equiv (\phi P/\pi)(P/p_1)^{\varphi(p_1)-1} mod\ p_1, \phi = \psi + \pi/2,$$
$$2\pi > \psi \geq 0, \psi = \begin{cases} \angle(\tilde{z}_1/\tilde{z}_5), & for\ \tilde{z}_1 \neq 0, \\ \angle(\tilde{z}_2/\tilde{z}_6), & for\ \tilde{z}_1 = 0, \end{cases}$$
$$k_3 \equiv (\vartheta P/\pi)(P/p_4)^{\varphi(p_4)-1} mod\ p_4. \qquad \blacksquare$$

2.4 Blind Receivers

In practical systems, the symbols transmitted from S_2 need to be detected at S_1 subject to fading channels and background noise, and vice versa. For brevity, we derive the blind receivers for S_1, while the same principles are applicable to the blind detection at S_2. Since the symbols transmitted from S_1 are known to itself, the source node has two options: (1) apply self-interference cancelation (SIC) by pre-processing the received signals in one block to eliminate the components related to the known symbols, and then apply the GLRT or LSE detection rules; or (2) apply the GLRT or LSE detection rules directly without the SIC. The latter provides better performance with slightly higher computational cost. The GLRT receiver is obtained by maximizing the likelihood of received signals conditioned on the fading channel coefficients and transmitted signals, and it requires knowledge of the noise variance for detection. On the other hand, the LSE receiver does not need the information of noise variance. Depending on whether SIC is applied or not, we propose four blind receivers: Receivers A1 and A2 (the GLRT and LSE receivers with SIC), and Receivers B1 and B2 (the GLRT and LSE receivers without SIC). While our derivations show that the GLRT and LSE receivers with SIC (or without SIC) have different detection schemes, the simulation results indicate that the performance of these schemes is almost identical, especially at higher SNRs. This is an interesting observation. The GLRT receivers can be replaced by the LSE receivers

for ease of implementation and to avoid the knowledge of noise variance in the blind detection for the two-way relay system.

2.4.1 Receivers A1 and A2: GLRT and LSE receivers with SIC

These two receivers perform SIC first, then blind detections using GLRT and LSE criterions.

Receiver A1: GLRT receiver with SIC. Performing the following linear combinations in (2.5), (2.6), and (2.7): $x_2\mathbf{r}_1-x_1\mathbf{r}_2$ and $x_2\mathbf{r}_3-x_3\mathbf{r}_2$, and collecting the resulting components into vector $\mathbf{z}=(z_1\ \ z_2\ \ z_3\ \ z_4)^T$, we have $\mathbf{z}=\mathbf{C}_{\rm A}\mathbf{h}+\mathbf{n}_{\rm A}$ where $\mathbf{C}_{\rm A}$ is a 4×2 signal matrix, $\mathbf{C}_{\rm A}=\begin{pmatrix} \xi_1\mathbf{I}_2 & \xi_2\mathbf{I}_2 \end{pmatrix}^T$, with $\xi_1=(y_1x_2+x_1y_2), \xi_2=(y_3x_2+x_3y_2)$, $\mathbf{n}_{\rm A}$ is the noise vector with $n_{\rm A}(1)=x_2v(2)-x_1v(5)$, $n_{\rm A}(2)=Ah_2x_2\big(\nu(1)+\nu(2)\big)+x_2v(3)-Ah_2x_1\big(\nu(4)+\nu(5)\big)-x_2v(6)$, $n_{\rm A}(3)=x_2v(8)-x_3v(5)$, $n_{\rm A}(4)=Ah_2x_2\big(\nu(7)+\nu(8)\big)+x_2v(9)-Ah_2x_3\big(\nu(4)+\nu(5)\big)-x_3v(6)$. Since $\mathbf{n}_{\rm A}$ is zero mean CSCG with covariance matrix $\mathrm{diag}\big(2\sigma^2, 2\sigma^2(1+2A^2|h_2|^2), 2\sigma^2, 2\sigma^2(1+2A^2|h_2|^2)\big)$, the log-likelihood function of $\mathbf{z}$ conditional on the channel coefficients, the transmitted signals $\mathbf{x}=(x_1\ \ x_2\ \ x_3)^T$, and $\mathbf{y}=(y_1\ \ -y_2\ \ y_3)^T$ is

$$\begin{aligned}
&\log\big(f(\mathbf{z}|h_1,h_2,g_1,q_2,\mathbf{x},\mathbf{y})\big)\\
&=-\log\big(16\pi^4\sigma^8(1+2A^2|h_2|^2)^2\big)-(\mathbf{z}-\mathbf{C}_{\rm A}\mathbf{h})^H\mathbf{\Sigma}_{\rm A}^{-1}(\mathbf{z}-\mathbf{C}_{\rm A}\mathbf{h})\\
&=-\log\big(16\pi^4\sigma^8(1+2A^2|h_2|^2)^2\big)-\frac{1}{2\sigma^2}\big(||\mathbf{z}_o-\sqrt{P_2}q_2\mathbf{v}||^2\big)\\
&\quad-\frac{1}{2\sigma^2(1+2A^2|h_2|^2)}\big(||\mathbf{z}_e-Ah_2g_1\sqrt{P_2}\mathbf{v}||^2\big) \qquad (2.16)
\end{aligned}$$

where $\mathbf{z}_o=(z_1\ z_3)^T, \mathbf{z}_e=(z_2\ z_4)^T, \mathbf{v}=(\xi_1\ \xi_2)^T$. Following the steps in Appendix B, Receiver A1 is obtained as

$$\hat{\mathbf{y}}_{\rm A1}=\arg\min_{\mathcal{Y}_{\rm A},\overline{\mathcal{Y}}_{\rm A}}\Big\{\min_{\mathbf{y}\in\mathcal{Y}_{\rm A}}\Big(\frac{\kappa}{2\sigma^2}+2\log\big(\frac{\omega}{4\sigma^2}\big)+2\Big), \min_{\mathbf{y}\in\overline{\mathcal{Y}}_{\rm A}}\Big(\frac{\kappa+\omega}{2\sigma^2}\Big)\Big\} \qquad (2.17)$$

where $\omega=\mathbf{z}_e^H\mathbf{z}_e-\mathbf{z}_e^H\mathbf{v}\mathbf{v}^H\mathbf{z}_e/(\mathbf{v}^H\mathbf{v})$, $\kappa=\mathbf{z}_{\rm o}^H\mathbf{z}_{\rm o}-\mathbf{z}_{\rm o}^H\mathbf{v}\mathbf{v}^H\mathbf{z}_{\rm o}/(\mathbf{v}^H\mathbf{v})$, $\mathcal{Y}_{\rm A}=\{\mathbf{y}:\omega>4\sigma^2\}$, and $\overline{\mathcal{Y}}_{\rm A}=\{\mathbf{y}:\omega\le 4\sigma^2\}$. Note that vector $\mathbf{x}$ is known to node $\rm S_1$. The optimization problem in (2.17) is solved over all possible values of $\mathbf{y}$ in $\mathcal{Y}_{\rm A}$ and $\overline{\mathcal{Y}}_{\rm A}$. When the constellation sizes of PSKs are small, a numerical exhaustive search can be used in finding the solution

to Receiver A1. However, the computational complexity increases dramatically for larger constellation sizes or longer blocks. More efficient algorithms for finding the solutions, instead of exhaustive search, need to be considered.

Receiver A2: LSE receiver with SIC. The LSE receiver is obtained by minimizing $(\mathbf{z}-\mathbf{C}_{\rm A}\mathbf{h})^H(\mathbf{z}-\mathbf{C}_{\rm A}\mathbf{h})$ over the unknown channels. The solution is given by

$$\begin{aligned}\hat{\mathbf{y}}_{\rm A2} &= \arg\max_{\mathbf{y}} \left(\mathbf{z}_{\rm o}^H\mathbf{v}\mathbf{v}^H\mathbf{z}_{\rm o}/(\mathbf{v}^H\mathbf{v}) + \mathbf{z}_e^H\mathbf{v}\mathbf{v}^H\mathbf{z}_e/(\mathbf{v}^H\mathbf{v})\right) \\ &= \arg\max_{\mathbf{y}} \left(\mathbf{z}_{\rm A2}^H\mathbf{S}_{\rm A2}(\mathbf{S}_{\rm A2}^H\mathbf{S}_{\rm A2})^{-1}\mathbf{S}_{\rm A2}^H\mathbf{z}_{\rm A2}\right) \end{aligned} \tag{2.18}$$

where $\mathbf{z}_{\rm A2} = (z_1\ z_3\ z_2\ z_4)^T$, and $\mathbf{S}_{\rm A2}$ is a 4×2 signal matrix given by $\mathbf{S}_{\rm A2} = \begin{pmatrix} \mathbf{v} & \mathbf{0} \\ \mathbf{0} & \mathbf{v} \end{pmatrix}$. The optimization problem in (2.18) is solved over all possible values of $\mathbf{y}$.

2.4.2 Receivers B1 and B2: GLRT and LSE receivers without SIC

In Receivers A1 and A2, the noise variance is doubled as a result of the linear combinations of the received signals in order to cancel the self-interference terms. Therefore the performance of the receivers is degraded. In this section, we establish blind receivers without self-interference cancelation to avoid doubling the noise variance.

Receiver B1: GLRT receiver without SIC. Stacking (2.5), (2.6), and (2.7) into one vector, we have

$$\mathbf{r} = \mathbf{Y}_{\rm B}\mathbf{h} + \mathbf{X}_{\rm B}\mathbf{w} + \mathbf{n}_{\rm B} \tag{2.19}$$

where $\mathbf{r} = \begin{pmatrix} r(2) & r(3) & r(5) & r(6) & r(8) & r(9) \end{pmatrix}^T$,

$$\mathbf{Y}_{\rm B} = \begin{pmatrix} y_1\mathbf{I}_2 & -y_2\mathbf{I}_2 & y_3\mathbf{I}_2 \end{pmatrix}^T, \mathbf{X}_{\rm B} = \begin{pmatrix} x_1\mathbf{I}_2 & x_2\mathbf{I}_2 & x_3\mathbf{I}_2 \end{pmatrix}^T,$$

$$\mathbf{n}_{\rm B} = \begin{pmatrix} v(2) \\ Ah_2\big(\nu(1)+\nu(2)\big)+v(3) \\ v(5) \\ Ah_2\big(\nu(4)+\nu(5)\big)+v(6) \\ v(8) \\ Ah_2\big(\nu(7)+\nu(8)\big)+v(9) \end{pmatrix}.$$

The distribution of the received vector $\mathbf{r}$ given the channel gains h_1, h_2, g_1, q_2, and transmitted vectors is Gaussian with covariance matrix $\mathbf{\Sigma}_{\rm B} = \text{diag}\big(\sigma^2, \sigma^2(1+2A^2|h_2|^2), \sigma^2, \sigma^2(1+2A^2|h_2|^2), \sigma^2, \sigma^2(1+2A^2|h_2|^2)\big)$. The log-likelihood function is expressed as

$$\begin{aligned}\log\big(f(\mathbf{r}|h_1,h_2,g_1,q_2,\mathbf{x},\mathbf{y})\big) &= -\log\big(\pi^6\sigma^{12}(1+2A^2|h_2|^2)^3\big) \\ &\quad - (\mathbf{r}-\mathbf{Y}_{\rm B}\mathbf{h}-\mathbf{X}_{\rm B}\mathbf{w})^H\mathbf{\Sigma}_{\rm B}^{-1}(\mathbf{r}-\mathbf{Y}_{\rm B}\mathbf{h}-\mathbf{X}_{\rm B}\mathbf{w}) \\ &= -\log\left(\pi^6\sigma^{12}(1+2A^2|h_2|^2)^3\right) - \frac{||\mathbf{r}_{\rm o}-\sqrt{P_2}q_2\mathbf{y}||^2}{\sigma^2} \\ &\quad - \frac{||\mathbf{r}_{\rm e}-Ah_2g_1\sqrt{P_2}\mathbf{y}-Ah_2h_1\sqrt{P_1}\mathbf{x})||^2}{\sigma^2(1+2A^2|h_2|^2)} \end{aligned} \tag{2.20}$$

where $\mathbf{r}_{\rm o} = \big(r(2)\ r(5)\ r(8)\big)^T$, and $\mathbf{r}_{\rm e} = \big(r(3)\ r(6)\ r(9)\big)^T$. Receiver B1 is obtained by maximizing (2.20) as shown in Appendix C. The solution is given by

$$\hat{\mathbf{y}}_{\rm B1} = \arg\min_{\mathcal{Y}_{\rm B},\overline{\mathcal{Y}}_{\rm B}}\left\{\min_{\mathbf{y}\in\mathcal{Y}_{\rm B}}\Big(\frac{\lambda}{\sigma^2}+3\log\frac{\varpi}{3\sigma^2}+3\Big), \min_{\mathbf{y}\in\overline{\mathcal{Y}}_{\rm B}}\Big(\frac{\lambda+\varpi}{\sigma^2}\Big)\right\} \tag{2.21}$$

where $\lambda = ||\mathbf{r}_{\rm o}||^2 - \frac{1}{3}\mathbf{r}_{\rm o}^H\mathbf{y}\mathbf{y}^H\mathbf{r}_{\rm o}$, $\mathbf{B} = (\mathbf{I}_3 - \frac{1}{3}\mathbf{y}\mathbf{y}^H) \succeq \mathbf{0}$, $\varpi = \left(\mathbf{r}_{\rm e}^H\mathbf{B}\mathbf{r}_{\rm e} - \frac{\mathbf{r}_{\rm e}^H\mathbf{B}\mathbf{x}\mathbf{x}^H\mathbf{B}\mathbf{r}_{\rm e}}{\mathbf{x}^H\mathbf{B}\mathbf{x}}\right)$, $\mathcal{Y}_{\rm B} = \{\mathbf{y} : \varpi > 3\sigma^2\}$, and $\overline{\mathcal{Y}}_{\rm B} = \{\mathbf{y} : \varpi \le 3\sigma^2\}$. The optimization problem in (2.21) is solved for all possible values of $\mathbf{y}$ in $\mathcal{Y}_{\rm B}$ and $\overline{\mathcal{Y}}_{\rm B}$.

Receiver B2: LSE receiver without SIC: The LSE receiver without self-interference cancelation is obtained by minimizing $(\mathbf{r}-\mathbf{Y}_{\rm B}\mathbf{h}-\mathbf{X}_{\rm B}\mathbf{w})^H(\mathbf{r}-\mathbf{Y}_{\rm B}\mathbf{h}-\mathbf{X}_{\rm B}\mathbf{w})$ over the unknown channels. Receiver B2 is given by

$$\hat{\mathbf{y}}_{\rm B2} = \arg\max_{\mathbf{y}}\big(\frac{1}{3}\mathbf{r}_{\rm o}^H\mathbf{y}\mathbf{y}^H\mathbf{r}_{\rm o} + \mathbf{r}_{\rm e}^H\mathbf{S}(\mathbf{S}^H\mathbf{S})^{-1}\mathbf{r}_{\rm e}\big) \tag{2.22}$$

$$= \arg\max_{\mathbf{y}}\big(\mathbf{r}_{\rm B2}^H\mathbf{S}_{\rm B}(\mathbf{S}_{\rm B}^H\mathbf{S}_{\rm B})^{-1}\mathbf{S}_{\rm B}\mathbf{r}_{\rm B2}\big) \tag{2.23}$$

where $\mathbf{r}_{\mathrm{B2}} = (\mathbf{r}_{\mathrm{o}}\ \mathbf{r}_{\mathrm{e}})^T, \mathbf{S}_{\mathrm{B}} = \begin{pmatrix} \mathbf{y} & \mathbf{0} & \mathbf{0} \\ \mathbf{0} & \mathbf{x} & \mathbf{y} \end{pmatrix}$. Note that $\mathbf{S}_{\mathrm{B}} = \mathbf{P}_{\mathrm{B}}\mathbf{C}_{\mathrm{B}}$, and $\mathbf{r} = \mathbf{P}_{\mathrm{B}}^H \mathbf{r}_{\mathrm{B2}}$, where

$$\mathbf{C}_{\mathrm{B}} = \begin{pmatrix} y_1 & 0 & 0 \\ 0 & y_1 & x_1 \\ -y_2 & 0 & 0 \\ 0 & -y_2 & x_2 \\ y_3 & 0 & 0 \\ 0 & y_3 & x_3 \end{pmatrix}, \mathbf{P}_{\mathrm{B}} = \begin{pmatrix} 1 & 0 & 0 & 0 & 0 & 0 \\ 0 & 0 & 1 & 0 & 0 & 0 \\ 0 & 0 & 0 & 0 & 1 & 0 \\ 0 & 1 & 0 & 0 & 0 & 0 \\ 0 & 0 & 0 & 1 & 0 & 0 \\ 0 & 0 & 0 & 0 & 0 & 1 \end{pmatrix}.$$

From (2.23), Receiver B2 can also be written as

$$\hat{\mathbf{y}}_{\mathrm{B2}} = \arg\max_{\mathbf{y}} \left(\mathbf{r}^H \mathbf{C}_{\mathrm{B}} (\mathbf{C}_{\mathrm{B}}^H \mathbf{C}_{\mathrm{B}})^{-1} \mathbf{C}_{\mathrm{B}} \mathbf{r}\right). \tag{2.24}$$

The optimization problem in (2.24) is solved for all possible values of $\mathbf{y}$. It is worth noting that (2.19) can be written as $\mathbf{r} = \mathbf{C}_{\mathrm{B}}\mathbf{h}_{\mathrm{B}} + \mathbf{n}_{\mathrm{B}}$, where $\mathbf{h}_{\mathrm{B}} = (\sqrt{P_2}q_2\ \sqrt{P_2}Ah_2g_1\ \sqrt{P_1}Ah_2h_1)^H$.

2.5 Performance of Derived Receivers

In this section, we examine the performance of Receiver A2 and show that it achieves full diversity. Due to the self-interference terms and noise forwarded by the relay node, the error performance of Receivers A1, B1, and B2 seems difficult to characterize. However, the simulation results show that these receivers outperform Receiver A2, it is expected that all derived receivers achieve full diversity.

Receiver A2 achieves full diversity: Note that $\mathbf{S}_{\mathrm{A2}} = \mathbf{P}_{\mathrm{A2}}\mathbf{C}_{\mathrm{A}}$ and $\mathbf{z} = \mathbf{P}_{\mathrm{A2}}^T \mathbf{z}_{\mathrm{A2}}$, where $\mathbf{P}_{\mathrm{A2}} = \begin{pmatrix} 1 & 0 & 0 & 0 \\ 0 & 0 & 1 & 0 \\ 0 & 1 & 0 & 0 \\ 0 & 0 & 0 & 1 \end{pmatrix}$ is a permutation matrix. From (2.18), Receiver A2 also admits the following form: $\hat{\mathbf{y}}_{\mathrm{A2}} = \arg\max_{\mathbf{y}} \left(\mathbf{z}^H \mathbf{C}_{\mathrm{A}} (\mathbf{C}_{\mathrm{A}}^H \mathbf{C}_{\mathrm{A}})^{-1} \mathbf{C}_{\mathrm{A}}^H \mathbf{z}\right)$. To justify that Receiver A2 achieves full diversity, we only need to show that matrix $\mathbf{R}_{\mathbf{C}\tilde{\mathbf{C}}} = \left(\mathbf{C}_{\mathrm{A}}\ \tilde{\mathbf{C}}_{\mathrm{A}}\right)^H \left(\mathbf{C}_{\mathrm{A}}\ \tilde{\mathbf{C}}_{\mathrm{A}}\right)$ is full rank for distinct vectors $\mathbf{y}$ and $\tilde{\mathbf{y}}$ [40]. It is enough to show that the following matrix is

full rank:

$$(\mathbf{v} \;\; \tilde{\mathbf{v}}) = \begin{pmatrix} \xi_1 & \tilde{\xi}_1 \\ \xi_2 & \tilde{\xi}_2 \end{pmatrix} = \begin{pmatrix} x_2y_1 + x_1y_2 & x_2\tilde{y}_1 + x_1\tilde{y}_2 \\ x_2y_3 + x_3y_2 & x_2\tilde{y}_3 + x_3\tilde{y}_2 \end{pmatrix},$$

where $\tilde{\mathbf{v}} = (\tilde{\xi}_1 \;\; \tilde{\xi}_2)^T, \tilde{\xi}_1 = x_2\tilde{y}_1 + x_1\tilde{y}_2$, $\tilde{\xi}_2 = x_2\tilde{y}_3 + x_3\tilde{y}_2$, and $\tilde{y}_1, \tilde{y}_2$, and $\tilde{y}_3$ are sybmols from, respectively, set $\mathcal{S}_1, \mathcal{S}_2$, and $\mathcal{S}_4$. To show that the matrix is full rank, it is sufficient to argue that $\det(\mathbf{v} \;\; \tilde{\mathbf{v}}) \neq 0$ for $\mathbf{y} \neq \tilde{\mathbf{y}}$. We use a contradiction for the proof. Suppose $\det(\mathbf{v} \;\; \tilde{\mathbf{v}}) = 0$ for a choice of $\mathbf{y} \neq \tilde{\mathbf{y}}$ as $y_i = \tilde{y}_i, i = 1, 2$, and $y_3 \neq \tilde{y}_3$. Note the determinant $\det(\mathbf{v} \;\; \tilde{\mathbf{v}}) = \sum_{i=1}^{3} \tau_i$, where $\tau_1 = x_2^2\big(y_1\tilde{y}_3 - y_3\tilde{y}_1\big), \tau_2 = x_1x_2\big(y_2\tilde{y}_3 - y_3\tilde{y}_2\big)$, and $\tau_3 = x_2x_3\big(y_1\tilde{y}_2 - y_2\tilde{y}_1\big)$. From the assumption, we then have $\tau_1 + \tau_2 = x_2(x_2y_1 + x_1y_2)(\tilde{y}_3 - y_3) = 0$. Note that $x_2y_1 \in \mathcal{S}_2$ and $x_1y_2 \in \mathcal{S}_1$. Since p_1 and p_2 are coprime, we have $x_2y_1 + x_1y_2 \neq 0$ by Fact 1 in Appendix A. Because $x_2 \neq 0$, we have $\tilde{y}_3 = y_3$, which contradicts the assumption.

2.6 Constellation Selection

In the proposed signaling scheme, the transmitted PSK symbols are from constellation sets with different sizes. As a result, the bit rates in each time slot at the source nodes are different. However, in practical communication systems, a uniform bit rate in each time slot is often preferred during transmissions. A constellation selection scheme is required to select the same number of constellation points from sets $\mathcal{S}_1, \cdots, \mathcal{S}_4$ to achieve a uniform bit rate for the system. Note that the transmission rate in one block for each source node will be reduced if constellation selections are applied.

Constellation selection for Receiver A2: The pairwise error probability that vector $\tilde{\mathbf{y}}$ is detected for $\mathbf{y} \neq \tilde{\mathbf{y}}$ transmitted by the LSE blind receiver is proportional to $\big(\det(\mathbf{C}_{\mathrm{A2}}^H \;\; \mathbf{C}_{\mathrm{A2}}) + \det(\tilde{\mathbf{C}}_{\mathrm{A2}}^H \;\; \tilde{\mathbf{C}}_{\mathrm{A2}})\big)/\det\big((\mathbf{C}_{\mathrm{A2}} \;\; \tilde{\mathbf{C}}_{\mathrm{A2}})^H(\mathbf{C}_{\mathrm{A2}} \;\; \tilde{\mathbf{C}}_{\mathrm{A2}})\big)$. Let $\mathcal{B}_i$ be a subset of $\mathcal{S}_i$ with $|\mathcal{B}_i| = M$, where $M \geq 2$ is the number of constellation points to be selected from $\mathcal{S}_i$, so that $\log_2 M$ bits are transmitted in one symbol. The constellation selection criterion for Receiver A2 can then be expressed as

$$\min_{\mathcal{B}_1, \cdots, \mathcal{B}_4} \max_{\substack{y_i, \tilde{y}_i \in \mathcal{B}_i \\ \mathbf{y} \neq \tilde{\mathbf{y}}}} \frac{\det(\mathbf{C}_{\mathrm{A2}}{}^H\mathbf{C}_{\mathrm{A2}}) + \det(\tilde{\mathbf{C}}_{\mathrm{A2}}^H\tilde{\mathbf{C}}_{\mathrm{A2}})}{\det\big((\mathbf{C}_{\mathrm{A2}} \;\; \tilde{\mathbf{C}}_{\mathrm{A2}})^H(\mathbf{C}_{\mathrm{A2}} \;\; \tilde{\mathbf{C}}_{\mathrm{A2}})\big)} \tag{2.25}$$

where

$$\tilde{\mathbf{C}}_{\mathrm{A2}} = \begin{pmatrix} \tilde{y}_1 x_2 + x_1 \tilde{y}_2 \mathbf{I}_2 \\ \tilde{y}_3 x_2 + x_3 \tilde{y}_2 \mathbf{I}_2 \end{pmatrix}. \tag{2.26}$$

The selected two-point constellation points with $M = 2$ for Receiver A2 are listed in Table 2.2.

Constellation selection for Receiver B2: The error performance of Receiver B2 seems difficult to characterize, we propose the following constellation selection scheme for it:

$$\min_{\mathcal{B}_1,\cdots,\mathcal{B}_4} \max_{\substack{y_i,\tilde{y}_i \in \mathcal{B}_i \\ \mathbf{y} \neq \tilde{\mathbf{y}}}} \frac{\det(\mathbf{C}_{\mathrm{B}}{}^H \mathbf{C}_{\mathrm{B}}) + \det(\tilde{\mathbf{C}}_{\mathrm{B}}^H \tilde{\mathbf{C}}_{\mathrm{B}})}{\det(\mathbf{G}\mathbf{G}^H)} \tag{2.27}$$

where

$$\mathbf{G} = \begin{pmatrix} x_1 & y_1 & \tilde{y}_1 \\ x_2 & -y_2 & -\tilde{y}_2 \\ x_3 & y_3 & \tilde{y}_3 \end{pmatrix}, \tilde{\mathbf{C}}_{\mathrm{B}} = \begin{pmatrix} \tilde{y}_1 & 0 & 0 \\ 0 & \tilde{y}_1 & x_1 \\ -\tilde{y}_2 & 0 & 0 \\ 0 & -\tilde{y}_2 & x_2 \\ \tilde{y}_3 & 0 & 0 \\ 0 & \tilde{y}_3 & x_3 \end{pmatrix}.$$

The selections with $M = 2$ for Receiver B2 are also listed in Table 2.2.

Table 2.2: Two-Point Constellation Selections

Selections	Set $\mathcal{S}_1$	Set $\mathcal{S}_2$	Set $\mathcal{S}_3$	Set $\mathcal{S}_4$
For Receiver A2	$(2,3)$	$(0,3)$	$(0,5)$	$(3,8)$
For Receiver B2	$(2,3)$	$(2,5)$	$(0,4)$	$(0,5)$

2.7 Simulation Results

In this section, we present simulation results to verify the derived receivers and the constellation selections, and to explore the power allocation schemes to further improve system performance. The symbol error rates (SERs) are plotted by averaging over 10^6

random channel realizations. The channel coefficients are generated by independent zero-mean CSCG random variables with different variances.

Constellation selections: Fig. 2.2 plots the SERs of the derived receivers at S_1 with the constellation points listed in Table 2.2. Receivers A1 and A2 use the selection points in the first row in Table 2.2, and Receivers B1 and B2 use those in the second row. The channel variances in all links are identical, $\delta_q^2 = \delta_g^2 = \delta_h^2 = 1$. The plots show that there is little difference between the performance of Receivers A1 and A2, and between the performance of Receivers B1 and B2. Receivers B1 and B2 significantly outperform A1 and A2. This is because the noise variance is doubled in Receivers A1 and A2 due to the self-interference cancelation. For the purpose of comparison, the SERs for coherent maximum likelihood (ML) detection are included, whereby the perfect channel state information is used in the detection. The SNR gap between Receiver B2 and coherent ML detection is reduced when two blocks are used in the detection.

The SERs are also plotted for the training-based scheme in which a least-square approach is applied in estimating the channel coefficients. For a fair comparison, the same information bits are transmitted per time slot for all schemes. In the proposed scheme, three symbols are transmitted in nine time slots. Therefore, a bit rate of 1/3 bits is transmitted for the two-point selections in Table 2.2. For the training-based scheme, we have

$$\mathbf{r}_t = \mathbf{T}\mathbf{h}_t + \mathbf{n}_t \tag{2.28}$$

where r_t denotes the received training signal at S_1, and $\mathbf{n}_t$ is the corresponding noise. Since the channel vector to be estimated $\mathbf{h}_t = [\mathbf{h}, \mathbf{w}]^T$ is a 4×1 vector, the training signal matrix T must achieve full column rank (which is four) in order to obtain the unique least squares solution of $\hat{\mathbf{h}}_t = \mathbf{T}^H(\mathbf{T}\mathbf{T}^H)^{-1}\mathbf{r}_t$, such that two pilot symbols need to be transmitted from each source node using six time slots in each block. Therefore, 8-PSK is used to achieve a bit rate of 1/3 in one-block detection, and BPSK and 3-PSK are used in two-block transmission for a bit rate $\big(1 + 3\log_2(3)\big)/18 \approx 0.32$ (two training and one BPSK information symbols are transmitted in the first block, and three 3-PSK symbols are transmitted in the second

block). The plots indicate that the proposed blind receivers provide significant SNR gains over the training based scheme.

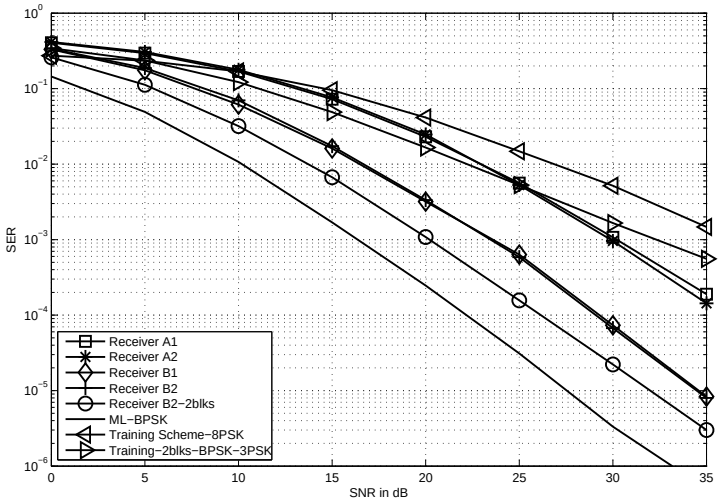

Figure 2.2: SER at S_1 and Constellation Selections for Blind Receivers, $\delta_q^2 = \delta_g^2 = \delta_h^2 = 1$.

Power allocation: We examine power allocation schemes among the source and relay nodes to further improve the system performance. Since the analytical expressions of the error probabilities for the proposed receivers are difficult to obtain, an obvious winning criterion to optimize the error performance seems hard to find. In this simulation, we present five criterions based on the signal to interference ratio (SINR) and SNR, and obtain power allocation schemes to improve the average SER the source nodes: $P_{e-avg} = P_{e1} + P_{e2}$, where P_{e1} and P_{e2} are the SERs at S_1 and S_2, respectively. Specifically, we seek the power allocations in P_1, P_2, and P_r subject to the total power constraint at the source and relay nodes, by solving (numerically) optimization problems with various cost functions. The optimization problems share a uniform format:

$$\begin{aligned} &\max_{P_1,P_2,P_r} \text{Cost Function} \\ \text{subject to } \; &A = \sqrt{Pr/(P_1\delta_h^2 + P_2\delta_g^2 + 2\sigma^2)} \\ &P_1 + P_2 + Pr \leq P_T \end{aligned} \tag{2.29}$$

where P_T is the total power in the system, including the power at the source nodes and the relay. The following five cost functions can be considered:

- Cost Function 1: $\min(\mu_1, \mu_2)$, where μ_1 and μ_2 are, respectively, the SINR for source nodes 1 and 2, $\mu_1 = \frac{P_2\delta_q^2+P_2A^2\delta_h^2\delta_g^2}{A^2\delta_h^4P_1+(2A^2\delta_h^2+2)\sigma^2}$, and $\mu_2 = \frac{P_1\delta_q^2+P_1A^2\delta_h^2\delta_g^2}{A^2\delta_g^4P_2+(2A^2\delta_g^2+2)\sigma^2}$.

- Cost Function 2: $\min(\mu_3, \mu_4)$, where μ_3 and μ_4 are, respectively, the SNR for source node 1 and 2, $\mu_3 = \frac{P_2\delta_q^2+P_2A^2\delta_h^2\delta_g^2}{(2A^2\delta_h^2+2)\sigma^2}$, and $\mu_4 = \frac{P_1\delta_q^2+P_1A^2\delta_h^2\delta_g^2}{(2A^2\delta_g^2+2)\sigma^2}$.

- Cost Function 3: $\min(\mu_5, \mu_6)$, where μ_5 and μ_6 are, respectively, the summation of the SNR in the direct link and the SINR in the relaying link for source nodes 1 and 2, $\mu_5 = \frac{P_2\delta_q^2}{\sigma^2} + \frac{P_2A^2\delta_h^2\delta_g^2}{A^2\delta_h^4P_1+(2A^2\delta_h^2+1)\sigma^2}$, and $\mu_6 = \frac{P_1\delta_q^2}{\sigma^2} + \frac{P_1A^2\delta_h^2\delta_g^2}{A^2\delta_g^4P_2+(2A^2\delta_g^2+1)\sigma^2}$.

- Cost Function 4: $\min(\mu_7, \mu_8)$, where $\mu_7 = \frac{P_2\delta_q^2}{\sigma^2} + \frac{P_2A^2\delta_h^2\delta_g^2}{(2A^2\delta_h^2+1)\sigma^2}$, and $\mu_8 = \frac{P_1\delta_q^2}{\sigma^2} + \frac{P_1A^2\delta_h^2\delta_g^2}{(2A^2\delta_g^2+1)\sigma^2}$.

- Cost Function 5: $\min(\mu_9, \mu_{10})$, where $\mu_9 = \frac{P_2\delta_q^2}{\sigma^2}\frac{P_2A^2\delta_h^2\delta_g^2}{(2A^2\delta_h^2+1)\sigma^2}$, and $\mu_{10} = \frac{P_1\delta_q^2}{\sigma^2}\frac{P_1A^2\delta_h^2\delta_g^2}{(2A^2\delta_g^2+1)\sigma^2}$.

The solutions to optimization problem in (2.29) using Cost Functions 1, 2, and 3 are very similar at a high SNR, in the sense that the values of P_1 and P_2 are identical to almost half of the total power, and the amplification coefficient approaches zero (implying that the relaying link is turned off). The diversity gain is therefore reduced to one. Table 2.3 lists the power allocations and amplification coefficients at different SNRs for Cost Functions 3, 4, and 5 by numerical calculations for $P_T = 3$.

Figs. 2.3 and 2.4 plot, respectively, the average SER P_{e-avg} and worst SER $\max(P_{e1}, P_{e2})$ for Receivers A2 and B2. The channel variances are, respectively, $\delta_q^2 = 1, \delta_g^2 = 5$, and $\delta_h^2 = 1$. The plots indicate that, if the power loading of Cost Function 3 is used, the performance of the receivers suffers significantly due to the loss in diversity gain. Cost Function 4 performs inferiorly to the uniform power loading with $P_1 = P_2 = P_T/3$. Cost Function 5 provides a small gain over the uniform power loading scheme at a high SNR.

Table 2.3: Power Allocations for Cost Functions 3, 4, and 5

	Cost Function 3			Cost Function 4			Cost Function 5		
SNR	P_1	P_2	A	P_1	P_2	A	P_1	P_2	A
0	1.46	1.45	.09	1.380	1.355	.162	1.200	.906	.340
5	1.48	1.47	.08	1.342	1.287	.210	1.222	.892	.375
10	1.493	1.48	.05	1.329	1.257	.230	1.232	.889	.387
15	1.498	1.495	.03	1.327	1.252	.235	1.234	.886	.392
20	1.498	1.498	.02	1.325	1.247	.238	1.235	.886	.393
25	1.498	1.498	.008	1.325	1.247	.238	1.235	.885	.394
30	1.498	1.498	.008	1.324	1.246	.238	1.235	.886	.394
35	1.498	1.498	.008	1.326	1.248	.237	1.234	.884	.395

Figs. 2.5 and 2.6 shows, respectively, the average and worst SERs for both source nodes for another channel condition with a poorer direct link and bigger difference in variances of the relaying channels: $\delta_q^2 = 0.1, \delta_g^2 = 10$, and $\delta_h^2 = 1$. The SNR gain of Cost Function 5 over the uniform power loading scheme is more noticeable with about 1dB.

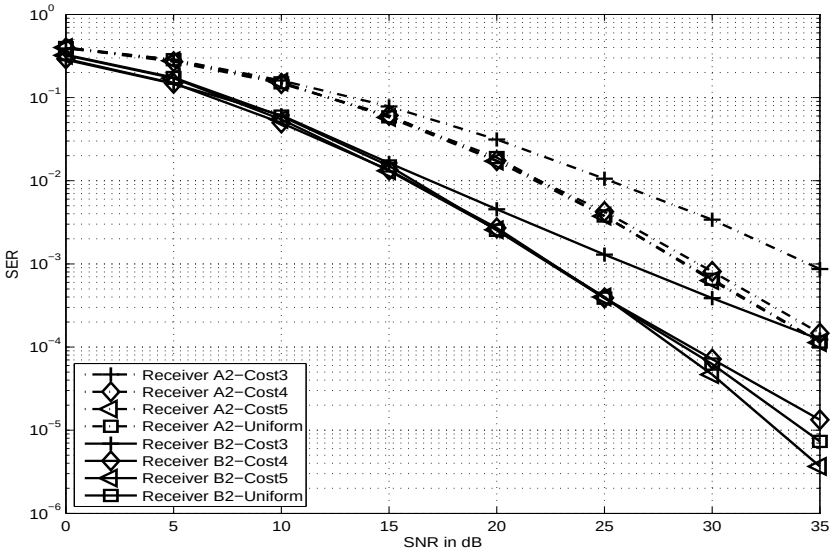

Figure 2.3: Average SER, $\delta_q^2 = 1, \delta_g^2 = 5$, and $\delta_h^2 = 1$.

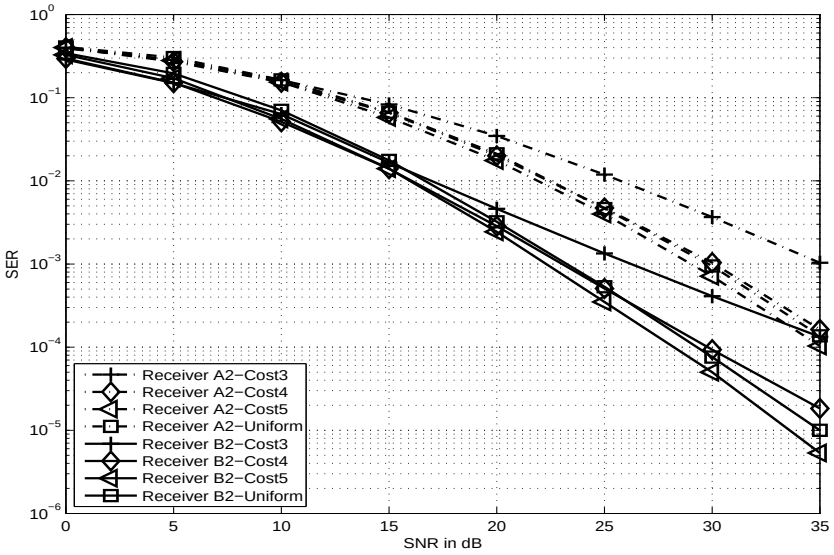

Figure 2.4: Worst SER, $\delta_q^2 = 1, \delta_g^2 = 5$, and $\delta_h^2 = 1$.

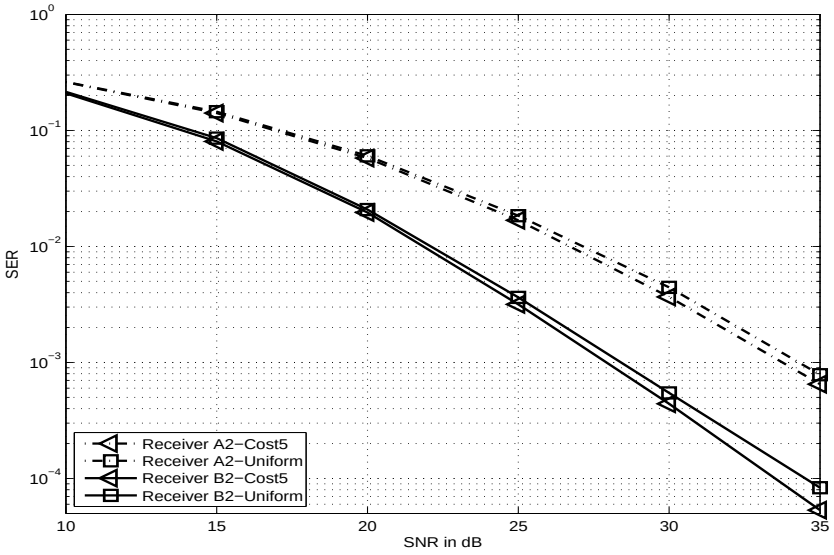

Figure 2.5: Average SER, $\delta_q^2 = 0.1, \delta_g^2 = 10$, and $\delta_h^2 = 1$.

Time varying channel: Fig. 2.7 plots the SERs at S_1 for Receivers A1 and B1 if time varying channels are applied to the system (the performance of Receivers A2 and B2 is not plotted, since it is very close to that of Receivers A1 and B1). The channel variance in each link is identical with $\delta_q^2 = \delta_g^2 = \delta_h^2 = 1$. Nine channel coefficients are generated for

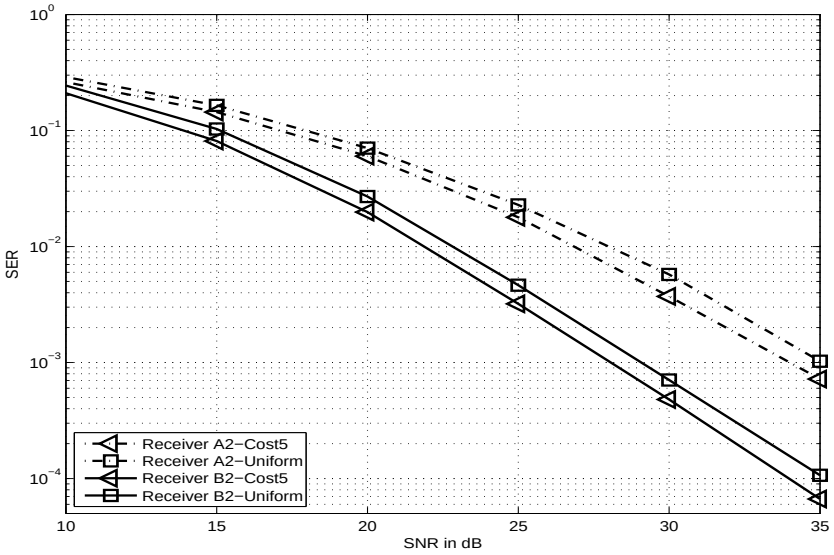

Figure 2.6: Worst SER, $\delta_q^2 = 0.1, \delta_g^2 = 10$, and $\delta_h^2 = 1$.

each transmission block based on the Jake's Model with the normalized doppler frequency $f_d T_s = 0.001, 0.003$, and 0.005, respectively. The constellation points listed in Table 2.2 are used. For the purpose of comparison, the SER for block fading channels with $f_d T_s = 0$ is also included in the figure. It is observed that the performance of the receivers in time varying channels degrades compared to that in block fading channels. This is because the condition that channels remain unchanged in one block does not hold anymore.

2.8 Conclusion

This chapter considers blind detection for an AF two-way relay system with non-reciprocal channels. An effective signalling and transmitting scheme is proposed to achieve unique identification of the transmitted symbols and channel coefficients in noise-free transmissions. The GLRT and LSE receivers with full diversity are derived for the Rayleigh fading channels with Gaussian noise. Simulations show that the performance of GLRT receivers is almost identical to that of the LSE receivers. This interesting observation suggests that one can replace the GLRT receiver by the LSE receiver in the blind detection to take advantage

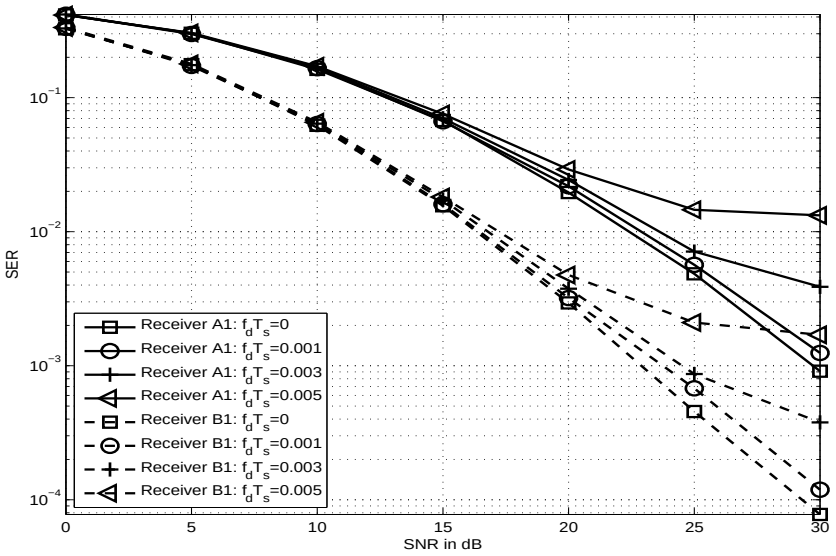

Figure 2.7: SER at S_1 in Time Varying Channels.

of a simpler implementation without sacrificing performance. Power allocation schemes are examined to further improve the system performance.

CHAPTER 3

Blind Detection Design over Frequency-Selective Fading Channels: AF Two-Way Relay Network without Direct Link

3.1 Introduction

We reported effective signaling and transmission schemes in Chapter 2 and [26,27] to deal with the ambiguity issues for the blind detections in two-way relay systems, in which flat fading channels are assumed between each nodes. Apprently, these research works only focus on flat fading environment, which cannot handle the multi-path fading. In radio propagation, the fading channels are not always flat [41–44]. When the coherence bandwidth of channel is less than the signal bandwidth, different frequency components of signals experience different magnitude of fading, which is frequency-selective fading [45]. Recently, blind estimations have been discussed for frequency selective fading two-way relay systems in which the CSI is assumed unavailable at the receivers [46–48]. However, these pilot-based or training-assisted blind estimation algorithms have achieved progress at the cost of certain spectral efficiency to transmit the training symbols, since these estimators are typically associated with a *phase or scalar* ambiguity, even in noise-free transmissions. As a result, a short training sequence has to be transmitted to resolve the inherent phase or scalar ambiguity. Consequently, unique identification of channel coefficients and transmitted signals in noise-free transmission is crucial to an efficient blind detection transmission design in noisy transmissions.

This chapter focuses on a two-way relay system model in which the channels between each nodes are assumed frequency selective fading [49–51]. The systems produce the inter-symbol interference introduced by transmitting the data stream in equal-size blocks. Some redundancy is padded to each block before transmission in order to eliminate interblock interference. There exists many methods of adding redundancy [52–54], however in this chapter we apply zero-padding redundancy scheme to alleviate the interblock interference [55–57]. To solve the channel ambiguity issue, we propose an effective signaling and transmission scheme

for the frequency-selective two-way relay system with zero-padded block transmission, in which neither the transmitter nor the receiver has the CSI. An iterative sphere decoder is then derived to approximate the LSE detection for Rayleigh fading channels and Gaussian noise. The contribution of this chapter is summarized as follows.

- A novel and effective modulation technique using four pairwise coprime PSK constellation is proposed to uniquely identify the transmitted signals and channel coefficients for frequency-selective two-way relay system with zero-padded block transmission.
- In the Gaussian noise and Rayleigh fading environment, the complexity of detection implementation is highly decreased by applying the joint sphere decoder derived. .

Here, we need to point out that the similar signaling and transmission schemes are applied in [26,27] for two-way flat-fading channels. However, theoretic analysis and computer simulations become much more complicated for frequency-selective channels, and worthwhile to be investigated.

The remainder of this chapter is organized as follows: Section 3.2 presents the system model and the transmission scheme with designed PSK symbols. Section 3.3 proposes an LSE blind receiver, and derives the iterative sphere decoder to approximate the LSE detection for the Rayleigh fading channels with Gaussian noise. Simulation results of blind receivers and complexity analysis are provided in Section 3.4. Section 3.5 concludes the chapter.

3.2 System Model

Fig. 3.1 illustrates a two-way relay system in which two source nodes S_1 and S_2 exchange information with each other with the assistance of a relay node R. The reciprocal channels between each nodes are assumed, which means that the channel coefficient from one node to another is identical to that in the reverse channel back to the same node. The channel gains from S_1 and S_2 to R are denoted by complex vectors $\mathbf{h}$ and $\mathbf{g}$, respectively, where we assume that the channels $\mathbf{h}$ and $\mathbf{g}$ are of length L_h and L_g, respectively. Then the channel impulse responses are denoted as $\mathbf{h} = \big(h(0), h(1), ..., h(L_h - 1)\big)^{\mathrm{T}}$, $\mathbf{g} = \big(g(0), g(1), ..., g(L_g -$

$1))^{\mathrm{T}}$, in which each element is CSCG distributed with zero mean and $1/L_h$, $1/L_g$ variance, respectively. The channel coefficients are not known at either both source nodes or the relay. Each source node recovers symbols from the other source based on prior knowledge of its own transmitted symbols in the signals forwarded by the relay. The system operates in a half duplex mode in which the transmissions and receptions are not carried out simultaneously.

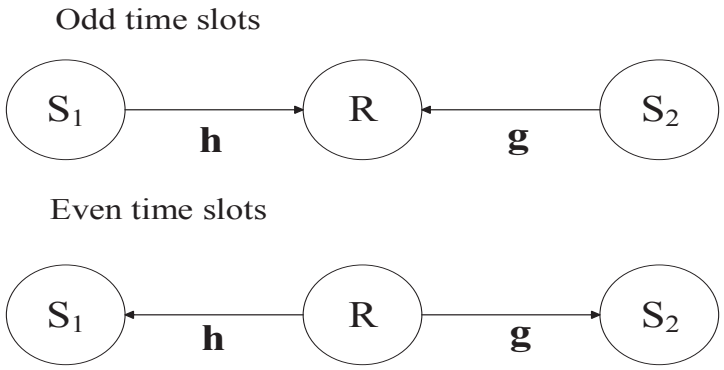

Figure 3.1: A Frequency-Selective Two-Way Relay System without Direct Link

To ensure unique identification of the channel coefficients and transmitted symbols in a noise-free transmission, we propose a novel and effective signaling and transmission scheme using PSK constellations.

It should be noted that it is impossible to develop the blind receivers in noisy transmissions if the unique identifiability is not guaranteed in the corresponding noise-free system. A four-block transmission scheme is first proposed, in which the channel coefficients do not change within four time blocks (eight time slots, since it takes two time slots to exchange information from two source nodes in each block) of observation; after that, they change to new independent values and stay unchanged in the next four blocks, and so on. The transmission scheme are carried out using four PSK constellations. Four symbol sequences are exchanged between the source nodes in every four time blocks. The theoretical proof

of unique identification in this scenario will be left for the future work since it is quite mathematically involved.

It should be pointed that if the channel coherence time is not long enough and the channel gains fail to remain unchanged in four blocks of transmission, the proposed scheme cannot be applied. Conversely, if the channel gains remain unchanged in more than four blocks, the proposed transmission and detection schemes can also be applied. The symbol error rate (SNR) performance of six block and eight block transmission schemes are included in section 3.4. In sections 3.2 and 3.3, we demonstrate the signaling scheme and blind receivers in four-block transmission.

Let $p_i,\ i = 1, 2, 3, 4$, denote pairwise coprime positive integers, and let constellation set $\mathcal{S}_i$ collect all p_i-PSK symbols, i.e., $\mathcal{S}_i = \{\exp(j2\pi m_i/p_i, m_i = 0, ..., p_i - 1\}$. Denote the transmitted symbol sequences in kth transmission block from S_1 and S_2, respectively, by $\mathbf{x}_k$ and $\mathbf{y}_k$, where $\mathbf{x}_k$ and $\mathbf{y}_k$ are of length $L_x,\ L_y$. They are thus given by $\mathbf{x}_k = \big(x_k(0), x_k(1), ..., x_k(L_x - 1)\big)^{\mathrm{T}}$, and $\mathbf{y}_k = \big(y_k(0), y_k(1), ..., y_k(L_y - 1)\big)^{\mathrm{T}}$, respectively, $k = 1, ..., 4$.

We define the equivalent channel sequences as $\mathbf{a} = \mathbf{h} \otimes \mathbf{h}$, $\mathbf{b} = \mathbf{g} \otimes \mathbf{h}$, $\mathbf{c} = \mathbf{g} \otimes \mathbf{g}$, and their lengths are $L_a,\ L_b,\ L_c$, respectively. Therefore, the lengths $L_a,\ L_b$, and L_c are calculated as $L_a = 2L_h - 1$, $L_b = L_h + L_g - 1$, $L_c = 2L_g - 1$. We only focus on the received signals at S_1 for the brevity of demonstration, whereas similar results hold for S_2. In order to avoid interblock interference, $L_a - 1$, and $L_b - 1$ zeros are appended to $\mathbf{x}_k$ and $\mathbf{y}_k$ to form $\mathbf{x}'_k$ and $\mathbf{y}'_k$, respectively, and are given as

$$\mathbf{x}'_k = \big(x_k(0), x_k(1), ..., x_k(L_x - 1), \underbrace{0, ..., 0}_{L_a - 1}\big)^{\mathrm{T}} \tag{3.1}$$

$$\mathbf{y}'_k = \big(y_k(0), y_k(1), ..., y_k(L_y - 1), \underbrace{0, ..., 0}_{L_b - 1}\big)^{\mathrm{T}} \tag{3.2}$$

The proposed signaling and transmission scheme in four blocks (eight time slots) is shown in details in Table 4.1 in order to be clearly explained.

Table 3.1: Signalling and Transmission Scheme for Frequency-Selective Fading Two-Way Relay System without Direct Link

Time Slots	Transmitting/Receiving	Symbols and Constellations
1	$S_1 \xrightarrow{\mathbf{x}'_1(\mathbf{x}_1)} R$, $S_2 \xrightarrow{\mathbf{y}'_1(\mathbf{y}_1)} R$	$\mathbf{x}_1 \in \mathcal{S}_1$, $\mathbf{y}_1 \in \mathcal{S}_2$
2	$R \xrightarrow{\mathbf{x}'_1,\mathbf{y}'_1} S_1$, S_2	
3	$S_1 \xrightarrow{\mathbf{x}'_2(\mathbf{x}_2)} R$, $S_2 \xrightarrow{-\mathbf{y}'_2(\mathbf{y}_2)} R$	$\mathbf{x}_2 \in \mathcal{S}_2$, $\mathbf{y}_2 \in \mathcal{S}_1$
4	$R \xrightarrow{\mathbf{x}'_2,\mathbf{y}'_2} S_1$, S_2	
5	$S_1 \xrightarrow{\mathbf{x}'_3(\mathbf{x}_3)} R$, $S_2 \xrightarrow{\mathbf{y}'_3(\mathbf{y}_3)} R$	$\mathbf{x}_3 \in \mathcal{S}_3$, $\mathbf{y}_3 \in \mathcal{S}_4$
6	$R \xrightarrow{\mathbf{x}'_3,\mathbf{y}'_3} S_1$, S_2	
7	$S_1 \xrightarrow{\mathbf{x}'_4(\mathbf{x}_4)} R$, $S_2 \xrightarrow{-\mathbf{y}'_4(\mathbf{y}_4)} R$	$\mathbf{x}_4 \in \mathcal{S}_4$, $\mathbf{y}_4 \in \mathcal{S}_3$
8	$R \xrightarrow{\mathbf{x}'_4,\mathbf{y}'_4} S_1$, S_2	

In the first time slot, S_1 transmits zero-padded signal $\mathbf{x}'_1$, in which $\mathbf{x}_1$ is from set $\mathcal{S}_1$, and S_2 transmits zero-padded signal $\mathbf{y}'_1$, in which $\mathbf{y}_1$ is from set $\mathcal{S}_2$. The received signal at the relay is $\mathbf{r}'_{R_1} = \mathbf{h} \otimes \mathbf{x}'_1 + \mathbf{g} \otimes \mathbf{y}'_1 + \mathbf{n}'_1$.

In the second time slot, the relay transmits $A\mathbf{r}'_{R_1}$ to both source nodes. The received signal at S_1 is $\mathbf{r}'_1 = A\mathbf{h} \otimes \mathbf{r}'_{R_1} + \mathbf{u}'_1 = A\mathbf{h} \otimes \mathbf{h} \otimes \mathbf{x}'_1 + A\mathbf{h} \otimes \mathbf{g} \otimes \mathbf{y}'_1 + A\mathbf{h} \otimes \mathbf{n}'_1 + \mathbf{u}'_1$, where $\mathbf{n}'_k$, and $\mathbf{u}'_k, (k = 1, ..., 4)$ are the additive white Gaussian noise (AWGN) in kth transmission block at nodes R, and S_1, respectively, whose element is i.i.d. CSCG distributed with zero mean and σ^2 variance, and $A = 1/(2+\sigma^2)^{1/2}$ is the amplification coefficient at the relay with the assumption of unit power at all three nodes in order to ensure that the average power in forwarding the received signals does not exceed the available power.

In the third time slot, S_1 transmits zero-padded signal $\mathbf{x}'_2$, in which $\mathbf{x}_2$ is from set $\mathcal{S}_2$, and S_2 transmits zero-padded signal $-\mathbf{y}'_2$, in which $\mathbf{y}_2$ is from set $\mathcal{S}_1$. The received signal at the relay is $\mathbf{r}'_{R_2} = \mathbf{h} \otimes \mathbf{x}'_2 - \mathbf{g} \otimes \mathbf{y}'_2 + \mathbf{n}'_2$.

In the fourth time slot, the relay transmits $A\mathbf{r}'_{R_2}$ to both source nodes. The received signal at S_1 is $\mathbf{r}'_2 = A\mathbf{h} \otimes \mathbf{r}'_{R_2} + \mathbf{u}'_2 = A\mathbf{h} \otimes \mathbf{h} \otimes \mathbf{x}'_2 - A\mathbf{h} \otimes \mathbf{g} \otimes \mathbf{y}'_2 + A\mathbf{h} \otimes \mathbf{n}'_2 + \mathbf{u}'_2$.

In the fifth time slot, S_1 transmits zero-padded signal $\mathbf{x}'_3$, in which $\mathbf{x}_3$ is from set $\mathcal{S}_3$,

and S_2 transmits zero-padded signal $\mathbf{y}'_3$, in which $\mathbf{y}_3$ is from set $\mathcal{S}_4$. The received signal at the relay is $\mathbf{r}'_{R_3} = \mathbf{h} \otimes \mathbf{x}'_3 + \mathbf{g} \otimes \mathbf{y}'_3 + \mathbf{n}'_3$.

In the sixth time slot, the relay transmits $A\mathbf{r}'_{R_3}$ to both source nodes. The received signal at S_1 is $\mathbf{r}'_3 = A\mathbf{h} \otimes \mathbf{r}'_{R_3} + \mathbf{u}'_3 = A\mathbf{h} \otimes \mathbf{h} \otimes \mathbf{x}'_3 + A\mathbf{h} \otimes \mathbf{g} \otimes \mathbf{y}'_3 + A\mathbf{h} \otimes \mathbf{n}'_3 + \mathbf{u}'_3$.

In the seventh time slot, S_1 transmits zero-padded signal $\mathbf{x}'_4$, in which $\mathbf{x}_4$ is from set $\mathcal{S}_4$, and S_2 transmits zero-padded signal $-\mathbf{y}'_4$, in which $\mathbf{y}_4$ is from set $\mathcal{S}_3$. The received signal at the relay is $\mathbf{r}'_{R_4} = \mathbf{h} \otimes \mathbf{x}'_4 - \mathbf{g} \otimes \mathbf{y}'_4 + \mathbf{n}'_4$.

In the eighth time slot, the relay transmits $A\mathbf{r}'_{R_4}$ to both source nodes. The received signal at S_1 is $\mathbf{r}'_4 = A\mathbf{h} \otimes \mathbf{r}'_{R_4} + \mathbf{u}'_4 = A\mathbf{h} \otimes \mathbf{h} \otimes \mathbf{x}'_4 - A\mathbf{h} \otimes \mathbf{g} \otimes \mathbf{y}'_4 + A\mathbf{h} \otimes \mathbf{n}'_4 + \mathbf{u}'_4$.

Then, the received signals at S_1 in kth block are written as

$$\begin{aligned} \mathbf{r}'_k &= A\mathbf{h} \otimes \mathbf{h} \otimes \mathbf{x}'_k + (-1)^{k+1} A\mathbf{h} \otimes \mathbf{g} \otimes \mathbf{y}'_k + A\mathbf{h} \otimes \mathbf{n}'_k + \mathbf{u}'_k \\ &= A\mathbf{a} \otimes \mathbf{x}'_k + (-1)^{k+1} A\mathbf{b} \otimes \mathbf{y}'_k + A\mathbf{h} \otimes \mathbf{n}'_k + \mathbf{u}'_k \end{aligned} \tag{3.3}$$

After discarding the padded zeros, the received signals in kth block of transmission at S_1 can be represented as

$$\mathbf{r}_k = A\mathcal{T}(\mathbf{a})\mathbf{x}_k + (-1)^{k+1} A\mathcal{T}(\mathbf{b})\mathbf{y}_k + A\mathcal{T}(\mathbf{h})\mathbf{n}_k + \mathbf{u}_k \tag{3.4}$$

where $\mathbf{r}_k$ is a $P \times 1$ received signal sequence, and $\mathbf{n}_k$ and $\mathbf{u}_k$ are the corresponding noises added to non-zero signals at R and S_1, respectively. $\mathcal{T}(\mathbf{a})$, $\mathcal{T}(\mathbf{b})$, and $\mathcal{T}(\mathbf{h})$ denote the Toeplitz channel matrices which consist of vectors $\mathbf{a}$, $\mathbf{b}$, and $\mathbf{h}$, respectively. Recall that the lengths of $\mathbf{a}$ and $\mathbf{b}$ are $L_a = 2L_h - 1$ and $L_b = L_h + L_g - 1$, then the minimum number of rows of channel matrix $\mathcal{T}(\mathbf{a})$ and $\mathcal{T}(\mathbf{b})$ is obtained as $P = 2\max(L_a, L_b) - 1 = 2L_h + 2\max(L_h, L_g) - 3$. For brevity of demonstration, we suppose $L_h \geq L_g$, (it has a similar result when $L_h < L_g$), so that $L_a \geq L_b$ and $L_x \geq L_y = L_b = L_h + L_g - 1$. Since the same length of the two terms of received signal transmitted from different sources is required, so that the length of the other transmitted signal $\mathbf{x}_k$ is calculated as $L_x = P - L_a$. Therefore, it is concluded that the length of $\mathbf{x}_k$ and $\mathbf{y}_k$ are $L_x = 2L_h - 2$, and $L_y = L_h + L_g - 1$, and the Toeplitz matrices

$\mathcal{T}(\mathbf{a})$, $\mathcal{T}(\mathbf{b})$, and $\mathcal{T}(\mathbf{h})$ can be written as

$$\mathcal{T}(\mathbf{a}) = \begin{pmatrix} a(0) & 0 & \cdots & 0 \\ a(1) & a(0) & \cdots & 0 \\ \vdots & a(1) & \ddots & \vdots \\ a(L_a-1) & \ddots & \ddots & a(0) \\ 0 & \ddots & \ddots & a(1) \\ \vdots & \ddots & \ddots & \vdots \\ 0 & \cdots & 0 & a(L_a-1) \end{pmatrix}_{P\times L_x} \quad \mathcal{T}(\mathbf{b}) = \begin{pmatrix} b(0) & 0 & \cdots & 0 \\ b(1) & b(0) & \cdots & 0 \\ \vdots & b(1) & \ddots & \vdots \\ b(L_b-1) & \ddots & \ddots & b(0) \\ 0 & \ddots & \ddots & b(1) \\ \vdots & \ddots & \ddots & \vdots \\ 0 & \cdots & 0 & b(L_b-1) \end{pmatrix}_{P\times L_y}$$

$$\mathcal{T}(\mathbf{h}) = \begin{pmatrix} h(0) & 0 & \cdots & 0 \\ h(1) & h(0) & \cdots & 0 \\ \vdots & h(1) & \ddots & \vdots \\ h(L_h-1) & \ddots & \ddots & h(0) \\ 0 & \ddots & \ddots & h(1) \\ \vdots & \ddots & \ddots & \vdots \\ 0 & \cdots & 0 & h(L_h-1) \end{pmatrix}_{P\times L_x}$$

For blind channel estimation, it is convenient to rewrite the channel model (3.4) as

$$\mathbf{r}_k = A\mathcal{T}(\mathbf{x}_k)\mathbf{a} + (-1)^{k+1}A\mathcal{T}(\mathbf{y}_k)\mathbf{b} + A\mathcal{T}(\mathbf{h})\mathbf{n}_k + \mathbf{u}_k \tag{3.5}$$

where we have used the fact:

$$\mathcal{T}(\mathbf{a})\mathbf{x}_k = \mathcal{T}(\mathbf{x}_k)\mathbf{a},\ \mathcal{T}(\mathbf{b})\mathbf{y}_k = \mathcal{T}(\mathbf{y}_k)\mathbf{b} \tag{3.6}$$

with the $P \times L_a$ and $P \times L_b$ Toeplitz signal matrix $\mathcal{T}(\mathbf{x}_k)$, $\mathcal{T}(\mathbf{y}_k)$ defined by

$$\mathcal{T}(\mathbf{x}_k) = \begin{pmatrix} x_k(0) & 0 & \cdots & 0 \\ x_k(1) & x_k(0) & \cdots & 0 \\ \vdots & x_k(1) & \ddots & \vdots \\ x_k(L_x-1) & \ddots & \ddots & x_k(0) \\ 0 & \ddots & \ddots & x_k(1) \\ \vdots & \ddots & \ddots & \vdots \\ 0 & \cdots & 0 & x_k(L_x-1) \end{pmatrix}_{P\times L_a} \quad \mathcal{T}(\mathbf{y}_k) = \begin{pmatrix} y_k(0) & 0 & \cdots & 0 \\ y_k(1) & y_k(0) & \cdots & 0 \\ \vdots & y_k(1) & \ddots & \vdots \\ y_k(L_y-1) & \ddots & \ddots & y_k(0) \\ 0 & \ddots & \ddots & y_k(1) \\ \vdots & \ddots & \ddots & \vdots \\ 0 & \cdots & 0 & y_k(L_y-1) \end{pmatrix}$$

3.3 Blind Receiver

In practical systems, the symbols transmitted from S_2 need to be detected at S_1 subjected to background noise, and vice versa. For brevity, we present the proposed receiver for S_1, while the same receiver designs are applicable to S_2. There are different ways for S_1 to blindly detect the symbols from S_2. One viable way is to apply least square error (LSE) detection rule to the received signals by doing an exhaustive search over the entire codeword. However, the complexity of this method exponentially increases as the size of constellation sets and transmission blocks, which is practically prohibitive. Therefore, a parallel iterative sphere decoder is also developed to deal with this complexity issue, such that the signaling and transmission scheme proposed can be applied in practice with larger number of transmission blocks.

3.3.1 LSE Receiver

LSE receiver at S_1 for our channel model deals with the following optimization problem:

$$\hat{\mathbf{Y}} = \arg\max_{\mathbf{S}(\mathbf{y})} \left(\mathbf{r}^H \mathbf{S} (\mathbf{S}^H \mathbf{S})^{-1} \mathbf{S}^H \mathbf{r} \right), \ \mathbf{S} = A \cdot (\mathbf{X}\ \mathbf{Y}) \tag{3.7}$$

where $\mathbf{X} = [\mathcal{T}(\mathbf{x}_1), \mathcal{T}(\mathbf{x}_2), \mathcal{T}(\mathbf{x}_3), \mathcal{T}(\mathbf{x}_4)]^{\mathrm{T}}$, and $\mathbf{Y} = [\mathcal{T}(\mathbf{y}_1), \mathcal{T}(-\mathbf{y}_2), \mathcal{T}(\mathbf{y}_3), \mathcal{T}(-\mathbf{y}_4)]^{\mathrm{T}}$ in which each sub-matrix is a Toeplitz matrix. The BER performance and computational complexity of this LSE receiver in frequency selective fading environment are examined in Section 3.4.

3.3.2 Parallel Iterative Sphere Decoder

In this subsection, inspired by [58], a parallel iterative sphere decoder is derived to reduce the computational complexity of blind receiver for two-way relay system in frequency-selective fading environment.

[59] proved that (3.7) is equivalent to the following least squares for jointly estimating

the channel coefficients and the signals.

$$\{\hat{\mathbf{Y}}, \hat{\bar{\mathbf{h}}}\} = \arg \min_{\mathbf{S}(\mathbf{Y}), \bar{\mathbf{h}}} ||\mathbf{r} - \mathbf{S}\bar{\mathbf{h}}||_2^2, \tag{3.8}$$

where $\bar{\mathbf{h}} = (\mathbf{a}, \mathbf{b})^{\mathrm{T}}$.

This optimization problem can be solved by employing iterative least squares with ML decoders. Given an initial estimate $\hat{\bar{\mathbf{h}}}^{(0)} = (\hat{\mathbf{a}}^{(0)}, \hat{\mathbf{b}}^{(0)})^{\mathrm{T}}$ of $\bar{\mathbf{h}}$, since $||\mathbf{r} - \mathbf{S}\bar{\mathbf{h}}^{(0)}||_2^2 = \sum_{k=1}^{4} ||\mathbf{r}_k - \big(\mathcal{T}(\mathbf{x}_k)\ \mathcal{T}(\mathbf{y}_k)\big)\bar{\mathbf{h}}^{(0)}||_2^2$, and the information symbols between each two codeword matrices $\mathcal{T}(\mathbf{y}_k)$ and $\mathcal{T}(\mathbf{y}_l)$ for $k \neq l$ are independent. The minimization problem of $||\mathbf{r} - \mathbf{S}\bar{\mathbf{h}}^{(0)}||_2^2$ with respect to the signal matrix $\mathbf{Y}$ is equivalent to each minimization problem with respect to the individual signal sub-matrix $\mathcal{T}(\mathbf{y}_k)$.

$$\begin{aligned} \hat{\mathbf{y}}_k^{(0)} &= \arg\min ||\mathbf{r}_k - \big(\mathcal{T}(\mathbf{x}_k)\ \mathcal{T}(\mathbf{y}_k)\big)\bar{\mathbf{h}}^{(0)}||_2^2 \\ &= \arg\min ||\mathbf{r}_k - \big(\mathcal{T}(\mathbf{a}^{(0)})\ \mathcal{T}(\mathbf{b}^{(0)})\big)\mathbf{s}_k||_2^2, \text{ for } k = 1, \cdots, 4 \end{aligned} \tag{3.9}$$

where $\mathbf{s}_k = (\mathbf{x}_k, \mathbf{y}_k)^{\mathrm{T}}$. Due to the structure of $\mathcal{T}(\mathbf{a}^{(0)})$ and $\mathcal{T}(\mathbf{b}^{(0)})$, the minimization problem of (3.9) can be efficiently solved using parallel sphere decoders or Viterbi algorithm if either L (suppose $L_a = L_b = L$) or the size of constellations is small. Once we have all the estimates $\hat{\mathbf{y}}_k^{(0)}$ of $\mathbf{y}_k$ for $k = 1, \cdots, 4$, then a better estimate of $\bar{\mathbf{h}}$ can be obtained by minimizing $||\mathbf{r} - \hat{\mathbf{S}}^{(0)}\bar{\mathbf{h}}||_2^2$ with respect to $\bar{\mathbf{h}}$, which gives $\hat{\bar{\mathbf{h}}}^{(1)} = \big((\mathbf{S}^{(0)})^H\mathbf{S}^{(0)}\big)^{-1}(\mathbf{S}^{(0)})^H\mathbf{r}$. We denote $\mathbf{S}^{(0)} = [\mathcal{T}(\mathbf{x}_1)^{\mathrm{T}}, \mathcal{T}(\hat{\mathbf{y}}_1^{(0)})^{\mathrm{T}}, \cdots, \mathcal{T}(\mathbf{x}_4)^{\mathrm{T}}, \mathcal{T}(\hat{\mathbf{y}}_4^{(0)})^{\mathrm{T}}]^{\mathrm{T}}$. We keep continuing this process until $||\hat{\bar{\mathbf{h}}}^{(m+1)} - \hat{\bar{\mathbf{h}}}^{(m)}||$ is less than a given threshold $\gamma > 0$. The above whole procedure can be summarized as the following proposition:

Proposition 1 *Iterative least squares with parallel sphere decoders or the Viterbi algorithm*

- *Initialization;* $\hat{\bar{\mathbf{h}}}^{(0)}$*, and estimate* $\hat{\mathbf{S}}^{(0)}$ *using the parallel lineal ML decoders or the Viterbi algorithm based on (3.9).*
- *Update:* $\hat{\bar{\mathbf{h}}}^{(m+1)} = ((\mathbf{S}^{(m)})^H\mathbf{S}^{(m)})^{-1}(\mathbf{S}^{(m)})^H\mathbf{r}$.
- *Stop: Continue until* $||\hat{\bar{\mathbf{h}}}^{(m+1)} - \hat{\bar{\mathbf{h}}}^{(m)}|| < \gamma$.

The performance of the decoding Proposition 1 heavily depends on how to properly choose the estimate of $\bar{\mathbf{h}}$, i.e., $\bar{\mathbf{h}}^{(0)}$. In this subsection, we develop an efficient algorithm to achieve an initial estimate of the channel. Let us consider the relationship between the inputs and outputs in four blocks of transmission, we have

$$\mathbf{r}_1 = A\mathcal{T}(\mathbf{x}_1)\mathbf{a} + A\mathcal{T}(\mathbf{y}_1)\mathbf{b} + \mathbf{u}_1 \tag{3.10}$$

$$\mathbf{r}_2 = A\mathcal{T}(\mathbf{x}_2)\mathbf{a} - A\mathcal{T}(\mathbf{y}_2)\mathbf{b} + \mathbf{u}_2 \tag{3.11}$$

$$\mathbf{r}_3 = A\mathcal{T}(\mathbf{x}_3)\mathbf{a} + A\mathcal{T}(\mathbf{y}_3)\mathbf{b} + \mathbf{u}_3 \tag{3.12}$$

$$\mathbf{r}_4 = A\mathcal{T}(\mathbf{x}_4)\mathbf{a} - A\mathcal{T}(\mathbf{y}_4)\mathbf{b} + \mathbf{u}_4 \tag{3.13}$$

First, we estimate $\bar{\mathbf{h}}$ in a forward processing direction, which means that we make use of the upper components of the Toeplitz signal matrix. After that we estimate $\bar{\mathbf{h}}$ in a reverse processing way by using the lower part of the signal matrix. Then, the first received signal components of (3.10), (3.11), (3.12), and (3.13) can be respectively written as

$$r_1(0) = Ax_1(0)a(0) + Ay_1(0)b(0) + u_1(0) \tag{3.14}$$

$$r_2(0) = Ax_2(0)a(0) - Ay_2(0)b(0) + u_2(0) \tag{3.15}$$

$$r_3(0) = Ax_3(0)a(0) + Ay_3(0)b(0) + u_3(0) \tag{3.16}$$

$$r_4(0) = Ax_4(0)a(0) - Ay_4(0)b(0) + u_4(0) \tag{3.17}$$

These received signals can be written in a more compact vector form as

$$\mathbf{r}_k(0) = \begin{pmatrix} r_1(0) \\ r_2(0) \\ r_3(0) \\ r_4(0) \end{pmatrix} = A \begin{pmatrix} x_1(0) & y_1(0) \\ x_2(0) & -y_2(0) \\ x_3(0) & y_3(0) \\ x_4(0) & -y_4(0) \end{pmatrix} \begin{pmatrix} a(0) \\ b(0) \end{pmatrix} + \begin{pmatrix} u_1(0) \\ u_2(0) \\ u_3(0) \\ u_4(0) \end{pmatrix} \tag{3.18}$$

$$= A\mathbf{B}_f(0)\bar{\mathbf{h}}_f(0) + \mathbf{u}_k(0) \tag{3.19}$$

where $\mathbf{B}_f(0) = \begin{pmatrix} x_1(0) & y_1(0) \\ x_2(0) & -y_2(0) \\ x_3(0) & y_3(0) \\ x_4(0) & -y_4(0) \end{pmatrix}$, and the subscript f refers to forward processing. Then,

the initial estimate of $\bar{\mathbf{h}}_f(0) = (a(0)\ b(0))^T$ is given by

$$\hat{\bar{\mathbf{h}}}_f^{(0)}(0) = \frac{1}{A}\hat{\mathbf{B}}_f^{+}(0)\mathbf{r}_k(0) \tag{3.20}$$

where $\hat{\mathbf{B}}_f^{+}(0)$ denotes the pseudo-inverse of matrix $\hat{\mathbf{B}}_f(0)$, and

$$\hat{\mathbf{B}}_f(0) = \begin{pmatrix} x_1(0) & \hat{y}_{1,f}(0) \\ x_2(0) & -\hat{y}_{2,f}(0) \\ x_3(0) & \hat{y}_{3,f}(0) \\ x_4(0) & -\hat{y}_{4,f}(0) \end{pmatrix} \tag{3.21}$$

where $\hat{y}_{1,f}(0)$, $\hat{y}_{2,f}(0)$, $\hat{y}_{3,f}(0)$, and $\hat{y}_{4,f}(0)$ can be obtained by solving the following optimization problem:

$$\{\hat{y}_{1,f}(0), \hat{y}_{2,f}(0), \hat{y}_{3,f}(0), \hat{y}_{4,f}(0)\} = \arg \max_{\substack{y_1(0)\in\mathcal{S}_2, y_2(0)\in\mathcal{S}_1, \\ y_3(0)\in\mathcal{S}_4, y_4(0)\in\mathcal{S}_3}} \mathbf{r}_k(0)\mathbf{B}_f(0)\mathbf{B}_f^{+}(0)\mathbf{r}_k(0) \tag{3.22}$$

In general, suppose that the estimates for both $\bar{\mathbf{h}}(i)$ and the signals $\mathbf{y}_k(i)$ are all correct, i.e., $\hat{\bar{\mathbf{h}}}_f^{(0)}(i) = \bar{\mathbf{h}}(i)$, and $\hat{\mathbf{y}}_{k,f}(i) = \mathbf{y}_k(i)$ for $i = 1, 2, \cdots, L_a$. Now, consider the $(n+1)$th signal components respectively in (3.10) to (3.13),

$$r_1(n) = A\Big(\sum_{i=1}^{n} x_1(n+1-i)a(i-1) + x_1(0)a(n) + \sum_{i=1}^{n} y_1(n+1-i)b(i-1) + \hat{y}_1(0)b(n)\Big) + u_1(n) \tag{3.23}$$

$$r_2(n) = A\Big(\sum_{i=1}^{n} x_2(n+1-i)a(i-1) + x_2(0)a(n) - \sum_{i=1}^{n} y_2(n+1-i)b(i-1) - \hat{y}_2(0)b(n)\Big) + u_2(n) \tag{3.24}$$

$$r_3(n) = A\Big(\sum_{i=1}^{n} x_3(n+1-i)a(i-1) + x_3(0)a(n) + \sum_{i=1}^{n} y_3(n+1-i)b(i-1) + \hat{y}_3(0)b(n)\Big) + u_3(n) \tag{3.25}$$

$$r_4(n) = A\Big(\sum_{i=1}^{n} x_4(n+1-i)a(i-1) + x_4(0)a(n) - \sum_{i=1}^{n} y_4(n+1-i)b(i-1) - \hat{y}_4(0)b(n)\Big) + u_4(n) \tag{3.26}$$

which can equivalently be rewritten as

$$w_1(n) = r_1(n) - A\Big(\sum_{i=2}^{n} x_1(n+1-i)a(i-1) - \sum_{i=2}^{n} y_1(n+1-i)b(i-1)\Big)$$
$$= A\Big(x_1(n)\hat{a}_f(0) + x_1(0)a(n) + y_1(n)\hat{b}_f(0) + \hat{y}_{1,f}(0)b(n)\Big) + u_1(n) \tag{3.27}$$

$$w_2(n) = r_2(n) - A\Big(\sum_{i=2}^{n} x_2(n+1-i)a(i-1) + \sum_{i=2}^{n} y_2(n+1-i)b(i-1)\Big)$$
$$= A\Big(x_2(n)\hat{a}_f(0) + x_2(0)a(n) - y_2(n)\hat{b}_f(0) - \hat{y}_{2,f}(0)b(n)\Big) + u_2(n) \tag{3.28}$$

$$w_3(n) = r_3(n) - A\Big(\sum_{i=2}^{n} x_3(n+1-i)a(i-1) - \sum_{i=2}^{n} y_3(n+1-i)b(i-1)\Big)$$
$$= A\Big(x_3(n)\hat{a}_f(0) + x_3(0)a(n) + y_3(n)\hat{b}_f(0) + \hat{y}_{3,f}(0)b(n)\Big) + u_3(n) \tag{3.29}$$

$$w_4(n) = r_4(n) - A\Big(\sum_{i=2}^{n} x_4(n+1-i)a(i-1) + \sum_{i=2}^{n} y_4(n+1-i)b(i-1)\Big)$$
$$= A\Big(x_4(n)\hat{a}_f(0) + x_4(0)a(n) - y_4(n)\hat{b}_f(0) - \hat{y}_{4,f}(0)b(n)\Big) + u_4(n) \tag{3.30}$$

Let $\mathbf{w}_k(n) = \Big(w_1(n)\ w_2(n)\ w_3(n)\ w_4(n)\Big)^T$, then we can further rewrite the equations above as:

$$\mathbf{w}_k(n) = A\begin{pmatrix} x_1(n) & y_1(n) \\ x_2(n) & -y_2(n) \\ x_3(n) & y_3(n) \\ x_4(n) & -y_4(n) \end{pmatrix}\begin{pmatrix} \hat{a}_f(0) \\ \hat{b}_f(0) \end{pmatrix} + A\begin{pmatrix} x_1(0) & \hat{y}_{1,f}(0) \\ x_2(0) & -\hat{y}_{2,f}(0) \\ x_3(0) & \hat{y}_{3,f}(0) \\ x_4(0) & -\hat{y}_{4,f}(0) \end{pmatrix}\begin{pmatrix} a(n) \\ b(n) \end{pmatrix} + \begin{pmatrix} u_1(n) \\ u_2(n) \\ u_3(n) \\ u_4(n) \end{pmatrix} \tag{3.31}$$

$$= A\mathbf{B}_f(n)\hat{\bar{\mathbf{h}}}_f(0) + A\hat{\mathbf{B}}_f(0)\bar{\mathbf{h}}_f(n) + \mathbf{u}_k(n) \tag{3.32}$$

where $\mathbf{B}_f(n) = \begin{pmatrix} x_1(n) & y_1(n) \\ x_2(n) & -y_2(n) \\ x_3(n) & y_3(n) \\ x_4(n) & -y_4(n) \end{pmatrix}$. Therefore, the initial least square error estimate of $\bar{\mathbf{h}}_f(n) = (a(n)\ b(n))^T$ in forward processing is given by

$$\hat{\bar{\mathbf{h}}}_f^{(0)}(n) = \frac{1}{A}\hat{\mathbf{B}}_f^{+}(0)\mathbf{w}_k(n) - \hat{\mathbf{B}}_f^{+}(0)\hat{\mathbf{B}}_f(n)\hat{\bar{\mathbf{h}}}_f^{(0)}(0) \tag{3.33}$$

where

$$\hat{\mathbf{B}}_f(n) = \begin{pmatrix} x_1(n) & \hat{y}_{1,f}(n) \\ x_2(n) & -\hat{y}_{2,f}(n) \\ x_3(n) & \hat{y}_{3,f}(n) \\ x_4(n) & -\hat{y}_{4,f}(n) \end{pmatrix} \tag{3.34}$$

where $\hat{y}_{1,f}(n)$, $\hat{y}_{2,f}(n)$, $\hat{y}_{3,f}(n)$, and $\hat{y}_{4,f}(n)$ can be obtained by solving the following optimization problem:

$$\{\hat{y}_{1,f}(n), \hat{y}_{2,f}(n), \hat{y}_{3,f}(n), \hat{y}_{4,f}(n)\} =$$

$$\arg \min_{\substack{y_1(n)\in\mathcal{S}_2, y_2(n)\in\mathcal{S}_1, \\ y_3(n)\in\mathcal{S}_4, y_4(n)\in\mathcal{S}_3}} ||\mathbf{w}_k(n) - A\mathbf{B}_f(n)\hat{\tilde{\mathbf{h}}}_f(0) - \hat{\mathbf{B}}_f(0)\hat{\mathbf{B}}_f^+(0)\mathbf{w}_k(n) + A\hat{\mathbf{B}}_f(0)\hat{\mathbf{B}}_f^+(0)\mathbf{B}_f(n)\hat{\tilde{\mathbf{h}}}_f(n)||^2 \tag{3.35}$$

Due to the structure of $\mathcal{T}(\mathbf{x}_k)$ and $\mathcal{T}(\mathbf{y}_k)$, we can also estimate $\bar{\mathbf{h}}$ in the reverse processing direction. The last received signal components of (3.10), (3.11), (3.12), and (3.13) can be respectively written as

$$\mathbf{r}_k(2L-1) = A \begin{pmatrix} x_1(2L-1) & y_1(2L-1) \\ x_2(2L-1) & -y_2(2L-1) \\ x_3(2L-1) & y_3(2L-1) \\ x_4(2L-1) & -y_4(2L-1) \end{pmatrix} \begin{pmatrix} a(2L-1) \\ b(2L-1) \end{pmatrix} + \begin{pmatrix} u_1(2L-1) \\ u_2(2L-1) \\ u_3(2L-1) \\ u_4(2L-1) \end{pmatrix} \tag{3.36}$$

$$= A\mathbf{B}_r(0)\bar{\mathbf{h}}_r(0) + \mathbf{u}_k(2L-1) \tag{3.37}$$

where $\mathbf{B}_r(0) = \begin{pmatrix} x_1(2L-1) & y_1(2L-1) \\ x_2(2L-1) & -y_2(2L-1) \\ x_3(2L-1) & y_3(2L-1) \\ x_4(2L-1) & -y_4(2L-1) \end{pmatrix}$, and the subscript r refers to the reverse processing. Then, the initial estimate of $\bar{\mathbf{h}}_r(0) = (a(2L-1)\ b(2L-1))^T$ is given by

$$\hat{\bar{\mathbf{h}}}_r^{(0)}(0) = \frac{1}{A}\hat{\mathbf{B}}_r^+(0)\mathbf{r}_k(2L-1) \tag{3.38}$$

and

$$\hat{\mathbf{B}}_r(0) = \begin{pmatrix} x_1(2L-1) & \hat{y}_{1,r}(2L-1) \\ x_2(2L-1) & -\hat{y}_{2,r}(2L-1) \\ x_3(2L-1) & \hat{y}_{3,r}(2L-1) \\ x_4(2L-1) & -\hat{y}_{4,r}(2L-1) \end{pmatrix} \tag{3.39}$$

where $\hat{y}_{1,r}(2L-1)$, $\hat{y}_{2,r}(2L-1)$, $\hat{y}_{3,r}(2L-1)$, and $\hat{y}_{4,r}(2L-1)$ can be obtained by solving the following optimization problem:

$$\begin{aligned} &\{\hat{y}_{1,r}(2L-1),\hat{y}_{2,r}(2L-1),\hat{y}_{3,r}(2L-1),\hat{y}_{4,r}(2L-1)\} \\ &\quad = \arg \max_{\substack{y_1(2L-1)\in\mathcal{S}_2, y_2(2L-1)\in\mathcal{S}_1, \\ y_3(2L-1)\in\mathcal{S}_4, y_4(2L-1)\in\mathcal{S}_3}} \mathbf{r}_k(2L-1)\mathbf{B}_r(0)\mathbf{B}_r^+(0)\mathbf{r}_k(2L-1) \end{aligned} \tag{3.40}$$

Then, taking the similar steps as we do for the forward processing, we have

$$\mathbf{w}_k(n) = A\mathbf{B}_r(n)\hat{\bar{\mathbf{h}}}_r(0) + A\hat{\mathbf{B}}_r(0)\bar{\mathbf{h}}_r(n) + \mathbf{u}_k(n) \tag{3.41}$$

The initial least square estimate of $\bar{\mathbf{h}}_r(n) = (a(n)\ b(n))^T$ can be obtained by

$$\hat{\bar{\mathbf{h}}}_r^{(0)}(n) = \frac{1}{A}\hat{\mathbf{B}}_r^+(0)\mathbf{w}_k(n) - \hat{\mathbf{B}}_r^+(0)\hat{\mathbf{B}}_r(n)\hat{\bar{\mathbf{h}}}_r^{(0)}(0) \tag{3.42}$$

where

$$\hat{\mathbf{B}}_r(n) = \begin{pmatrix} x_1(n) & \hat{y}_{1,r}(n) \\ x_2(n) & -\hat{y}_{2,r}(n) \\ x_3(n) & \hat{y}_{3,r}(n) \\ x_4(n) & -\hat{y}_{4,r}(n) \end{pmatrix} \tag{3.43}$$

where $\hat{y}_{1,r}(n)$, $\hat{y}_{2,r}(n)$, $\hat{y}_{3,r}(n)$, and $\hat{y}_{4,r}(n)$ can be obtained by solving the following optimization problem:

$$\begin{aligned} &\{\hat{y}_{1,r}(n), \hat{y}_{2,r}(n), \hat{y}_{3,r}(n), \hat{y}_{4,r}(n)\} = \\ &\arg \min_{\substack{y_1(n)\in\mathcal{S}_2, y_2(n)\in\mathcal{S}_1, \\ y_3(n)\in\mathcal{S}_4, y_4(n)\in\mathcal{S}_3}} ||\mathbf{w}_k(n) - A\mathbf{B}_r(n)\hat{\bar{\mathbf{h}}}_r(0) - \hat{\mathbf{B}}_r(0)\hat{\mathbf{B}}_r^+(0)\mathbf{w}_k(n) + A\hat{\mathbf{B}}_r(0)\hat{\mathbf{B}}_r^+(0)\mathbf{B}_r(n)\hat{\bar{\mathbf{h}}}_r(0)||^2 \end{aligned} \tag{3.44}$$

Now, we have two estimates of $\mathbf{y}_k$, $k = 1, \cdots, 4$ by doing iterative estimation processed in two different directions for the signal matrix, we can compare $\mathbf{r}^H \hat{\mathbf{S}}_f (\hat{\mathbf{S}}_f^H \hat{\mathbf{S}}_f)^{-1} \hat{\mathbf{S}}_f^H \mathbf{r}$ and $\mathbf{r}^H \hat{\mathbf{S}}_r (\hat{\mathbf{S}}_r^H \hat{\mathbf{S}}_r)^{-1} \hat{\mathbf{S}}_r^H \mathbf{r}$, and choose the greater one in order to decrease the loss of diversity, where $\hat{\mathbf{S}}_f = A \cdot (\mathbf{X}\ \hat{\mathbf{Y}}_f)$, and $\hat{\mathbf{S}}_r = A \cdot (\mathbf{X}\ \hat{\mathbf{Y}}_r)$. Then, the initial estimate of channel coefficients for this parallel iterative sphere decoder is given as

$$\hat{\tilde{\mathbf{h}}}^{(0)} = \begin{cases} (\hat{\mathbf{S}}_f^H \hat{\mathbf{S}}_f)^{-1} \hat{\mathbf{S}}_f^H \mathbf{r} & \text{if } \mathbf{r}^H \hat{\mathbf{S}}_f (\hat{\mathbf{S}}_f^H \hat{\mathbf{S}}_f)^{-1} \hat{\mathbf{S}}_f^H \mathbf{r} > r^H \hat{\mathbf{S}}_r (\hat{\mathbf{S}}_r^H \hat{\mathbf{S}}_r)^{-1} \hat{\mathbf{S}}_r^H \mathbf{r} \\ (\hat{\mathbf{S}}_r^H \hat{\mathbf{S}}_r)^{-1} \hat{\mathbf{S}}_r^H \mathbf{r} & \text{if } \mathbf{r}^H \hat{\mathbf{S}}_f (\hat{\mathbf{S}}_f^H \hat{\mathbf{S}}_f)^{-1} \hat{\mathbf{S}}_f^H \mathbf{r} < r^H \hat{\mathbf{S}}_r (\hat{\mathbf{S}}_r^H \hat{\mathbf{S}}_r)^{-1} \hat{\mathbf{S}}_r^H \mathbf{r} \end{cases} \tag{3.45}$$

3.4 Simulation Results

In this section, we present simulation results to verify the derived receivers. In all our computer simulations, we fix $L_h = L_g = 2$, such that one transmission sequence of both $\mathbf{x}_k$ and $\mathbf{y}_k$ consist of three signals, namely $\mathbf{x}_k = \big(x_k(0), x_k(1), x_k(2)\big)^{\mathrm{T}}$, $\mathbf{y}_k = \big(y_k(0), y_k(1), y_k(2)\big)^{\mathrm{T}}$, $k = 1, 2, 3, 4$. The symbols error rates (SERs) are plotted by averaging over 10^6 random channel realizations. The channel coefficients are generated by i.i.d. zero-mean CSCG random variables with unit variance.

SER Performance: In the proposed signaling scheme, the transmitted PSK symbols are from constellation sets with different sizes. Therefore, the bit rate of each time frame of transmission is different. The constellation selection Method 2 in [26] is utilized here to pick the same number of constellation points from sets $\mathcal{S}_1, \cdots, \mathcal{S}_4$ in order to achieve a uniform bit rate for the practical communication system. The specific constellation points in $\mathcal{S}_i$, $i = 1, \cdots 4$, are given, respectively, by (2,4),(1,3),(1,3),(0,6).

Fig.3.2 plots the SERs for the blind LSE receiver using the constellation selection and a training-based receiver. For the purpose of the comparison, the SERs of coherent ML detection are also included, whereby the perfect channel state information is assumed to be available. The SER marked by "ML-Coherent-Selection" is plotted using constellation points given above, and the "ML-Coherent-BPSK" is obtained for binary phase shift keying (BPSK) symbols. In the training-based scheme, six pilot symbols need to be transmitted from each source node, and a least-square approach is applied in estimating the channel

coefficients. For a fair comparison, the same information bits are transmitted per time block for all systems. The system with blind LSE receiver transmits two-point constellation symbols with three bits per time block transmitted. The system with training-based receiver transmits quadrature phase shift keying (QPSK) signals in four-block of transmission (two time blocks are required to transmit the pilots in a four-block transmission, and the similar explanation is given in detail in 2.7). In this case, the bit rate of training-based scheme is three bits per time block as well, which is fairly comparable with the blind LSE receiver. Fig.3.2 shows that the blind LSE receiver provides a significant gain compared with the training-based receiver.

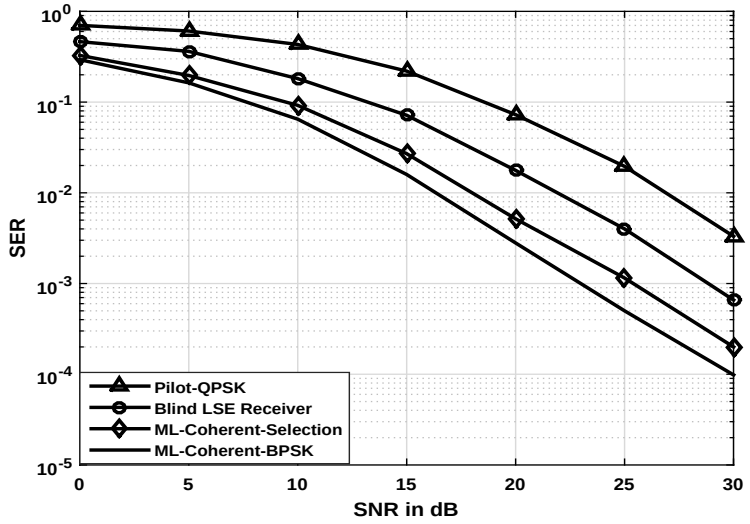

Figure 3.2: SER for LSE blind detector

As explained in Section 3.3, the complexity of the derived parallel sphere decoder linearly increases instead of exponentially increased as the number of transmission blocks increases, which makes it feasible for practical systems to implement the proposed blind transmission and signaling scheme with more transmission blocks. Fig.3.3 plots the SERs for the iterative sphere decoder and LSE receiver with different number of transmission blocks using the same constellation selection given by (2,4),(1,3),(1,3),(0,6). Fig.3.3 suggests that

the iterative detector with larger transmission blocks outperforms that with less transmission blocks, since it is more accurate to estimate the channel coefficients that stay unchanged in longer transmission time. It can be observed that the SER of iterative sphere decoder becomes closer to that of LSE receiver as the number of transmission blocks increases, provides almost identical performance as LSE receiver with eight transmission blocks, and is only 1-2 dB away from that for the ML coherent detection with perfect knowledge of CSI.

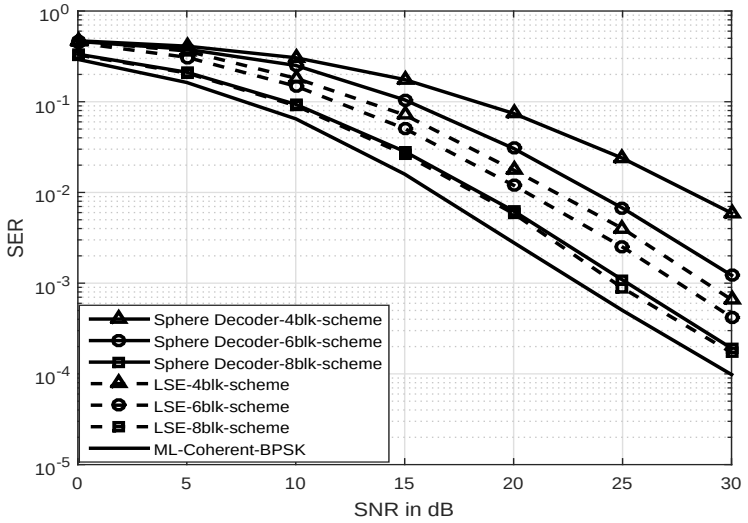

Figure 3.3: SER for parallel iterative sphere decoder

Complexity Analysis: In this subsection, we compare the computational complexity between the LSE receiver and the iterative sphere decoder. For the LSE receiver, since the symbol detection is implemented by doing exhaustive search over the entire codeword, the time complexity of LSE blind receiver can be expressed as $T_{LSE}(n) = O(n^{N_b N_s})$, where N_b denotes the block numbers of the transmission scheme (the number of blocks that the channels remain unchanged), and N_s denotes the number of symbols that one source node transmits to another in each block. For the derived parallel iterative sphere decoder, since it is simplifies the minimization problem by operating N_b parallel sub-minimization problem, the time complexity of sphere decoder is summarized as $T_{SD}(n) = O(N_b n^{N_s})$. It can be

concluded that the complexity of derived iterative sphere decoder linearly increases as N_b increases comparing to exponentially increase of the complexity of LSE receiver.

Table 3.2: Number of Flops Algorithms for Various Operations

Function	Operation	Algorithm
$flop\_sqrt$	$\sqrt{a}$	$f = 8$
$flop\_div$	a/b	$f = 8$
$flop\_exp$	$\exp(a)$	$f = 40$
$flop\_log$	$\log(a)$	$f = 20$
$flop\_mul(r, m, c)$	$\mathbf{A} \cdot \mathbf{B}$, $\mathbf{A} : r \times m$, $\mathbf{B} : m \times c$	$f = r \cdot c \cdot (2m - 1)$
$flop\_lu(n)$	LU($\mathbf{C}$), $\mathbf{C} : n \times n$	$f = n(n - 0.5)(n - 1) + (n - 1)flop\_div$
$flop\_inv(n)$	$\mathbf{D}^{-1}$, where $\mathbf{D} : n \times n$	$f = flop\_lu(n) + 2flop\_mul(n, n, n) - nflop\_div$

In order to evaluate the analysis of computational complexity above, the number of floating-point operations per second (flops) is calculated and compared for both proposed blind receivers in $i5$ CPU platform. The major algorithm of calculating number of flops for matrix are listed in Table 3.2, where f denotes the number of flops.. Fig.3.4 plots the number of flops against the transmission schemes with different number of blocks in one trial of simulation. This result suggests that the derived sphere decoder has a significant lower complexity than the LSE receiver in the case of four transmission block scheme, and grows linearly with the increasing of the number of blocks. It shows an enormous advantage for implementation due to the complexity of LSE receiver increasing exponentially.

3.5 Conclusion

This chapter considers an AF two-way relay network with frequency-selective fading channels. An effective signaling and transmission scheme is proposed to achieve the unique identifiability of frequency selective fading channel coefficients and transmitted symbols in noise-free environment. An LSE blind receiver is proposed for the Rayleigh fading channels

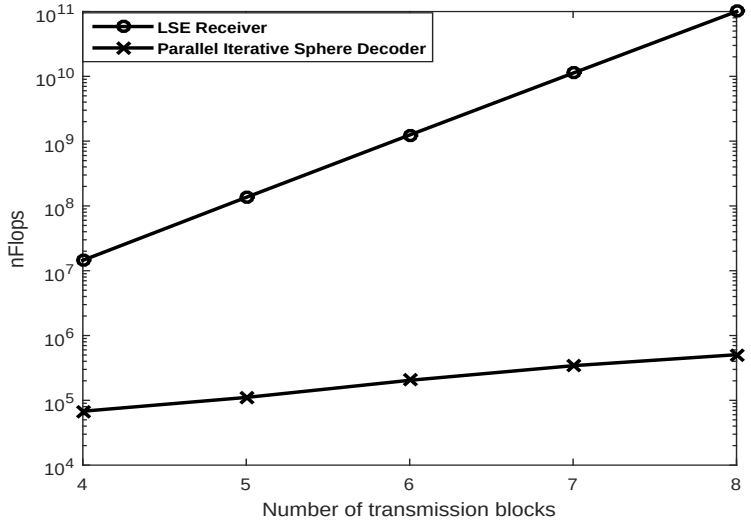

Figure 3.4: Complexity comparison between two blind detectors

with Gaussian noise. In order to reduce the complexity of symbol detection, a parallel iterative sphere decoder with initial channel estimate is derived. Simulation results show that the blind LSE detector outperforms the training-based scheme in terms of same data rate. The complexity comparison results suggest that the derived sphere decoder significantly reduce the implementation complexity compared to the LSE detector.

CHAPTER 4

Time-Reversal Space Time Block Coded Blind Detection Design over Frequency-Selective Fading Channels: Two Antenna AF Relay Network without Direct Link

4.1 Introduction

Relay networks have drawn a large number of attention in the past decades since they exploit diversity and spatial gain by allowing users to share their antennas and transmit cooperatively, such that the performance of wireless communication systems can be enhanced [12,60,61]. Recently, two-way relaying scheme has been studied due to its spectral efficiency comparing to the conventional one-way relaying [4]. In two-way relay networks, source nodes exchange information via one or more relay nodes [5, 6]. The source nodes transmit the signals to the relays simultaneously, and the relay nodes forward the received signals to the source based on two popular relaying protocols, which are amplify-and-forward (AF) [62–65] and decode-and-forward (DF) [66,67], respectively. In an AF relaying network, the relay node scales the sum of the signals received from the source nodes by multiplying the amplification coefficient, then transmits the scaled version of the signal to the source nodes, while in a DF protocol, the relay node first decodes the received signal, and then sends the re-encoded signal. The AF relaying protocol has been popular due to its simplicity of implementation comparing to the DF relaying. Nonetheless, the AF relaying protocol requires the knowledge of channel state information (CSI) for all links.

In practice, CSI can hardly be obtained at source nodes. Therefore, various channel estimations based on pilots or training have been investigated for two-way relay systems [14–16]. Nonetheless, these research works only focus on flat fading environment, which cannot handle the multi-path fading. Recently, blind estimations have been discussed for frequency selective fading two-way relay systems in which the CSI is assumed unavailable at the receivers [20–22]. However, these pilot-based or training-assisted blind estimation

algorithms have achieved progress at the cost of certain spectral efficiency to transmit the training symbols, since these estimators are typically associated with a *phase or scalar* ambiguity, even in noise-free transmissions. As a result, a short training sequence has to be transmitted to resolve the inherent phase or scalar ambiguity. Consequently, unique identification of channel coefficients and transmitted signals in noise-free transmission is crucial to an efficient blind detection transmission design in noisy transmissions.

Two effective signaling and transmission schemes are reported in [26,27], respectively, to deal with the ambiguity issues for the blind detections in two-way relay systems, in which flat fading channels are assumed between each nodes. In radio propagation, the fading channels are not always flat. When the coherence bandwidth of channel is less than the signal bandwidth, different frequency components of signals experience different magnitude of fading, which is frequency-selective fading. This paper focuses on a two-way relay system model in which the channels between each nodes are assumed frequency selective fading. The systems produce the intersymbol interference introduced by transmitting the data stream in equal-size blocks. Some redundancy is padded to each block before transmission in order to eliminate interblock interference. There exists many methods of adding redundancy [52,53], however in this paper, we apply zero-padding redundancy scheme to alleviate the interblock interference. To solve the channel ambiguity issue, we propose an effective signaling and transmission scheme for the frequency-selective two-way relay system with zero-padded block transmission, in which neither the transmitter nor the receiver has the CSI.

In order to enhance the performance of the two-way relay system by exploring the diversity gain, the multiple-input multiple-output (MIMO) technique has been widely utilized [68–72]. In the system studied in this chapter, multiple antennas are deployed at the source nodes, and time-reversal space time block code (TR-STBC) [73–76] is then applied to deal with the multi-path fading. An iterative sphere decoder is finally derived to approximate the LSE detection for Rayleigh fading channels and Gaussian noise.

4.2 System Model

Fig.4.1 and Fig.4.2 illustrate a frequency-selective fading two-way relay system equipped with two antennas at source nodes S_1, S_2 and single antenna at relay node R, where two source nodes exchange information with each other with the assistance of the relay. Time-reversal space-time block codes extend conventional STBC for transmission over frequency-selective channels by encoding time-reversed contiguous blocks of symbols. Denote the time domain signals $\mathbf{x}_k(i)$, $\mathbf{y}_k(i)$ that are transmitted in kth ($k = 1, 2, 3$) block at the ith ($i = 1, 2$) transmit antenna. They are generated from S_1 and S_2 respectively by taking the N-point inverse fast Fourier transform (IFFT) of the signals in frequency domain $\mathbf{s}_k(i) = [s_k(i, 0), ..., s_k(i, N-1)]$, and $\mathbf{u}_k(i) = [u_k(i, 0), ..., u_k(i, N-1)]$. Each transmitted signal sequence is divided to two sub-sequence $\mathbf{x}_{k,l}(i) = [x_{k,l}(i, 0), ..., x_{k,l}(i, N-1)]$, and $\mathbf{y}_{k,l}(i) = [y_{k,l}(i, 0), ..., y_{k,l}(i, N-1)]$, where $l = 1, 2$ indexes the sub-sequence transmitted in each TR-STBC block.

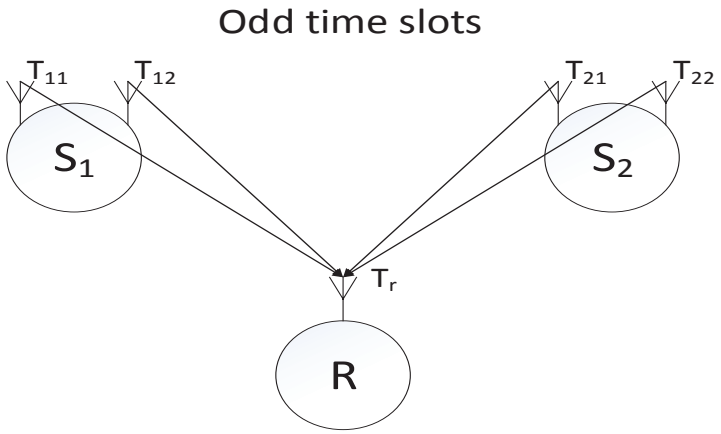

Figure 4.1: TR-STBC Two-Way Relay Transmission in Odd Time Slots

An effective signaling and transmission scheme using PSK constellations is proposed in this chapter. The transmission scheme we propose is carried out in three transmission blocks (twelve time slots, since each block needs four time slots to operate TR-STBC) using

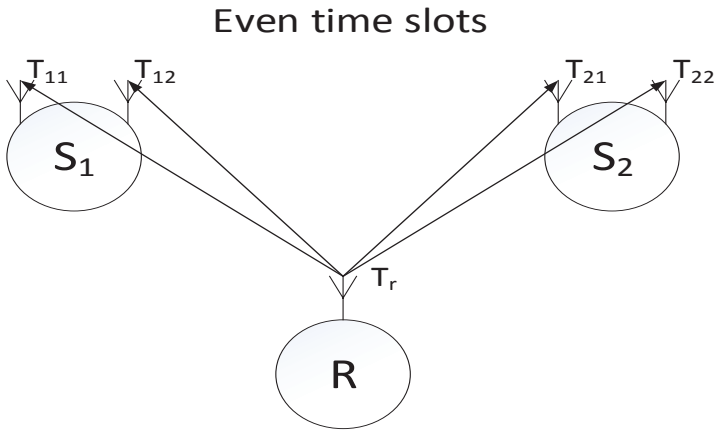

Figure 4.2: TR-STBC Two-Way Relay Transmission in Even Time Slots

four PSK constellations. Two symbol sequences are exchanged between the source nodes in each block.

It should be pointed that if the channel coherence time is not long enough and the channel gains fail to remain unchanged in three blocks of transmission, the proposed scheme cannot be applied. Conversely, if the channel gains remain unchanged in more than three blocks, the proposed transmission and detection schemes can also be applied.

Denote the antennas at S_1 by T_{11}, T_{12}, the antennas at S_2 by T_{21}, T_{22}, and the antennas at R by T_r, respectively. The reciprocal channels between each antennas are assumed, which means that the channel coefficient from one antenna to another is identical to that in the reverse channel back to the same antenna. The channel coefficients from T_{11} and T_{12} to R are denoted by $\mathbf{h}(1)$ and $\mathbf{h}(2)$, and the channel coefficients from T_{21} and T_{22} to R are denoted by $\mathbf{g}(1)$ and $\mathbf{g}(2)$. We assume that the channels of the different antennas from the same source node to the relay have the same length, which are denoted as L_h and L_g, respectively. Then the channel impulse responses are denoted as $\mathbf{h}(i) = \big(h(i,0), h(i,1), ..., h(i,L_h-1)\big)^{\mathrm{T}}$, and $\mathbf{g}(i) = \big(g(i,0), g(i,1), ..., g(i,L_g-1)\big)^{\mathrm{T}}$, $i = 1, 2$, and each component of $\mathbf{h}(i)$, $\mathbf{g}(i)$ are zero mean and $1/L_h$, $1/L_g$ variance distributed, respectively. The channel coefficients are not known at either both source nodes or the relay. Each source

node recovers symbols from the other source based on prior knowledge of its own transmitted symbols in the signals forwarded by the relay. The system operates in a half duplex mode in which the transmissions and receptions are not carried out simultaneously. The channel coefficients do not change within three time blocks of observation; after that, they change to new independent values according to Rayleigh fading and are fixed in the next block, and so on.

Let p_i, $i = 1, 2, 3, 4$, denote pairwise coprime positive integers, and let constellation set $\mathcal{S}_i$ collect all p_i-PSK symbols, i.e., $\mathcal{S}_i = \{\exp(j2\pi m_i/p_i, m_i = 0, ..., p_i - 1\}$. The proposed signaling and transmission scheme in one block is shown in Table 4.1, where $\mathbf{F}$ denotes the IFFT matrix.

Then, we can obtain that $\mathbf{x}_{k,2}(1) = -\mathbf{P}\mathbf{x}_{k,1}(2)^*$, and $\mathbf{x}_{k,2}(2) = \mathbf{P}\mathbf{x}_{k,1}(1)^*$, where $\mathbf{P}$ is the time reversal precoding matrix, which is shown as:

$$\mathbf{P} = \begin{pmatrix} 1 & 0 & 0 & 0 & \cdots \\ 0 & 0 & 0 & \cdots & 1 \\ 0 & 0 & \cdots & 1 & 0 \\ \cdots & \cdots & \cdots & \cdots & \cdots \\ 0 & 1 & 0 & \cdots & 0 \end{pmatrix} \tag{4.1}$$

It should be pointed out that the zero-padding scheme applied in this system is similar with that has been presented in Chapter 3. In this chapter, the signals with padded zeros are used for notation simplicity.

In the first time slot, T_{11}, T_{12}, T_{21}, and T_{21} transmit signals $\mathbf{x}_{1,1}(1)$, $\mathbf{x}_{1,1}(2)$, $\mathbf{y}_{1,1}(1)$, and $\mathbf{y}_{1,1}(2)$, respectively. The received signal at the relay is $\mathbf{r}_{R_{1,1}} = \mathbf{h}(1) \otimes \mathbf{x}_{1,1}(1) + \mathbf{h}(2) \otimes \mathbf{x}_{1,1}(2) + \mathbf{g}(1) \otimes \mathbf{y}_{1,1}(1) + \mathbf{g}(2) \otimes \mathbf{y}_{1,1}(2) + \mathbf{n}_{1,1}$.

In the second time slot, the relay transmits $A\mathbf{r}_{R_{1,1}}$ to four antennas at both source nodes. For brevity, we focus on the received signals at T_{11} for the illustration, while similar results hold for T_{12}, T_{21}, and T_{21} as well. The received signal at T_{11} is $\mathbf{r}_{1,1} = A\mathbf{h}(1) \otimes \mathbf{r}_{R_{1,1}} + \mathbf{u}_{1,1} = A\mathbf{h}(1) \otimes \mathbf{h}(1) \otimes \mathbf{x}_{1,1}(1) + A\mathbf{h}(1) \otimes \mathbf{h}(2) \otimes \mathbf{x}_{1,1}(2) + A\mathbf{h}(1) \otimes \mathbf{g}(1) \otimes \mathbf{y}_{1,1}(1) + A\mathbf{h}(1) \otimes \mathbf{g}(2) \otimes \mathbf{y}_{1,1}(2) + A\mathbf{h}(1) \otimes \mathbf{n}_{1,1} + \mathbf{u}_{1,1}$, where $A = 1/(2 + \sigma^2)^{1/2}$ is the amplification coefficient

Table 4.1: Signalling and Transmission Scheme for TR-STBC Frequency-Selective Fading Two-Way Relay System without Direct Link

Time slot	Transmitting/receiving	Symbols and constellations
1	$\mathrm{T}_{11} \overset{\mathbf{x}_{1,1}(1)=\mathbf{F}\mathbf{s}_1(1)}{\longrightarrow} \mathrm{T}_r$, $\mathrm{T}_{12} \overset{\mathbf{x}_{1,1}(2)=\mathbf{F}\mathbf{s}_1(2)}{\longrightarrow} \mathrm{T}_r$, $\mathrm{T}_{21} \overset{\mathbf{y}_{1,1}(1)=\mathbf{F}\mathbf{u}_1(1)}{\longrightarrow} \mathrm{T}_r$, $\mathrm{T}_{22} \overset{\mathbf{y}_{1,1}(2)=\mathbf{F}\mathbf{u}_1(2)}{\longrightarrow} \mathrm{T}_r$	$\mathbf{x}_{1,l}(i) \in \mathcal{S}_1$ $\mathbf{y}_{1,l}(i) \in \mathcal{S}_2$
2	$\mathrm{T}_r \overset{\mathbf{x}_{1,1}(1),\mathbf{x}_{1,1}(2),\mathbf{y}_{1,1}(1),\mathbf{y}_{1,1}(2)}{\longrightarrow} \mathrm{T}_{11}, \mathrm{T}_{12}, \mathrm{T}_{21}, \mathrm{T}_{22}$	
3	$\mathrm{T}_{11} \overset{\mathbf{x}_{1,2}(1)=\mathbf{F}(-\mathbf{s}_1^*(2))}{\longrightarrow} \mathrm{T}_r$, $\mathrm{T}_{12} \overset{\mathbf{x}_{1,2}(2)=\mathbf{F}(\mathbf{s}_1^*(1))}{\longrightarrow} \mathrm{T}_r$, $\mathrm{T}_{21} \overset{\mathbf{y}_{1,2}(1)=\mathbf{F}(-\mathbf{u}_1^*(2))}{\longrightarrow} \mathrm{T}_r$, $\mathrm{T}_{22} \overset{\mathbf{y}_{1,2}(2)=\mathbf{F}(\mathbf{u}_1^*(1))}{\longrightarrow} \mathrm{T}_r$	
4	$\mathrm{T}_r \overset{\mathbf{x}_{1,2}(1),\mathbf{x}_{1,2}(2),\mathbf{y}_{1,2}(1),\mathbf{y}_{1,2}(2)}{\longrightarrow} \mathrm{T}_{11}, \mathrm{T}_{12}, \mathrm{T}_{21}, \mathrm{T}_{22}$	
5	$\mathrm{T}_{11} \overset{\mathbf{x}_{2,1}(1)=\mathbf{F}\mathbf{s}_2(1)}{\longrightarrow} \mathrm{T}_r$, $\mathrm{T}_{12} \overset{\mathbf{x}_{2,1}(2)=\mathbf{F}\mathbf{s}_2(2)}{\longrightarrow} \mathrm{T}_r$, $\mathrm{T}_{21} \overset{\mathbf{y}_{2,1}(1)=\mathbf{F}\mathbf{u}_2(1)}{\longrightarrow} \mathrm{T}_r$, $\mathrm{T}_{22} \overset{\mathbf{y}_{2,1}(2)=\mathbf{F}\mathbf{u}_2(2)}{\longrightarrow} \mathrm{T}_r$	$\mathbf{x}_{2,l}(i) \in \mathcal{S}_2$ $\mathbf{y}_{2,l}(i) \in \mathcal{S}_1$
6	$\mathrm{T}_r \overset{\mathbf{x}_{2,1}(1),\mathbf{x}_{2,1}(2),\mathbf{y}_{2,1}(1),\mathbf{y}_{2,1}(2)}{\longrightarrow} \mathrm{T}_{11}, \mathrm{T}_{12}, \mathrm{T}_{21}, \mathrm{T}_{22}$	
7	$\mathrm{T}_{11} \overset{\mathbf{x}_{2,2}(1)=\mathbf{F}(-\mathbf{s}_2^*(2))}{\longrightarrow} \mathrm{T}_r$, $\mathrm{T}_{12} \overset{\mathbf{x}_{2,2}(2)=\mathbf{F}(\mathbf{s}_2^*(1))}{\longrightarrow} \mathrm{T}_r$, $\mathrm{T}_{21} \overset{\mathbf{y}_{2,2}(1)=\mathbf{F}(-\mathbf{u}_2^*(2))}{\longrightarrow} \mathrm{T}_r$, $\mathrm{T}_{22} \overset{\mathbf{y}_{2,2}(2)=\mathbf{F}(\mathbf{u}_2^*(1))}{\longrightarrow} \mathrm{T}_r$	
8	$\mathrm{T}_r \overset{\mathbf{x}_{2,2}(1),\mathbf{x}_{2,2}(2),\mathbf{y}_{2,2}(1),\mathbf{y}_{2,2}(2)}{\longrightarrow} \mathrm{T}_{11}, \mathrm{T}_{12}, \mathrm{T}_{21}, \mathrm{T}_{22}$	
9	$\mathrm{T}_{11} \overset{\mathbf{x}_{3,1}(1)=\mathbf{F}\mathbf{s}_3(1)}{\longrightarrow} \mathrm{T}_r$, $\mathrm{T}_{12} \overset{\mathbf{x}_{3,1}(2)=\mathbf{F}\mathbf{s}_3(2)}{\longrightarrow} \mathrm{T}_r$, $\mathrm{T}_{21} \overset{\mathbf{y}_{3,1}(1)=\mathbf{F}\mathbf{u}_3(1)}{\longrightarrow} \mathrm{T}_r$, $\mathrm{T}_{22} \overset{\mathbf{y}_{3,1}(2)=\mathbf{F}\mathbf{u}_3(2)}{\longrightarrow} \mathrm{T}_r$	$\mathbf{x}_{3,l}(i) \in \mathcal{S}_3$ $\mathbf{y}_{3,l}(i) \in \mathcal{S}_4$
10	$\mathrm{T}_r \overset{\mathbf{x}_{3,1}(1),\mathbf{x}_{3,1}(2),\mathbf{y}_{3,1}(1),\mathbf{y}_{3,1}(2)}{\longrightarrow} \mathrm{T}_{11}, \mathrm{T}_{12}, \mathrm{T}_{21}, \mathrm{T}_{22}$	
11	$\mathrm{T}_{11} \overset{\mathbf{x}_{3,2}(1)=\mathbf{F}(-\mathbf{s}_3^*(2))}{\longrightarrow} \mathrm{T}_r$, $\mathrm{T}_{12} \overset{\mathbf{x}_{3,2}(2)=\mathbf{F}(\mathbf{s}_3^*(1))}{\longrightarrow} \mathrm{T}_r$, $\mathrm{T}_{21} \overset{\mathbf{y}_{3,2}(1)=\mathbf{F}(-\mathbf{u}_3^*(2))}{\longrightarrow} \mathrm{T}_r$, $\mathrm{T}_{22} \overset{\mathbf{y}_{3,2}(2)=\mathbf{F}(\mathbf{u}_3^*(1))}{\longrightarrow} \mathrm{T}_r$	
12	$\mathrm{T}_r \overset{\mathbf{x}_{3,2}(1),\mathbf{x}_{3,2}(2),\mathbf{y}_{3,2}(1),\mathbf{y}_{3,2}(2)}{\longrightarrow} \mathrm{T}_{11}, \mathrm{T}_{12}, \mathrm{T}_{21}, \mathrm{T}_{22}$	

at the relay with the assumption of unit power at all three nodes in order to ensure that the average power in forwarding the received signals does not exceed the available power.

In the third time slot, T_{11}, T_{12}, T_{21}, and T_{21} transmit signals $\mathbf{x}_{1,2}(1)$, $\mathbf{x}_{1,2}(2)$, $\mathbf{y}_{1,2}(1)$, and $\mathbf{y}_{1,2}(2)$, respectively. The received signal at the relay is $\mathbf{r}_{R_{1,2}} = \mathbf{h}(1) \otimes \mathbf{x}_{1,2}(1) + \mathbf{h}(2) \otimes \mathbf{x}_{1,2}(2) + \mathbf{g}(1) \otimes \mathbf{y}_{1,2}(1) + \mathbf{g}(2) \otimes \mathbf{y}_{1,2}(2) + \mathbf{n}_{1,2}$.

In the fourth time slot, the relay transmits $A\mathbf{r}_{R_{1,2}}$ to four antennas at both source

nodes. The received signal at T_{11} is $\mathbf{r}_{1,2} = A\mathbf{h}(1) \otimes \mathbf{r}_{R_{1,2}} + \mathbf{u}_{1,2} = A\mathbf{h}(1) \otimes \mathbf{h}(1) \otimes \mathbf{x}_{1,2}(1) + A\mathbf{h}(1) \otimes \mathbf{h}(2) \otimes \mathbf{x}_{1,2}(2) + A\mathbf{h}(1) \otimes \mathbf{g}(1) \otimes \mathbf{y}_{1,2}(1) + A\mathbf{h}(1) \otimes \mathbf{g}(2) \otimes \mathbf{y}_{1,2}(2) + A\mathbf{h}(1) \otimes \mathbf{n}_{1,2} + \mathbf{u}_{1,2}$. It should be noted that the signals $\mathbf{x}_{1,l}(i) \in \mathcal{S}_1$ and $\mathbf{y}_{1,l}(i) \in \mathcal{S}_2$.

In the fifth time slot, T_{11}, T_{12}, T_{21}, and T_{21} transmit signals $\mathbf{x}_{2,1}(1)$, $\mathbf{x}_{2,1}(2)$, $\mathbf{y}_{2,1}(1)$, and $\mathbf{y}_{2,1}(2)$, respectively. The received signal at the relay is $\mathbf{r}_{R_{2,1}} = \mathbf{h}(1) \otimes \mathbf{x}_{2,1}(1) + \mathbf{h}(2) \otimes \mathbf{x}_{2,1}(2) + \mathbf{g}(1) \otimes \mathbf{y}_{2,1}(1) + \mathbf{g}(2) \otimes \mathbf{y}_{2,1}(2) + \mathbf{n}_{2,1}$.

In the sixth time slot, the relay transmits $A\mathbf{r}_{R_{2,1}}$ to four antennas at both source nodes. The received signal at T_{11} is $\mathbf{r}_{2,1} = A\mathbf{h}(1) \otimes \mathbf{r}_{R_{2,1}} + \mathbf{u}_{2,1} = A\mathbf{h}(1) \otimes \mathbf{h}(1) \otimes \mathbf{x}_{2,1}(1) + A\mathbf{h}(1) \otimes \mathbf{h}(2) \otimes \mathbf{x}_{2,1}(2) + A\mathbf{h}(1) \otimes \mathbf{g}(1) \otimes \mathbf{y}_{2,1}(1) + A\mathbf{h}(1) \otimes \mathbf{g}(2) \otimes \mathbf{y}_{2,1}(2) + A\mathbf{h}(1) \otimes \mathbf{n}_{2,1} + \mathbf{u}_{2,1}$.

In the seventh time slot, T_{11}, T_{12}, T_{21}, and T_{21} transmit signals $\mathbf{x}_{2,2}(1)$, $\mathbf{x}_{2,2}(2)$, $\mathbf{y}_{2,2}(1)$, and $\mathbf{y}_{2,2}(2)$, respectively. The received signal at the relay is $\mathbf{r}_{R_{2,2}} = \mathbf{h}(1) \otimes \mathbf{x}_{2,2}(1) + \mathbf{h}(2) \otimes \mathbf{x}_{2,2}(2) + \mathbf{g}(1) \otimes \mathbf{y}_{2,2}(1) + \mathbf{g}(2) \otimes \mathbf{y}_{2,2}(2) + \mathbf{n}_{2,2}$.

In the eighth time slot, the relay transmits $A\mathbf{r}_{R_{2,2}}$ to four antennas at both source nodes. The received signal at T_{11} is $\mathbf{r}_{2,2} = A\mathbf{h}(1) \otimes \mathbf{r}_{R_{2,2}} + \mathbf{u}_{2,2} = A\mathbf{h}(1) \otimes \mathbf{h}(1) \otimes \mathbf{x}_{2,2}(1) + A\mathbf{h}(1) \otimes \mathbf{h}(2) \otimes \mathbf{x}_{2,2}(2) + A\mathbf{h}(1) \otimes \mathbf{g}(1) \otimes \mathbf{y}_{2,2}(1) + A\mathbf{h}(1) \otimes \mathbf{g}(2) \otimes \mathbf{y}_{2,2}(2) + A\mathbf{h}(1) \otimes \mathbf{n}_{2,2} + \mathbf{u}_{2,2}$. It should be noted that the signals $\mathbf{x}_{2,l}(i) \in \mathcal{S}_2$ and $\mathbf{y}_{2,l}(i) \in \mathcal{S}_1$.

In the ninth time slot, T_{11}, T_{12}, T_{21}, and T_{21} transmit signals $\mathbf{x}_{3,1}(1)$, $\mathbf{x}_{3,1}(2)$, $\mathbf{y}_{3,1}(1)$, and $\mathbf{y}_{3,1}(2)$, respectively. The received signal at the relay is $\mathbf{r}_{R_{3,1}} = \mathbf{h}(1) \otimes \mathbf{x}_{3,1}(1) + \mathbf{h}(2) \otimes \mathbf{x}_{3,1}(2) + \mathbf{g}(1) \otimes \mathbf{y}_{3,1}(1) + \mathbf{g}(2) \otimes \mathbf{y}_{3,1}(2) + \mathbf{n}_{3,1}$.

In the tenth time slot, the relay transmits $A\mathbf{r}_{R_{3,1}}$ to four antennas at both source nodes. The received signal at T_{11} is $\mathbf{r}_{3,1} = A\mathbf{h}(1) \otimes \mathbf{r}_{R_{3,1}} + \mathbf{u}_{3,1} = A\mathbf{h}(1) \otimes \mathbf{h}(1) \otimes \mathbf{x}_{3,1}(1) + A\mathbf{h}(1) \otimes \mathbf{h}(2) \otimes \mathbf{x}_{3,1}(2) + A\mathbf{h}(1) \otimes \mathbf{g}(1) \otimes \mathbf{y}_{3,1}(1) + A\mathbf{h}(1) \otimes \mathbf{g}(2) \otimes \mathbf{y}_{3,1}(2) + A\mathbf{h}(1) \otimes \mathbf{n}_{3,1} + \mathbf{u}_{3,1}$.

In the eleventh time slot, T_{11}, T_{12}, T_{21}, and T_{21} transmit signals $\mathbf{x}_{3,2}(1)$, $\mathbf{x}_{3,2}(2)$, $\mathbf{y}_{3,2}(1)$, and $\mathbf{y}_{3,2}(2)$, respectively. The received signal at the relay is $\mathbf{r}_{R_{3,2}} = \mathbf{h}(1) \otimes \mathbf{x}_{3,2}(1) + \mathbf{h}(2) \otimes \mathbf{x}_{3,2}(2) + \mathbf{g}(1) \otimes \mathbf{y}_{3,2}(1) + \mathbf{g}(2) \otimes \mathbf{y}_{3,2}(2) + \mathbf{n}_{3,2}$.

In the twelfth time slot, the relay transmits $A\mathbf{r}_{R_{3,2}}$ to four antennas at both source nodes. The received signal at T_{11} is $\mathbf{r}_{3,2} = A\mathbf{h}(1) \otimes \mathbf{r}_{R_{3,2}} + \mathbf{u}_{3,2} = A\mathbf{h}(1) \otimes \mathbf{h}(1) \otimes \mathbf{x}_{3,2}(1) +$

$A\mathbf{h}(1)\otimes\mathbf{h}(2)\otimes\mathbf{x}_{3,2}(2)+A\mathbf{h}(1)\otimes\mathbf{g}(1)\otimes\mathbf{y}_{3,2}(1)+A\mathbf{h}(1)\otimes\mathbf{g}(2)\otimes\mathbf{y}_{3,2}(2)+A\mathbf{h}(1)\otimes\mathbf{n}_{3,2}+\mathbf{u}_{3,2}$. It should be noted that the signals $\mathbf{x}_{3,l}(i)\in\mathcal{S}_3$ and $\mathbf{y}_{3,l}(i)\in\mathcal{S}_4$.

Therefore, the received signal at R in kth block of transmission is denoted as $\mathbf{r}_{R_k}=(\mathbf{r}_{R_{k_1}},\mathbf{r}_{R_{k,2}})^T$, and can be written as:

$$\begin{aligned}\mathbf{r}_{R_k}=&\begin{pmatrix}\mathbf{h}(1)\otimes\mathbf{x}_{k,1}(1)\\ \mathbf{h}(1)\otimes\mathbf{x}_{k,2}(1)\end{pmatrix}+\begin{pmatrix}\mathbf{h}(2)\otimes\mathbf{x}_{k,1}(2)\\ \mathbf{h}(2)\otimes\mathbf{x}_{k,2}(2)\end{pmatrix}\\&+\begin{pmatrix}\mathbf{g}(1)\otimes\mathbf{y}_{k,1}(1)\\ \mathbf{g}(1)\otimes\mathbf{y}_{k,2}(1)\end{pmatrix}+\begin{pmatrix}\mathbf{g}(2)\otimes\mathbf{y}_{k,1}(2)\\ \mathbf{g}(2)\otimes\mathbf{y}_{k,2}(2)\end{pmatrix}+\mathbf{n}_k\end{aligned}\tag{4.2}$$

The received signal at T_{11} in kth block of transmission is denoted by $\mathbf{r}_k=(\mathbf{r}_{k,1},\mathbf{r}_{k,2})^T$, then the received signal in three blocks of transmission is denoted by $\mathbf{r}=(\mathbf{r}_1^T,\mathbf{r}_2^T,\mathbf{r}_3^T)^T$, and $\mathbf{r}_k=A\mathbf{h}(1)\otimes\mathbf{r}_{R_k}+\mathbf{v}_k$, where $\mathbf{n}_k$, $\mathbf{v}_k$ are the i.i.d. CSCG noises at R, T_{11}, in which the elements are zero mean Gaussian distributed with variance σ^2.

We define the equivalent channel vectors as $\mathbf{a}(1)=\mathbf{h}(1)\otimes\mathbf{h}(1)$, $\mathbf{a}(2)=\mathbf{h}(1)\otimes\mathbf{h}(2)$, $\mathbf{b}(1)=\mathbf{h}(1)\otimes\mathbf{g}(1)$, $\mathbf{b}(2)=\mathbf{h}(1)\otimes\mathbf{g}(2)$, and their lengths are $L_{a(1)}$, $L_{a(2)}$, $L_{b(1)}$, $L_{b(2)}$ respectively. Therefore, the lengths $L_{a(1)}$, $L_{a(2)}$, $L_{b(1)}$, and $L_{b(2)}$ are calculated as $L_{a(1)}=L_{a(2)}=2L_h-1$, $L_{b(1)}=L_{b(2)}=L_h+L_g-1$. The received signals at T_{11} for kth block of transmission is thus expressed as:

$$\tilde{\mathbf{r}}_k=A\begin{pmatrix}\mathbf{H}_1 & \mathbf{H}_2\\ \mathbf{H}_2^*\mathbf{P} & -\mathbf{H}_1^*\mathbf{P}\end{pmatrix}\begin{pmatrix}\mathbf{x}_{k,1}(1)\\ \mathbf{x}_{k,2}(1)\\ \mathbf{x}_{k,1}(2)\\ \mathbf{x}_{k,2}(2)\end{pmatrix}+A\begin{pmatrix}\mathbf{G}_1 & \mathbf{G}_2\\ \mathbf{G}_2^*\mathbf{P} & -\mathbf{G}_1^*\mathbf{P}\end{pmatrix}\begin{pmatrix}\mathbf{y}_{k,1}(1)\\ \mathbf{y}_{k,2}(1)\\ \mathbf{y}_{k,1}(2)\\ \mathbf{y}_{k,2}(2)\end{pmatrix}+\tilde{\mathbf{z}}\tag{4.3}$$

$$=A\mathbf{H}(\mathbf{a})\mathbf{x}_k+A\mathbf{G}(\mathbf{b})\mathbf{y}_k+\tilde{\mathbf{z}}\tag{4.4}$$

where $\tilde{\mathbf{r}}_k=(\mathbf{r}_{k,1},\mathbf{r}_{k,2}{}^*)^T$, $\mathbf{H}(\mathbf{a})=\begin{pmatrix}\mathbf{H}_1 & \mathbf{H}_2\\ \mathbf{H}_2^*\mathbf{P} & -\mathbf{H}_1^*\mathbf{P}\end{pmatrix}$, $\mathbf{G}(\mathbf{b})=\begin{pmatrix}\mathbf{G}_1 & \mathbf{G}_2\\ \mathbf{G}_2^*\mathbf{P} & -\mathbf{G}_1^*\mathbf{P}\end{pmatrix}$, and $\mathbf{x}_k=(\mathbf{x}_{k,1}(1)^T,\mathbf{x}_{k,2}(1)^T,\mathbf{x}_{k,1}(2)^T,\mathbf{x}_{k,2}(2)^T)^T$, $\mathbf{y}_k=(\mathbf{y}_{k,1}(1)^T,\mathbf{y}_{k,2}(1)^T,\mathbf{y}_{k,1}(2)^T,\mathbf{y}_{k,2}(2)^T)^T$. The simplest two-tap channel case is studied here for brevity, such that the channel gains are written as $\mathbf{h}(i)=(h(i,0),h(i,1))^T$, and $\mathbf{g}(i)=(g(i,0),g(i,1))^T$, respectively. Therefore, the equivalent channel gains can be written as $\mathbf{a}(i)=(a(i,0),a(i,1),a(i,2))^T$ and

$\mathbf{b}(i) = (b(i,0), b(i,1), b(i,2))^T$. $\mathbf{H}_1$, $\mathbf{H}_2$, $\mathbf{G}_1$, and $\mathbf{G}_2$ are Toeplitz matrix ,and are expressed as:

$$\mathbf{H}_1 = \begin{pmatrix} a(1,0) & 0 & 0 \\ a(1,1) & a(1,0) & 0 \\ a(1,2) & a(1,1) & a(1,0) \\ 0 & a(1,2) & a(1,1) \\ 0 & 0 & a(1,2) \end{pmatrix} \tag{4.5}$$

$$\mathbf{H}_2 = \begin{pmatrix} a(2,0) & 0 & 0 \\ a(2,1) & a(2,0) & 0 \\ a(2,2) & a(2,1) & a(2,0) \\ 0 & a(2,2) & a(2,1) \\ 0 & 0 & a(2,2) \end{pmatrix} \tag{4.6}$$

$$\mathbf{G}_1 = \begin{pmatrix} b(1,0) & 0 & 0 \\ b(1,1) & b(1,0) & 0 \\ b(1,2) & b(1,1) & b(1,0) \\ 0 & b(1,2) & b(1,1) \\ 0 & 0 & b(1,2) \end{pmatrix} \tag{4.7}$$

$$\mathbf{G}_2 = \begin{pmatrix} b(2,0) & 0 & 0 \\ b(2,1) & b(2,0) & 0 \\ b(2,2) & b(2,1) & b(2,0) \\ 0 & b(2,2) & b(2,1) \\ 0 & 0 & b(2,2) \end{pmatrix} \tag{4.8}$$

For blind channel estimation, it is convenient to rewrite the channel model (4.3) as:

$$\mathbf{r}_k = A \begin{pmatrix} \mathbf{X}_k(1) & \mathbf{X}_k(2) \\ -\tilde{\mathbf{X}}_k^*(2) & \tilde{\mathbf{X}}_k^*(1) \end{pmatrix} \begin{pmatrix} \mathbf{a}(1) \\ \mathbf{a}(2) \end{pmatrix} + A \begin{pmatrix} \mathbf{Y}_k(1) & \mathbf{Y}_k(2) \\ -\tilde{\mathbf{Y}}_k^*(2) & \tilde{\mathbf{Y}}_k^*(1) \end{pmatrix} \begin{pmatrix} \mathbf{b}(1) \\ \mathbf{b}(2) \end{pmatrix} + \mathbf{z} \tag{4.9}$$

$$= A\mathbf{X}_k\mathbf{a} + A\mathbf{Y}_k\mathbf{b} + \mathbf{z} \tag{4.10}$$

where $\mathbf{X}_k(1)$, $\mathbf{X}_k(2)$, $\mathbf{Y}_k(1)$, and $\mathbf{Y}_k(2)$ denote the Toeplitz matrices which consist of $\mathbf{x}_k(1) = (\mathbf{x}_{k,1}(1)^T, \mathbf{x}_{k,2}(1)^T)^T$, $\mathbf{x}_k(2) = (\mathbf{x}_{k,1}(2)^T, \mathbf{x}_{k,2}(2)^T)^T$, $\mathbf{y}_k(1) = (\mathbf{y}_{k,1}(1)^T, \mathbf{y}_{k,2}(1)^T)^T$, and $\mathbf{y}_k(2) = (\mathbf{y}_{k,1}(2)^T, \mathbf{y}_{k,2}(2)^T)^T$ respectively. $\tilde{\mathbf{X}}_k(1)$, $\tilde{\mathbf{X}}_k(2)$, $\tilde{\mathbf{Y}}_k(1)$, and $\tilde{\mathbf{Y}}_k(2)$ denote the Toeplitz matrix which consists of $\mathbf{P}\mathbf{x}_k(1)$, $\mathbf{P}\mathbf{x}_k(2)$, $\mathbf{P}\mathbf{y}_k(1)$, and $\mathbf{P}\mathbf{y}_k(2)$, repectively. $\mathbf{X}_k$, $\mathbf{Y}_k$ can be written as $\mathbf{X}_k = \begin{pmatrix} \mathbf{X}_k(1) & \mathbf{X}_k(2) \\ -\tilde{\mathbf{X}}_k^*(2) & \tilde{\mathbf{X}}_k^*(1) \end{pmatrix}$, $\mathbf{Y}_k = \begin{pmatrix} \mathbf{Y}_k(1) & \mathbf{Y}_k(2) \\ -\tilde{\mathbf{Y}}_k^*(2) & \tilde{\mathbf{Y}}_k^*(1) \end{pmatrix}$, respectively, and $\mathbf{a} = (\mathbf{a}(1), \mathbf{a}(2))^T$, $\mathbf{b} = (\mathbf{b}(1), \mathbf{b}(2))^T$. The noise term $\mathbf{z}$ is written as $\mathbf{z} = A\mathbf{h}(1) \otimes \mathbf{n} + \mathbf{u}$.

4.3 Blind Receiver

In practical systems, the symbols transmitted from T_{12}, T_{21}, and T_{22} need to be detected at T_{11} subjected to background noise, and vice versa. For brevity, we present the proposed receiver for T_{11}, while the same receiver designs are applicable to other antennas. The LSE receiver at T_{11} for our channel model deals with the following optimization problem:

$$\hat{\mathbf{Y}} = \arg\max_{\mathbf{y},\mathbf{x}(2)} \left(\mathbf{r}^H \mathbf{S}(\mathbf{S}^H\mathbf{S})^{-1}\mathbf{S}^H\mathbf{r} \right), \ \mathbf{S} = A \cdot (\mathbf{X}\ \mathbf{Y}) \tag{4.11}$$

where $\mathbf{X} = (\mathbf{X}_1, \mathbf{X}_2, \mathbf{X}_3)^{\mathrm{T}}$, and $\mathbf{Y} = (\mathbf{Y}_1, \mathbf{Y}_2, \mathbf{Y}_3)^{\mathrm{T}}$ $\mathbf{y}$ and $\mathbf{x}(2)$ can be respectively written as $\mathbf{y} = (\mathbf{y}_1, \mathbf{y}_2, \mathbf{y}_3)^T$, and $\mathbf{x}(2) = (\mathbf{x}_{1,1}(2), \mathbf{x}_{1,2}(2), \mathbf{x}_{2,1}(2), \mathbf{x}_{2,2}(2), \mathbf{x}_{3,1}(2), \mathbf{x}_{3,2}(2))^T$.

4.3.1 Sphere Decoding

The global solution can be found by doing an exhaustive search over the entire codeword. However, the complexity of this method exponentially increases as the size of constellation sets and transmission frame, which is practically prohibitive. It is proved that this optimization problem is equivalent to the following least squares for jointly estimating the channel coefficients and the signals.

$$\{\hat{\mathbf{y}}, \hat{\mathbf{x}}(2), \hat{\bar{\mathbf{h}}}\} = \arg \min_{\mathbf{S}(\mathbf{y},\mathbf{x}(2)),\bar{\mathbf{h}}} ||\mathbf{r} - \mathbf{S}\bar{\mathbf{h}}||_2^2, \tag{4.12}$$

where $\bar{\mathbf{h}} = (\mathbf{a}, \mathbf{b})^T$.

This optimization problem can be approached by employing iterative least squares with ML decoders. Given an initial estimate $\hat{\bar{\mathbf{h}}}^{(0)} = (\hat{\mathbf{a}}^{(0)}, \hat{\mathbf{b}}^{(0)})^{\mathrm{T}}$ of $\bar{\mathbf{h}}$, since $||\mathbf{r} - \mathbf{S}\bar{\mathbf{h}}^{(0)}||_2^2 =$

$\sum_{k=1}^{3} ||\mathbf{r}_k - A\big(\mathbf{X}_k \ \mathbf{Y}_k\big)\bar{\mathbf{h}}^{(0)}||_2^2$, and the information symbols between each two codeword matrices $(\mathbf{X}_k, \mathbf{Y}_k)$ and $(\mathbf{X}_l, \mathbf{Y}_l)$ for $k \neq l$ are independent. The minimization problem of $||\mathbf{r} - \mathbf{S}\bar{\mathbf{h}}^{(0)}||_2^2$ with respect to the signal matrix $\mathbf{Y}$ and $\mathbf{X}$ is equivalent to each minimization problem with respect to the individual signal sub-matrix $(\mathbf{X}_k, \mathbf{Y}_k)$.

$$\begin{aligned}\{\hat{\mathbf{x}}_k^{(0)}(2), \hat{\mathbf{y}}_k^{(0)}\} &= \arg\min ||\mathbf{r}_k - A\big(\mathbf{X}_k \ \mathbf{Y}_k\big)\bar{\mathbf{h}}^{(0)}||_2^2 \\ &= \arg\min ||\tilde{\mathbf{r}}_k - A\big(\mathbf{H}(\mathbf{a}^{(0)}) \ \mathbf{G}(\mathbf{b}^{(0)})\big)\mathbf{s}_k||_2^2, \qquad \text{for } k = 1, 2, 3 \end{aligned} \tag{4.13}$$

where $\mathbf{s}_k = (\mathbf{x}_k^T, \mathbf{y}_k^T)^T$. Due to the structure of $\mathbf{H}(\mathbf{a}^{(0)})$ and $\mathbf{G}(\mathbf{b}^{(0)})$, the minimization problem of (4.13) can be efficiently solved using parallel sphere decoders or Viterbi algorithm if either L (the number of channel taps) or the size of constellations is small. Once we have all the estimates $\hat{\mathbf{y}}_k^{(0)}$ of $\mathbf{y}_k$, and $\hat{\mathbf{x}}_k^{(0)}(2)$ of $\mathbf{x}_k(2)$, for $k = 1, \cdots, 3$, then a better estimate of $\bar{\mathbf{h}}$ can be obtained by minimizing $||\mathbf{r} - \hat{\mathbf{S}}^{(0)}\bar{\mathbf{h}}||_2^2$ with respect to $\bar{\mathbf{h}}$, which gives $\hat{\bar{\mathbf{h}}}^{(1)} = \big((\mathbf{S}^{(0)})^H\mathbf{S}^{(0)}\big)^{-1}(\mathbf{S}^{(0)})^H\mathbf{r}$. We denote $\mathbf{S}^{(0)} = (\mathbf{X}_1(\hat{\mathbf{x}}_1^{(0)}(2))^T, \mathbf{Y}_1(\hat{\mathbf{y}}_1^{(0)})^T, \cdots, \mathbf{X}_3(\hat{\mathbf{x}}_3^{(0)}(2))^T, \mathbf{Y}_3(\hat{\mathbf{y}_3}^{(0)})^T)^{\mathrm{T}}$. We keep continuing this process until $||\hat{\bar{\mathbf{h}}}^{(m+1)} - \hat{\bar{\mathbf{h}}}^{(m)}||$ is less than a given threshold $\gamma > 0$. The above whole procedure can be summarized similarly as Proposition 1 in Chapter 3.

4.3.2 Initialization of Channel Estimation

The performance of the decoding proposition 1 heavily depends on how to properly choose the estimate of $\bar{\mathbf{h}}$, i.e., $\hat{\bar{\mathbf{h}}}^{(0)}$. In this section, we develop an efficient algorithm especially for this system to achieve an initial estimate of the channel. Let us consider the relationship between the inputs and outputs in the kth block of transmission. In this case, we have

$$\mathbf{r}_k(1) = A\mathbf{X}_k(1)\mathbf{a}(1) + A\mathbf{X}_k(2)\mathbf{a}(2) + A\mathbf{Y}_k(1)\mathbf{b}(1) + A\mathbf{Y}_k(2)\mathbf{b}(2) + \mathbf{z}_k(1) \tag{4.14}$$

$$\mathbf{r}_k(2) = -A\tilde{\mathbf{X}}_k^*(2)\mathbf{a}(1) + A\tilde{\mathbf{X}}_k^*(1)\mathbf{a}(2) - A\tilde{\mathbf{Y}}_k^*(2)\mathbf{b}(1) + A\tilde{\mathbf{Y}}_k^*(1)\mathbf{b}(2) + \mathbf{z}_k(2) \tag{4.15}$$

Then, from the first two equations of (4.14), (4.15), we have

$$\begin{aligned} r_k(1,0) =& Ax_{k,1}(1,0)a(1,0) + Ax_{k,1}(2,0)a(2,0) \\ &+ Ay_{k,1}(1,0)b(1,0) + Ay_{k,1}(1,0)b(2,0) + z_k(1,0) \end{aligned} \tag{4.16}$$

$$\begin{aligned} r_k(2,0) =& - Ax^*_{k,1}(2,0)a(1,0) + Ax^*_{k,1}(1,0)^*a(2,0) \\ &- Ay^*_{k,1}(2,0)b(1,0) + Ay^*_{k,1}(1,0)b(2,0) + z_k(2,0) \end{aligned} \tag{4.17}$$

These two equations can be written in three blocks of transmission as

$$\begin{aligned} \mathbf{r}_k(0) =& (r_1(1,0), r_1(2,0), r_2(1,0), r_2(2,0), r_3(1,0), r_3(2,0))^T \\ =& A \begin{pmatrix} x_{1,1}(1,0) & x_{1,1}(2,0) & y_{1,1}(1,0) & y_{1,1}(2,0) \\ -x^*_{1,1}(2,0) & x^*_{1,1}(1,0) & -y^*_{1,1}(2,0) & y^*_{1,1}(1,0) \\ x_{2,1}(1,0) & x_{2,1}(2,0) & y_{2,1}(1,0) & y_{2,1}(2,0) \\ -x^*_{2,1}(2,0) & x^*_{2,1}(1,0) & -y^*_{2,1}(2,0) & y^*_{2,1}(1,0) \\ x_{3,1}(1,0) & x_{3,1}(2,0) & y_{3,1}(1,0) & y_{3,1}(2,0) \\ -x^*_{3,1}(2,0) & x^*_{3,1}(1,0) & -y^*_{3,1}(2,0) & y^*_{3,1}(1,0) \end{pmatrix} \begin{pmatrix} a(1,0) \\ a(2,0) \\ b(1,0) \\ b(2,0) \end{pmatrix} + \begin{pmatrix} z_{1,1}(0) \\ z_{1,2}(0) \\ z_{2,1}(0) \\ z_{2,2}(0) \\ z_{3,1}(0) \\ z_{3,2}(0) \end{pmatrix} \end{aligned} \tag{4.18}$$

$$= A\mathbf{B}_0\bar{\mathbf{h}}_0 + \mathbf{z}_k(0) \tag{4.19}$$

Then, the initial estimate of $\bar{\mathbf{h}}_0 = (a(1,0), a(2,0), b(1,0), b(2,0))^T$ is given by

$$\hat{\bar{\mathbf{h}}}_0^{(0)} = A^{-1}\hat{\mathbf{B}}_0^+\mathbf{r}_k(0) \tag{4.20}$$

where $\hat{\mathbf{B}}_0^+$ denotes the pseudo-inverse of matrix $\hat{\mathbf{B}}_0$, and

$$\hat{\mathbf{B}}_0 = \begin{pmatrix} x_{1,1}(1,0) & \hat{x}_{1,1}(2,0) & \hat{y}_{1,1}(1,0) & \hat{y}_{1,1}(2,0) \\ -\hat{x}^*_{1,1}(2,0) & x^*_{1,1}(1,0) & -\hat{y}^*_{1,1}(2,0) & \hat{y}^*_{1,1}(1,0) \\ x_{2,1}(1,0) & x_{2,1}(2,0) & \hat{y}_{2,1}(1,0) & \hat{y}_{2,1}(2,0) \\ -\hat{x}^*_{2,1}(2,0) & x^*_{2,1}(1,0) & -\hat{y}^*_{2,1}(2,0) & \hat{y}^*_{2,1}(1,0) \\ x_{3,1}(1,0) & \hat{x}_{3,1}(2,0) & \hat{y}_{3,1}(1,0) & \hat{y}_{3,1}(2,0) \\ -\hat{x}^*_{3,1}(2,0) & x^*_{3,1}(1,0) & -\hat{y}^*_{3,1}(2,0) & \hat{y}^*_{3,1}(1,0) \end{pmatrix} \tag{4.21}$$

where $\hat{\mathbf{x}}_{k,1}(2,0)$, $\hat{\mathbf{y}}_{k,1}(1,0)$ and $\hat{\mathbf{y}}_{k,1}(2,0)$, $k = 1, 2, 3$, can be obtained by solving the following optimization problem:

$$\{\hat{\mathbf{x}}_{k,1}(2,0), \hat{\mathbf{y}}_{k,1}(1,0), \hat{\mathbf{y}}_{k,1}(2,0)\} = \arg\max \ \mathbf{r}_k(0)\mathbf{B}_0\mathbf{B}_0^+\mathbf{r}_k(0) \tag{4.22}$$

In general, suppose that both the estimates of $\bar{\mathbf{h}}_i$ and those of signals $\mathbf{x}_{k,i}(2)$, $\mathbf{y}_{k,i}(1)$, and $\mathbf{y}_{k,i}(2)$ are all correct. Now, consider the $(n+1)$th equations in (4.14) and (4.15), i.e.,

$$\begin{aligned} r_k(1,n) =& A\Big(\sum_{i=1}^{n} x_{k,1}(1,n+1-i)a(1,i-1) + x_{k,1}(1,0)a(1,n) \\ &+ \sum_{i=1}^{n} x_{k,1}(2,n+1-i)a(2,i-1) + x_{k,1}(2,0)a(2,n) \\ &+ \sum_{i=1}^{n} y_{k,1}(1,n+1-i)b(1,i-1) + y_{k,1}(1,0)b(1,n) \\ &+ \sum_{i=1}^{n} y_{k,1}(2,n+1-i)b(2,i-1) + y_{k,1}(2,0)b(2,n)\Big) + z_k(1,n) \end{aligned} \tag{4.23}$$

$$\begin{aligned} r_k(2,n) =& A\Big(- \sum_{i=1}^{n} x^*_{k,1}(2,n+1-i)a(1,i-1) - x^*_{k,1}(2,0)a(1,n) \\ &+ \sum_{i=1}^{n} x^*_{k,1}(1,n+1-i)a(2,i-1) + x^*_{k,1}(1,0)a(2,n) \\ &- \sum_{i=1}^{n} y^*_{k,1}(2,n+1-i)b(1,i-1) - y^*_{k,1}(2,0)^*b(1,n) \\ &+ \sum_{i=1}^{n} y^*_{k,1}(1,n+1-i)^*b(2,i-1) + y^*_{k,1}(1,0)b(2,n)\Big) + z_k(2,n) \end{aligned} \tag{4.24}$$

which can be equivalently rewritten as

$$\begin{aligned} w_k(1,n) = r_k(1,n) - A\Big(& \sum_{i=2}^{n} x_{k,1}(1,n+1-i)a(1,i-1) + x_{k,1}(1,0)a(1,n) \\ &+ \sum_{i=2}^{n} x_{k,1}(2,n+1-i)a(2,i-1) + x_{k,1}(2,0)a(2,n) \\ &+ \sum_{i=2}^{n} y_{k,1}(1,n+1-i)b(1,i-1) + y_{k,1}(1,0)b(1,n) \\ &+ \sum_{i=2}^{n} y_{k,1}(2,n+1-i)b(2,i-1) + y_{k,1}(2,0)b(2,n)\Big) + z_k(1,n) \end{aligned} \tag{4.25}$$

$$
\begin{aligned}
w_k(2,n) = r_k(2,n) - A\Big(& -\sum_{i=2}^{n} x^*_{k,1}(2,n+1-i)a(1,i-1) - x^*_{k,1}(2,0)a(1,n) \\
& + \sum_{i=2}^{n} x^*_{k,1}(1,n+1-i)a(2,i-1) + x^*_{k,1}(1,0)a(2,n) \\
& - \sum_{i=2}^{n} y^*_{k,1}(2,n+1-i)b(1,i-1) - y^*_{k,1}(2,0)b(1,n) \\
& + \sum_{i=2}^{n} y^*_{k,1}(1,n+1-i)b(2,i-1) + y^*_{k,1}(1,0)b(2,n)\Big) + z_k(2,n)
\end{aligned}
\tag{4.26}
$$

Let $\mathbf{w}_k(n) = \Big(w_1(1,n), w_1(2,n), w_2(1,n), w_2(2,n), w_3(1,n), w_3(2,n)\Big)^T$, then we can further rewrite the equations above as:

$$
\mathbf{w}_k(n) = A\mathbf{B}_n\bar{\mathbf{h}}_0 + A\mathbf{B}_0\bar{\mathbf{h}}_n + \mathbf{z}_k(n) \tag{4.27}
$$

Therefore, the least square error estimate of $\bar{\mathbf{h}}_n = (a(1,n), a(2,n), b(1,n), b(2,n))^T$ is given by

$$
\hat{\bar{\mathbf{h}}}_n^{(0)} = A^{-1}\mathbf{B}_0^{+}\mathbf{w}_k(n) - \mathbf{B}_0^{+}\hat{\mathbf{B}}_n\bar{\mathbf{h}}_0 \tag{4.28}
$$

where

$$
\hat{\mathbf{B}}_n = \begin{pmatrix}
x_{1,1}(1,n) & \hat{x}_{1,1}(2,n) & \hat{y}_{1,1}(1,n) & \hat{y}_{1,1}(2,n) \\
-\hat{x}^*_{1,1}(2,n) & x^*_{1,1}(1,n) & -\hat{y}^*_{1,1}(2,n) & \hat{y}^*_{1,1}(1,n) \\
x_{2,1}(1,n) & x_{2,1}(2,n) & \hat{y}_{2,1}(1,n) & \hat{y}_{2,1}(2,n) \\
-\hat{x}^*_{2,1}(2,n) & x^*_{2,1}(1,n) & -\hat{y}^*_{2,1}(2,n) & \hat{y}^*_{2,1}(1,n) \\
x_{3,1}(1,n) & \hat{x}_{3,1}(2,n) & \hat{y}_{3,1}(1,n) & \hat{y}_{3,1}(2,n) \\
-\hat{x}^*_{3,1}(2,n) & x^*_{3,1}(1,n) & -\hat{y}^*_{3,1}(2,n) & \hat{y}^*_{3,1}(1,n)
\end{pmatrix}
\tag{4.29}
$$

where $\hat{\mathbf{x}}_{k,1}(2,n)$, $\hat{\mathbf{y}}_{k,1}(1,n)$ and $\hat{\mathbf{y}}_{k,1}(2,n)$, $k = 1,2,3$, can be obtained by solving the following optimization problem:

$$
\{\hat{\mathbf{x}}_{k,1}(2,n), \hat{\mathbf{y}}_{k,1}(1,n), \hat{\mathbf{y}}_{k,1}(2,n)\} = \arg\min ||\mathbf{w}_k(n) - A\mathbf{B}_n\bar{\mathbf{h}}_0 - \mathbf{B}_0\mathbf{B}_0^{+}\mathbf{w}_k(n) + A\mathbf{B}_0\mathbf{B}_0^{+}\mathbf{B}_n\bar{\mathbf{h}}_0||^2 \tag{4.30}
$$

4.4 Simulation Results

In this section, we present simulation results to verify the derived receivers. In our computer simulations, we fix $L_h = L_g = 2$. The symbols error rates (SERs) are plotted in Fig. 4.3 by averaging over 10^6 random channel realizations. The channel coefficients are generated by i.i.d. zero-mean CSCG random variables with 1/2 variance. We choose $p_1 = 5$, $p_2 = 7$, $p_3 = 9$, and $p_4 = 11$ for the simulations. In the proposed signaling scheme, the transmitted PSK symbols are from constellation sets with different sizes. Therefore, the bit rate of each time frame of transmission is different. The constellation selection Method 2 in [26] is utilized here to pick the same number of constellation points from sets $\mathcal{S}_1, \cdots, \mathcal{S}_4$ in order to achieve a uniform bit rate for the practical communication system. The specific constellation points in $\mathcal{S}_i$, $i = 1, \cdots 4$, are given, respectively, by (2,4),(1,3),(1,3),(0,6).

In Fig.4.3, the SERs of LSE blind receiver and iterative parallel sphere decoders are plotted by respectively using (4.11) and Proposition 1 for TR-STBC two-way relay system comparing to those for one-antenna two-way network. The simulation results demonstrate the diversity gain benefitted from the TR-STBC scheme.

Fig.4.4 plots the SERs for the iterative sphere decoder and LSE receiver with different number of transmission blocks using the same constellation selection given by (2,4),(1,3),(1,3),(0,6). Here, we must point out clearly that in spite of the fact that (4.11) enables full diversity, the joint detection we develop in the previous section is just a suboptimal decoding algorithm, and in general, it cannot assure full diversity. However, it can be observed that the iterative detector with larger transmission blocks outperforms that with less transmission blocks, and the SER of iterative sphere decoder becomes closer to that of LSE receiver as the number of transmission blocks increases. It suggests that the derived iterative parallel sphere decoder provides similar diversity gain as LSE receiver, since it is more accurate to estimate the channel coefficients that stay unchanged in longer transmission time.

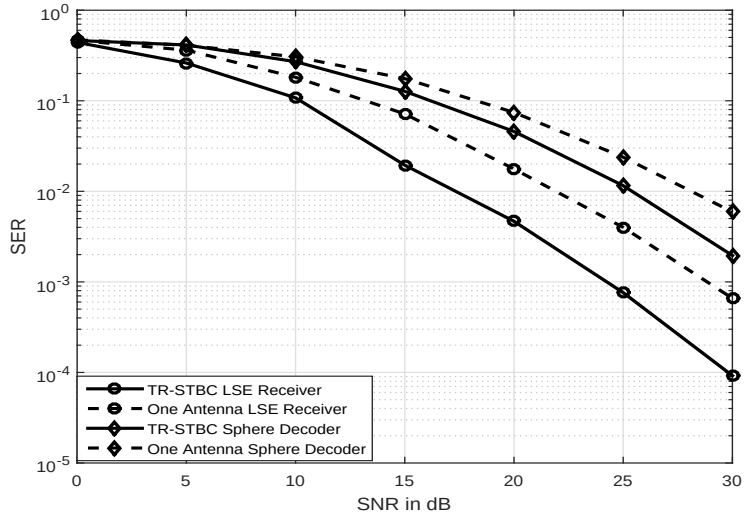

Figure 4.3: Symbol error rate

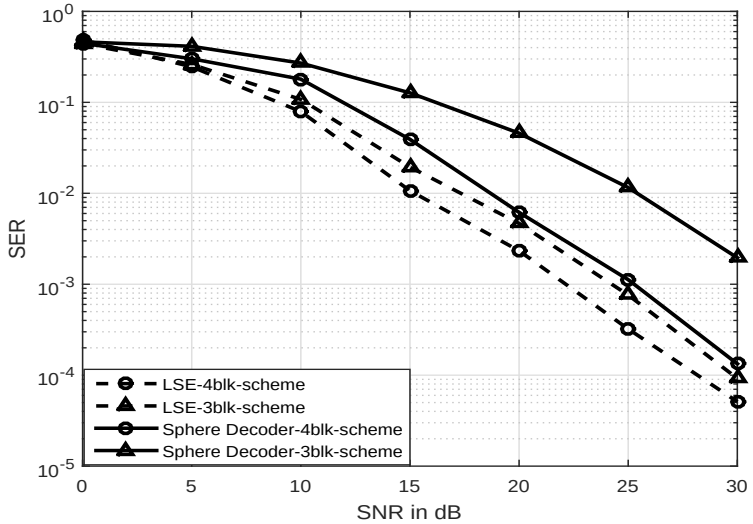

Figure 4.4: Symbol error rate

4.5 Conclusion

In this chapter, an effective signaling and transmission scheme is proposed for amplify-and-forward MIMO two-way relay system over frequency-selective fading channels. The transmitted symbols are carefully chosen from four PSK constellation sets in order to get the transmitted symbols reliably recovered in Gaussian noise environment. The time reversal space time block code is applied to deal with the multi-path fading. We have provided the iterative least squares with parallel sphere decoders to approximate the LSE detector by taking advantage of the linearity and triangular structure of our signal design.

CHAPTER 5

Conclusion

In this dissertation, three blind detection designs with unique identification are developed for three different AF two-way relay systems, which are presented in three chapters respectively.

The first chapter considers blind detection for an AF two-way relay system with non-reciprocal flat-fading channels. An effective signalling and transmitting scheme is proposed to achieve unique identification of the transmitted symbols and channel coefficients in noise-free transmissions. The GLRT and LSE receivers with full diversity are derived for the Rayleigh fading channels with Gaussian noise. Simulations show that the performance of GLRT receivers is almost identical to that of the LSE receivers. This interesting observation suggests that one can replace the GLRT receiver by the LSE receiver in the blind detection to take advantage of a simpler implementation without sacrificing performance. Power allocation schemes are examined to further improve the system performance.

The second chapter develops blind detection design for an AF two-way relay system over frequency-selective channels. An effective signalling and transmitting scheme is proposed using four PSK modulation.The iterative sphere decoder is derived for the Rayleigh fading channels with Gaussian noise to decrease the complexity of LSE optimization problem.

The third chapter applies the time-reversal space time block code (TR-STBC) to two-way relay system equipped with multiple antennas. An effective signalling and transmitting scheme is also proposed for AF two-way relay system with multiple antennas under frequency-selective fading environments. The iterative sphere decoder is developed to decrease the complexity, such that the proposed scheme is able to operate in practice.

Based on the simulation results, the proposed blind detection schemes outperform the training-based or pilot-assisted symbol detection algorithm.

REFERENCES

LIST OF REFERENCES

[1] C. E. Shannon, "Two-way communications channels," in *Proc. Berkeley Symp. Math. Stat. Prob.*, Chicago, IL, Jun. 1961, pp. 611–644.

[2] E. van der Meulen, "Three-terminal communication channels," *Adv. Appl. Prob.*, vol. 3, pp. 120–154, 1971.

[3] T. M. Cover and J. A. Thomas, *Elements of Information Theory.* New York: John Wiley & Sons, 1991.

[4] B. Rankov and A. Wittneben, "Spectral efficient signaling for half-duplex relay channels," in *Proc. Asilomar Conf. Signals, Systems and Computers*, Pacific Grove, CA, Oct./Nov. 2005, pp. 1066–1071.

[5] S. Kim, P. Mitran, and V. Tarokh, "Performance bounds for bi-directional coded cooperation protocols," *IEEE Trans. Inform. Theory*, vol. 54, no. 11, pp. 5235–5241, Nov. 2008.

[6] T. Oechtering and H. Boche, "Optimal tranmsit strategies in multiantenna bidirectional relaying," in *Proc. IEEE Int. Conf. Acoustics, Speech, Signal Processing (ICASSP)*, vol. 3, Honolulu, HI, Apr. 2007, pp. 145–148.

[7] T.-H. Pham, Y.-C. Liang, A. Nallanathan, and H. K. Garg, "Optimal training sequences for channel estimation in bi-directional relay networks with multiple antennas," *IEEE. Trans. Commun.*, vol. 58, no. 2, pp. 474–479, Feb. 2010.

[8] S. Zhang, S. C. Liew, and P. P. Lam, "Hot topic: Physical-layer network coding," in *Proc. ACM MobiCom*, Los Angeles, CA, 2006, pp. 358–365.

[9] C. Peng, Q. Zhang, M. Zhao, Y. Yao, and W. Jia, "On the performance analysis of network-coded cooperation in wireless networks," *IEEE Trans. Wireless Commun.*, vol. 7, no. 8, pp. 3090–3097, Aug. 2008.

[10] R. H. Y. Louie, Y. Li, and B. Vucetic, "Practical physical layer network coding for two-way relay channels: Performance analysis and comparison," *IEEE Trans. Wireless Commun.*, vol. 9, no. 2, pp. 764–777, Feb. 2010.

[11] S. Wang, Q. Song, X. Wang, and A. Jamalipour, "Rate and power adaptation for analog network coding," *IEEE Trans. Veh. Technol.*, vol. 60, no. 5, pp. 2302–2313, May 2011.

[12] J. N. Laneman, D. N. C. Tse, and G. W. Wornell, "Cooperative diversity in wireless networks: Efficient protocols and outage behavior," *IEEE Trans. Inform. Theory*, vol. 50, pp. 3062–3080, Dec. 2004.

LIST OF REFERENCES (continued)

[13] R. U. Nabar, H. Bölcskei, and F. W. Kneubühler, "Fading relay channel: Performance limits and space-time signal design," *IEEE J. Select. Areas Commun.*, vol. 22, pp. 1099–1109, Aug. 2004.

[14] L. P. W. Jr., R. M. T. Jr., and D. M. Warme, "Echo-MIMO: A two-way channel training method for matched cooperative beamforming," *IEEE Trans. Sig. Proc.*, vol. 56, no. 9, pp. 4419–4432, Sept. 2008.

[15] F. Gao, R. Zhang, and Y. C. Liang, "Optimal channel estimation and training design for two-way relay networks," *IEEE Trans. Commun.*, vol. 57, no. 10, pp. 3024–3033, Oct. 2009.

[16] B. Jiang, F. Gao, X. Gao, and A. Nallanathan, "Channel estimation and training design for two-way relay networks with power allocation," *IEEE Trans. Wireless Commun.*, vol. 9, no. 6, pp. 2022–2032, Jun. 2010.

[17] S. Abdallah and I. N. Psaromiligkos, "Blind channel estimation for MPSK-based amplify-and-forward two-way relaying," in *Proc. IEEE Int. Conf. Acoustics, Speech, Signal Processing (ICASSP)*, Prague, 2011, pp. 2828–2831.

[18] X. Liao, L. Fan, and G. Gao, "Blind channel estimation for OFDM modulated two-way relay network," in *Proc. IEEE Wireless Commun. and Networking Conf. (WCNC)*, Sydney, Australia, 2010, pp. 1–5.

[19] S. Abdallah and I. N. Psaromiligkos, "Semi-blind channel estimation for amplify-and-forward two-way relay networks employing constant-modulus constellations," in *Proc. Conf. on Information Sciences and Systems (CISS)*, 2011, pp. 1–5.

[20] P. Cheng, L. Gui, Y. Rui, Y. Guo, X. Huang, and W. Zhang, "Compressed sensing based channel estimation for two-way relay networks," *IEEE Wireless Communications Letters*, vol. 1, pp. 201 – 204, 2012.

[21] X. Xu, J. Wu, S. Ren, X. Luan, and X. H, "Superimposed training and channel estimation for two-way relay networks," in *16th International Conference on Advanced Communication Technology (ICACT)*, Pyeongchang, Feb. 2014, pp. 1050 – 1054.

[22] S. Zhang, F. Gao, and C. Pei, "Optimal training design for individual channel estimation in two-way relay networks," *IEEE Tran. Signal Processing.*, vol. 60, pp. 4987 – 4991, May 2012.

[23] J.-K. Zhang and F. Huang, "Blind unique identification of MIMO channels using signal designs and high-order moments," *IEEE Sig. Proc. Lett.*, vol. 17, pp. 539–542, Jun. 2010.

LIST OF REFERENCES (continued)

[24] J.-K. Zhang and Y. Chau, "Full diversity blind signal designs for unique identification of frequency selective channels," in *Proc. IEEE Int. Symp. Inform. Theory (ISIT)*, Seoul, Korea, 2009.

[25] J.-K. Zhang, C. Yuen, and F. Huang, "Full diversity blind signal designs for unique identification of frequency selective channels," vol. 61, no. 5, pp. 2172 – 2184, Jun. 2012.

[26] L. Li, Y. Ding, J.-K. Zhang, and R. Zhang, "Blind detection with unique identification in two-way relay channel," *IEEE Trans. Wireless Commun.*, vol. 11, no. 7, pp. 2640–2648, Jul. 2012.

[27] Y. Ding, L. Li, and J.-K. Zhang, "Blind transmission and detection designs with unique identification and full diversity for noncoherent two-way relay networks," *IEEE Trans. Veh. Technol.*, Jan. 2014.

[28] A. E. Gamal and S. Zahedi, "Capacity of a class of relay channels with orthogonal components," *IEEE Trans. Inform. Theory*, vol. 51, no. 5, pp. 1815–1817, May 2005.

[29] C. S. Patel and G. L. Stüber, "Channel estimation for amplify and forward relay based cooperative diversity systems," *IEEE Trans. Wireless Commun.*, vol. 6, no. 6, pp. 2348–2356, Jun. 2007.

[30] I. Krikidis, J. Thompson, S. Mclaughlin, and N. Goertz, "Amplify-and-forward with partial relay selection," *IEEE Commun. Lett.*, vol. 12, no. 4, pp. 235–237, Apr. 2008.

[31] G. Farhadi and N. C. Beaulieu, "A decentralized power allocation scheme for amplify-and-forward multi-hop relaying systems," in *Proc. IEEE Int. Conf. in Commun. (ICC)*, 2010, pp. 1–6.

[32] A. S. Behbahani and A. M. Eltawil, "Amplify-and-forward relay networks under received power constraint," *IEEE Trans. Wireless Commun.*, vol. 8, no. 11, pp. 5422–5426, Nov. 2009.

[33] B. Shen and K. Kwak, "Semi-blind iterative relay selection schemes for amplify-and-forward cooperative relay network," in *Proc. Int. Conf. Ubiquitous and Future Networks (ICUFN)*, 2011, pp. 140–145.

[34] H. Ghozlan, Y. Mohasseb, H. E. Gamal, and G. Kramer, "The MIMO wireless switch: Relaying can increase the multiplexing gain," in *Proc. IEEE Int. Symp. Inform. Theory (ISIT)*, Seoul, Korea, Jun. 2009, pp. 1448–1452.

[35] Y. Hu, K. H. Li, and K. C. Teh, "Performance of two-way amplify-and-forward relay networks over asymmetric channels," in *IEEE Milit. Commun. Conf.*, 2009, pp. 1–6.

LIST OF REFERENCES (continued)

[36] X. Zhang, A. Ghrayeb, and M. Hasna, "Relay assignment in network-coded cooperative systems with M-PSK modulation over asymmetric channels," 2010, pp. 470–475.

[37] N. Yi, Y. Ma, and R. Tafazolli, "Incremental decode-forward relaying over asymmetric fading channels: Outage probability and location-aided relay selection," in *Proc. IEEE Statistical Signal Processing Workshop (SSP)*, 2011, pp. 181–184.

[38] L. Zheng and D. N. C. Tse, "Communicaton on the grassmann manifold: A geometric approach to the noncoherent multi-antenna channel," *IEEE Trans. Inform. Theory*, vol. 48, no. 2, pp. 359–383, Feb. 2002.

[39] M. Brehler and M. K. Varanasi, "Asymptotic error probability analysis of quadratic receiver in Rayleigh-fading channels with applications to a unified analysis of coherent and noncoherent space-time receivers," *IEEE Trans. Inform. Theory*, vol. 47, pp. 2383–2399, Sept. 2001.

[40] S. Ma and J.-K. Zhang, "Noncoherent diagonal distributed space-time block codes for amplify-and-forward half-duplex cooperative relay channels," *IEEE Trans. Veh. Technol.*, vol. 60, no. 5, pp. 2400–2405, Jun. 2011.

[41] R. Mittra, C. H. Chan, and T. Cwik, "Techniques for analyzing frequency selective surfaces-a review," *Proc. IEEE*, vol. 76, pp. 1593–1615, 1988.

[42] Y.-S. Choi, P. J. Voltz, and F. A. Cassara, "On channel estimation and detection for multicarrier signals in fast and selective Rayleigh fading channels," *IEEE Tran. Commun.*, vol. 49, pp. 1375–1387, 2001.

[43] C. Xiao and Y. R. Zheng, "Simulation models with correct statistical properties for Rayleigh fading channels," *IEEE Trans. Commun.*, vol. 53, no. 6, pp. 920–928, Jun. 2003.

[44] T. Koike-Akino, P. Popovski, and V. Tarokh, "Two-way relaying with network coding for frequency-selective fading channels," in *42nd Asilomar Conference on Signals, Systems and Computers*, 2008.

[45] C. Xiao, Y. R. Zheng, and N. Beaulieu, "Statistical simulation models for Rayleigh and Rician fading," in *IEEE Int. Commun. Conf*, vol. 65, Anchorage, AK, May 2003, pp. 3524–3529.

[46] C. W. R. Chiong and Y. X. Y. Rong, "Channel estimation for two-way MIMO relay systems in frequency-selective fading environments," *IEEE Tran. Wireless Commun.*, 2015.

LIST OF REFERENCES (continued)

[47] T.-H. Pham, Y. C. Liang, H. K. Garg, and A. Nallanathan, "Joint channel estimation and data detection for MIMO-OFDM two-way relay networks," in *Global Telecommunications Conference (GLOBECOM)*, 2010.

[48] F. Gao, R. Zhang, and Y.-C. Liang, "Channel estimation for OFDM modulated two-way relay networks," *IEEE Tran. Signal Processing.*, 2010.

[49] H. Yan and H. H. Nguyen, "Adaptive physical-layer network coding in two-way relaying with OFDM," in *IEEE Global Communications Conference (GLOBECOM)*, 2013.

[50] R. Vahidnia and S. Shahbazpanahi, "Single-carrier equalization for asynchronous two-way relay networks," *IEEE Tran. Signal Processing.*, vol. 62, pp. 5793–5808, 2014.

[51] S.-L. Wang and T.-M. Wu, "Performance analyses of two-way AF relaying over Nakagami-m frequency-selective fading channels," in *IEEE 80th Vehicular Technology Conference (VTC2014-Fall)*, 2014.

[52] Z.Wang and G.B.Giannakis, "Wireless multicarrier communications: Where Fourier meets Shannon," *IEEE Signal Process. Mag.*, vol. 17, no. 3, pp. 29–48, May 2000.

[53] N. Al-Dhahir and N. Diggavi, "Guard sequence optimization for block transmission over linear frequency-selective channels," *IEEE Trans. Commun.*, vol. 50, pp. 938–946, Jun. 2002.

[54] H. Liu and K. S. Kwak, "Resource allocation for cyclic prefixed single-carrier cognitive two-way relay networks," in *IEEE International Conference on COnsumer Electronics (ICCE)*, 2013.

[55] C.-C. Weng and P. P. Vaidyanathan, "Block diagonal gmd for zero-padded MIMO frequency selective channels," *IEEE Tran. Signal Processing.*, vol. 59, pp. 713–727, 2011.

[56] R. Rajashekar, K. V. S. Hari, and L. Hanzo, "Spatial modulation aided zero-padded single carrier transmission for dispersive channels," *IEEE Tran. Commun.*, vol. 61, pp. 2318 – 2329, 2013.

[57] C. R. N. Athaudage and R. R. V. Angiras, "Sensitivity of FFT-equalised zero-padded OFDM systems to time and frequency synchronisation errors," *IEE Proceedings - Communications*, vol. 152, pp. 945–951, 2005.

[58] J.-K. Zhang, C. Yuen, and F. Huang, "Full diversity blind signal designs for unique identification of frequency selective channels," *IEEE Tran. Vehicular Technology*, 2012.

LIST OF REFERENCES (continued)

[59] G. H. Golub and V. Pereyra, "The differentiation of pseudo-inverses and nonlinear least squares problems whose variables separate," *SIAM J. Numer. Anal.*, vol. 10, no. 2, pp. 413–432, Apr. 1973.

[60] G. Kramer, M. Gastpar, and P. Gupta, "Cooperative strategies and capacity theorems for relay networks," *IEEE Trans. Inform. Theory*, vol. 51, no. 9, Sept. 2005.

[61] A. Sendonaris, E. Erkip, and B. Aazhang, "User cooperation diversity — Part I: System description," *IEEE Trans. Comm.*, vol. 51, pp. 1927–1938, Nov. 2003.

[62] D. E. Simmons and J. P. Coon, "Two-way OFDM-based nonlinear amplify-and-forward relay systems," *IEEE Tran. Vehicular Technology*, vol. 65, pp. 3808–3812, 2016.

[63] G. Amarasuriya, C. Tellambura, and M. Ardakani, "Two-way amplify-and-forward multiple-input multiple-output relay networks with antenna selection," *IEEE Journal Sel. Areas Commun.*, vol. 30, pp. 1513–1529, 2012.

[64] J. Ping and S. Ting, "Rate performance of AF two-way relaying in low SNR region," *Communications Letters, IEEE*, vol. 13, pp. 233 – 235, Apr. 2009.

[65] J. Gao, S. Vorobyov, H. Jiang, J. Zhang, and M. Haardt, "Relay selection for two-way relay channels with MABC DF: A diversity perspective," *IEEE Tran. Signal Processing.*, vol. 62, pp. 3563 – 3577, Jul. 2013.

[66] F. He, Y. Sun, X. Chen, L. Xiao, and S. Zhou, "Optimal power allocation for two-way decode-and-forward OFDM relay networks," in *IEEE International Conference on Communications (ICC)*, 2012.

[67] A. Sheikh and A. Olfat, "New beamforming and relay selection for two-way decode-and-forward relay networks," *IEEE Tran. Vehicular Technology*, vol. 65, pp. 1354–1366, 2016.

[68] K. Lee, H. Sun, E. Park, and I. Lee, "Joint optimization for one and two-way MIMO AF multiple-relay systems," *IEEE Trans. Wireless Comm.*, vol. 9, pp. 3671–3681, 2010.

[69] I. Hammerstrom, M. Kuhn, C. Esli, J. Zhao, A. Wittneben, and G. Bauch, "MIMO two-way relaying with transmit CSI at the relay," in *IEEE 8th Workshop on Signal Processing Advances in Wireless Communications*, 2007.

[70] L. Sanguinetti, A. A. D'Amico, and Y. Rong, "A tutorial on the optimization of amplify-and-forward MIMO relay systems," *IEEE J. Sel. Areas Commun.*, vol. 30, pp. 1331 – 1346, 2012.

LIST OF REFERENCES (continued)

[71] R. Vaze and R. W. Heath, "On the capacity and diversity-multiplexing tradeoff of the two-way relay channel," *IEEE Tran. Information Theory*, vol. 57, pp. 4219–4234, 2011.

[72] D. Gunduz, A. Goldsmith, and H. V. Poor, "MIMO two-way relay channel: Diversity-multiplexing tradeoff analysis," in *42nd Asilomar Conference on Signals, Systems and Computers*, 2008.

[73] H. Mheidat, M. Uysal, and N. Al-Dhahir, "Equalization techniques for distributed space-time block codes with amplify-and-forward relaying," *IEEE Trans Signal Processing*, vol. 55, pp. 1839–1852, 2007.

[74] Y. Zhu and K. B. Letaief, "Single-carrier frequency-domain equalization with decision-feedback processing for time-reversal space-time block-coded systems," *IEEE Tran. Commun.*, vol. 53, pp. 1127–1131, 2005.

[75] E. G. Larsson, P. Stoica, E. Lindskog, and J. Li, "Space-time block coding for frequency-selective channels," in *Acoustics, Speech, and Signal Processing (ICASSP), IEEE International Conference on*, 2002.

[76] N. Ammar and Z. Ding, "Frequency selective channel estimation in time-reversed space-time coding," in *IEEE Wireless Communications and Networking Conference (WCNC)*, vol. 3, 2004, pp. 1838–1843.

[77] L.-K. Hua, *Introduction to Number Theory*. New York: Springer-Verlag, 1982.

APPENDICES

APPENDIX A

Proof for Theorem 1

To prove Theorem 1, we first introduce the Euler's theorem, the proof of which can be found in [77].

Lemma 1 *If integers a and b are coprime, then $a^{\varphi(b)} \equiv 1 (mod\ b)$.* ■

We also state the following fact about PSK symbols:

Fact 1 *Let $\alpha_i = \exp(\frac{2\pi\ell_{\alpha_i}}{L_i}), i = 1, 2, \ell_{\alpha_i} = 0, \cdots, L_i - 1$ be L_i-PSK symbols, and L_1 and L_2 are coprime; then, $\alpha_1 + \alpha_2 \neq 0$.*

Proof: We use a contradiction. Suppose $\alpha_1+\alpha_2 = 0$. Note that $\alpha_1+\alpha_2 = 2\cos\left(\frac{\pi(\ell_{\alpha_1}L_2-\ell_{\alpha_2}L_1)}{L_1L_2}\right)$ $\exp\left(\frac{j\pi(\ell_{\alpha_1}L_2+\ell_{\alpha_2}L_1)}{L_1L_2}\right)$. The assumption $\alpha_1 + \alpha_2 = 0$ suggests $\cos\left(\frac{\pi(\ell_{\alpha_1}L_2+\ell_{\alpha_2}L_1)}{L_1L_2}\right) = 0$. Then, there must exist some values of L_1, L_2 satisfying $\frac{(\ell_{\alpha_1}L_2-\ell_{\alpha_2}L_1)}{L_1L_2} = 1/2 + K$, where K is an integer. We have $2(\ell_{\alpha_1}L_2 - \ell_{\alpha_2}L_1) = (1+2K)L_1L_2$. Since $(1+2K)$ is odd, the product L_1L_2 becomes an even number due to the factor of 2 on the left-hand side. This contradicts the assumption that L_1 and L_2 are coprime. Hence Fact 1.

For a given non-zero vector $\tilde{\mathbf{z}} \neq \mathbf{0}$, there is at least one non-zero component in vector $\tilde{\mathbf{z}}$. Let's assume $\tilde{z}_1 \neq 0$ (the case for $\tilde{z}_1 = 0$ will be discussed later). Recall the first elements in vectors (2.11), (2.12), and (2.13) as follows:

$$\tilde{z}_1 = x_2\tilde{r}(2) - x_1\tilde{r}(5) = \sqrt{P_2}q_2(x_2y_1 + x_1y_2) \tag{A.1}$$

$$\tilde{z}_3 = x_2\tilde{r}(8) - x_3\tilde{r}(5) = \sqrt{P_2}q_2(x_2y_3 + x_3y_2) \tag{A.2}$$

$$\tilde{z}_5 = x_3\tilde{r}(2) - x_1\tilde{r}(8) = \sqrt{P_2}q_2(x_3y_1 - x_1y_3) \tag{A.3}$$

Under condition $\tilde{z}_1 \neq 0$, channel q_2 in (A.1) must not be zero by fact 1. We then observe $\tilde{z}_3 \neq 0$ in (A.2) by $q_2 \neq 0$ and fact 1. Furthermore, we have $\tilde{z}_5 \neq 0$ in (A.3). The reason is:

$x_3y_1 - x_1y_3 = 0$ holds only when $x_3 = x_1 = y_1 = y_3 = 1$. Note that $x_1 \neq 1$ always holds from (2.1), since $x_1 \in \mathcal{S}_1$ in which the PSK symbol "0" is removed.

The channel coefficients and the transmitted symbols can be uniquely identified by the equations (A.1) to (A.3). Let $\tilde{z}_1/\tilde{z}_3 = \gamma e^{j\vartheta}, \tilde{z}_1/\tilde{z}_5 = \beta e^{j\psi}, \gamma, \beta > 0$, $2\pi > \vartheta, \psi \geq 0$. Revoking the definitions in (2.1) to (2.4), we have $x_1y_2 = \exp\left(\frac{j2\pi t_1}{p_1}\right), x_2y_1 = \exp\left(\frac{j2\pi t_2}{p_2}\right), x_3y_2 = \exp\left(\frac{j2\pi(\ell_3p_1+k_2p_3)}{p_1p_3}\right)$, and $x_2y_3 = \exp\left(\frac{j2\pi(\ell_2p_4+k_3p_2)}{p_2p_4}\right)$, where $t_1 \equiv (\ell_1 + k_2)\text{mod } p_1$ and $t_2 \equiv (\ell_2 + k_1)\text{mod } p_2$. The ratios $\tilde{z}_1/\tilde{z}_3$ and $\tilde{z}_1/\tilde{z}_5$ are further expressed, respectively, as

$$\begin{aligned}\gamma e^{j\vartheta} = &\frac{\cos\left(\frac{\pi(t_1p_2-t_2p_1)}{p_1p_2}\right)}{\cos\left(\frac{\pi\left((\ell_3p_1+k_2p_3)p_2p_4-(\ell_2p_4+k_3p_2)p_1p_3\right)}{p_1p_2p_3p_4}\right)}\\ &\times\frac{\exp\left(\frac{j\pi(t_1p_2+t_2p_1)}{p_1p_2}\right)}{\exp\left(\frac{j\pi\left((\ell_3p_1+k_2p_3)p_2p_4+(\ell_2p_4+k_3p_2)p_1p_3\right)}{p_1p_2p_3p_4}\right)}\end{aligned} \tag{A.4}$$

$$\begin{aligned}\beta e^{j\psi} = &\frac{\cos\left(\frac{\pi(t_1p_2-t_2p_1)}{p_1p_2}\right)}{\sin\left(\frac{\pi\left((\ell_3p_2+k_1p_3)p_1p_4-(\ell_1p_4+k_3p_1)p_2p_3\right)}{p_1p_2p_3p_4}\right)}\\ &\times\frac{\exp\left(\frac{j\pi(t_1p_2+t_2p_1)}{p_1p_2}\right)}{j\exp\left(\frac{j\pi\left((\ell_3p_2+k_1p_3)p_1p_4+(\ell_1p_4+k_3p_1)p_2p_3\right)}{p_1p_2p_3p_4}\right)}.\end{aligned} \tag{A.5}$$

Comparing the real and imaginary parts of both sides of (A.4) and (A.5), the imaginary parts of exponentials: $\exp\left(j\pi\left(\frac{t_1p_2+t_2p_1}{p_1p_2} - \frac{(\ell_3p_1+k_2p_3)p_2p_4+(\ell_2p_4+k_3p_2)p_1p_3}{p_1p_2p_3p_4} - \frac{\vartheta}{\pi}\right)\right)$ and $\exp\left(j\pi\left(\frac{t_1p_2+t_2p_1}{p_1p_2} - \frac{(\ell_3p_2+k_1p_3)p_1p_4+(\ell_1p_4+k_3p_1)p_2p_3}{p_1p_2p_3p_4} - \frac{\phi}{\pi}\right)\right)$ must equal zero, where $\phi = \psi + \pi/2$. We obtain the following congruent equations:

$$\begin{aligned}&(t_1p_2+t_2p_1)p_3p_4-\left((\ell_3p_1+k_2p_3)p_2p_4+(\ell_2p_4+k_3p_2)p_1p_3\right)\\ &\equiv(\vartheta P/\pi)\text{mod } P\end{aligned} \tag{A.6}$$

$$\begin{aligned}&(t_1p_2+t_2p_1)p_3p_4-\left((\ell_3p_2+k_1p_3)p_1p_4+(\ell_1p_4+k_3p_1)p_2p_3\right)\\ &\equiv(\phi P/\pi)\text{mod } P\end{aligned} \tag{A.7}$$

Simplifying the left-hand sides of (A.6) and (A.7) yields

$$\begin{aligned}&\big((t_1-k_2)p_2+(t_2-\ell_2)p_1\big)p_3p_4-(\ell_3p_4+k_3p_3)p_1p_2\\&\equiv(\vartheta P/\pi)\text{mod } P\end{aligned}\tag{A.8}$$

$$\begin{aligned}&\big((t_1-\ell_1)p_2+(t_2-k_1)p_1\big)p_3p_4-(\ell_3p_4+k_3p_3)p_1p_2\\&\equiv(\phi P/\pi)\text{mod } P.\end{aligned}\tag{A.9}$$

Since p_3p_4 and p_1p_2 are coprime, applying the Chinese remainder theorem [77], the solutions to k_1 and k_3 can be obtained from (A.8), and the solution to k_2 can be obtained from (A.9). Note that $k_1 \equiv (t_2-\ell_2)\text{mod } p_2$, and $k_2 \equiv (t_1-\ell_1)\text{mod } p_1$. Applying Lemma 1, we obtain

$$k_1 \equiv (\vartheta P/\pi)(P/p_2)^{\varphi(p_2)-1}\text{mod } p_2,\tag{A.10}$$

$$k_2 \equiv (\phi P/\pi)(P/p_2)^{\varphi(p_1)-1}\text{mod } p_1,\tag{A.11}$$

$$k_3 \equiv (\vartheta P/\pi)(P/p_4)^{\varphi(p_4)-1}\text{mod } p_4.\tag{A.12}$$

The values of k_1, k_2, and k_3 given in (A.10), (A.11), and (A.12) enable a unique identification of the transmitted symbols y_1, y_2, and y_3. The solutions are given, respectviely, by

$$y_1=\exp\Big(\frac{j2\pi k_1}{p_2}\Big), y_2=\exp\Big(\frac{j2\pi k_2}{p_1}\Big), y_3=\exp\Big(\frac{j2\pi k_3}{p_4}\Big).$$

Since symbols x_1, x_2, and x_3 are known to S_1, the entries in channel vector $\mathbf{h}$ can be determined by (2.11), (2.12), or (2.13). Theorem 1 lists the solution given by (2.11). The second entry in vector $\mathbf{w}$ can be determined by plugging the obtained $\mathbf{h}$ into (2.8), (2.9), or (2.10). Theorem 1 lists the solution given by (2.8).

If $\tilde{z}_1 = 0$ for a given non-zero $\tilde{\mathbf{z}} \neq 0$, then $\tilde{z}_2$ must not equal zero by Fact 1. The channel coefficients and transmitted symbols can be obtained using the second equations in (2.11), (2.12), and (2.13). In this case, Theorem 1 can be proven following the same steps in the case $\tilde{z}_1 \neq 0$ by defining $\tilde{z}_2/\tilde{z}_4 = \gamma e^{j\vartheta}$ and $\tilde{z}_2/\tilde{z}_6 = \beta e^{j\psi}$.

APPENDIX B

Proof of Receiver A1

Taking the derivative of the log-likelihood function in (2.16) with respect to q_2^*, an optimal q_2 is obtained by $\breve{q}_2 = \mathbf{v}^H\mathbf{z}_o/(\sqrt{P_2}\mathbf{v}^H\mathbf{v})$. Inserting $\breve{q}_2$ into (2.16), we have

$$\begin{aligned}\log\big(f(\mathbf{z}|h_1,h_2,\breve{q}_2,g_1,\mathbf{x},\mathbf{y})\big) = &-\log\big(16\pi^4\sigma^8(1+2A^2|h_2|^2)^2\big)\\ &-\frac{\kappa}{2\sigma^2}-\frac{\big(||\mathbf{z}_e - Ah_2g_1\sqrt{P_2}\mathbf{v}||^2\big)}{2\sigma^2(1+2A^2|h_2|^2)}.\end{aligned} \tag{B.1}$$

Taking the derivative with respect to g_1^* in (B.1), we obtain an optimal g_1 as $\breve{g}_1 = \frac{\mathbf{v}^H\mathbf{z}_e}{Ah_2\sqrt{P_2}\mathbf{v}^H\mathbf{v}}$. Inserting $\breve{g}_1$, we have

$$\begin{aligned}\log\big(f(\mathbf{r}|h_1,h_2,\breve{g}_1,\breve{q}_2,\mathbf{x},\mathbf{y})\big) = &-\log\big(16\pi^4\sigma^8(1+2A^2|h_2|^2)^2\big)\\ &-\frac{\kappa}{2\sigma^2}-\frac{\omega}{2\sigma^2(1+2A^2|h_2|^2)}.\end{aligned} \tag{B.2}$$

Denote $\eta = |h_2|^2$. Taking the derivative with respect to η, we have $\frac{d\log\left(f(\mathbf{r}|h_1,h_2,\breve{g}_1,\breve{q}_2,\mathbf{x},\mathbf{y})\right)}{d\eta} = -2\frac{2A^2}{(1+2A^2\eta)} + \frac{2A^2}{2\sigma^2(1+2A^2\eta)^2}\omega$. Note that $|h_2|^2$ is non-negative. An optimal solution to $|h_2|^2$ is given by $|\breve{h}_2|^2 = \left\lceil \frac{1}{2A^2}\left(\frac{\omega}{4\sigma^2}-1\right), 0\right\rceil$, where $\lceil(\cdot,\cdot)\rceil$ is the ceiling function. Inserting the solution into (B.2), the log likelihood function becomes

$$\begin{aligned}&\log\left(f(\mathbf{r}|\breve{h}_1,\breve{h}_2,\breve{g}_1,\breve{q}_2,\mathbf{x},\mathbf{y})\right)\\ =&\begin{cases}-\log(16\pi^4\sigma^8)-\frac{\kappa}{2\sigma^2}-2\log\left(\frac{\omega}{4\sigma^2}\right)-2, & \text{if } \frac{\omega}{4\sigma^2}>1\\ -\log(16\pi^4\sigma^8)-\frac{\kappa+\omega}{2\sigma^2}, & \text{if } \frac{\omega}{4\sigma^2}\le 1\end{cases}.\end{aligned}$$

Receiver A1 in (2.17) is obtained by maximizing the log-likelihood function.

APPENDIX C

Proof for Receiver B1

The derivative of (2.20) with respect to q_2^* is $\frac{\partial \log\left(f(\mathbf{r}|h_1,h_2,g_1,q_2,\mathbf{x},\mathbf{y})\right)}{\partial q_2^*} = -\frac{1}{\sigma^2}\big(-\sqrt{P_2}\mathbf{y}^H\mathbf{r}_{\rm o} + P_2\mathbf{y}^H\mathbf{y}q_2\big)$. Setting it to zero, the optimal solution to q_2 is given by $\breve{q}_2 = \frac{1}{3\sqrt{P_2}}\mathbf{y}^H\mathbf{r}_{\rm o}$. Inserting $\breve{q}_2$ into (2.20) yields

$$\log\big(f(\mathbf{r}|h_1,h_2,g_1,\breve{q}_2,\mathbf{x},\mathbf{y})\big) = -\log\big(\pi^6\sigma^{12}(1+2A^2|h_2|^2)^3\big) - \frac{\lambda}{\sigma^2} - \frac{||\mathbf{r}_{\rm e} - Ah_2g_1\sqrt{P_2}\mathbf{y} - Ah_2h_1\sqrt{P_1}\mathbf{x}||^2}{\sigma^2(1+2A^2|h_2|^2)}. \tag{C.1}$$

Taking the derivative of (C.1) with respect to g_1^*, the optimal solution to g_1 is given by

$$\breve{g}_1 = \frac{\mathbf{y}^H(\mathbf{r}_{\rm e} - Ah_1h_2\sqrt{P_1}\mathbf{x})}{Ah_2\mathbf{y}^H\mathbf{y}} = \frac{1}{3Ah_2}\mathbf{y}^H(\mathbf{r}_{\rm e} - Ah_1h_2\sqrt{P_1}\mathbf{x}).$$

Inserting $\breve{g}_1$ into (C.1) yields

$$\log(f(\mathbf{r}|h_1,h_2,\breve{g}_1,\breve{q}_2,\mathbf{x},\mathbf{y})\big) = -\log\left(\pi^6\sigma^{12}(1+2A^2|h_2|^2)^3\right) - \frac{\lambda}{\sigma^2} - \frac{(\mathbf{r}_{\rm e} - Ah_1h_2\sqrt{P_1}\mathbf{x})^H\mathbf{B}(\mathbf{r}_{\rm e} - Ah_1h_2\sqrt{P_1}\mathbf{x})}{\sigma^2(1+2A^2|h_2|^2)}. \tag{C.2}$$

Taking the derivative with respect to h_1^*, we obtain $\breve{h}_1 = \frac{\mathbf{x}^H\mathbf{B}\mathbf{r}_{\rm e}}{Ah_2\sqrt{P_1}\mathbf{x}^H\mathbf{B}\mathbf{x}}$. Inserting $\breve{h}_1$, we have

$$\log(f(\mathbf{r}|\breve{h}_1,h_2,\breve{g}_1,\breve{q}_2,\mathbf{x},\mathbf{y})\big) = -\log\left(\pi^6\sigma^{12}(1+2A^2|h_2|^2)^3\right) - \frac{\lambda}{\sigma^2} - \frac{\varpi}{\sigma^2(1+2A^2|h_2|^2)}. \tag{C.3}$$

Let $\eta = |h_2|^2$. The derivative with respect to η in (C.3) is,

$$\frac{\partial \log\big(f(\mathbf{r}|\breve{h}_1,h_2,\breve{g}_1,\breve{q}_2,\mathbf{x},\mathbf{y})\big)}{\partial\eta} = -\frac{6A^2}{1+2A^2\eta} + \frac{2A^2\varpi}{\sigma^2(1+2A^2\eta)^2}.$$

An optimal solution is found $|\breve{h}_2|^2 = \left\lceil \frac{1}{2A^2}\big(\frac{\varpi}{3\sigma^2} - 1\big), 0\right\rfloor$. Inserting $|\breve{h}_2|^2$ into (C.3), we have

$$\log\left(f(\mathbf{r}|\breve{h}_1,\breve{h}_2,\breve{g}_1,\breve{q}_2,\mathbf{x},\mathbf{y})\right) = \begin{cases} -\log(\pi^6\sigma^{12}) - \frac{\lambda}{\sigma^2} - 3\log\frac{\varpi}{3\sigma^2} - 3, & \text{if } \frac{\varpi}{3\sigma^2} > 1 \\ -\log(\pi^6\sigma^{12}) - \frac{\lambda+\varpi}{\sigma^2}, & \text{if } \frac{\varpi}{3\sigma^2} \le 1 \end{cases}.$$

Maximizing the log-likelihood function, one can obtain Receiver B1 in (2.21).